TO STUDY THE PERFORMANCE OF A PARABOLIC SOLAR COLLECTOR USING SiO_2-H_2O AND CuO-H_2O BASED NANOFLUIDS

A Project Report Submitted
in partial fulfillment of the requirements for
the award of degree of

MASTER OF ENGINEERING
IN
THERMAL ENGINEERING

Submitted by
SUNIL KUMAR
Roll No.: 801283027

Under the Guidance of

Mr. Sumeet Sharma
(Associate Professor)
Mr. Kundan Lal
(Assistant Professor)

DEPARTMENT OF MECHANICAL ENGINEERING
THAPAR UNIVERSITY
PATIALA-147004, INDIA

July 2014

DECLARATION

I, "**Sunil Kumar**", hereby certify that the work which is being presented in this project report entitled "**To study the performance of a parabolic solar collector using SiO_2-H_2O and CuO-H_2O based nanofluids**" by me in partial fulfillment of the requirements for the award of degree of Master of Engineering in Thermal Engineering from Thapar University, Patiala is an authentic record of my own work carried out under the supervision of **Mr. Sumeet Sharma**, Associate Professor and **Mr. Kundan Lal,** Assistant Professor, Department of Mechanical Engineering, Thapar University, Patiala.

The matter embodied in this thesis has not been submitted in any other University / Institute for the award of any other degree.

Date: 15/7/2014

Sunil Kumar

(Sunil Kumar)

Reg. No. 801283027

This is to certify that the above statement made by the student concerned is correct to the best of my knowledge and belief.

Sumeet Sharma

(Mr. Sumeet Sharma)
Associate Professor
Mechanical engineering Department
Thapar University, Patiala

(Mr. Kundan Lal)
Assistant Professor
Mechanical Engineering Department
Thapar University, Patiala

Countersigned by

Dr. Ajay Batish
Professor & Head
Mechanical engineering Department
Thapar University, Patiala

Dr. S.K. Mohapatra
Senior Professor and
Dean of Academic Affairs
Thapar University, Patiala

2

ACKNOWLEDGEMENT

Words are often less to reveals one's deep regards. This project work would not have been possible without the encouragement and able guidance of supervisors Mr. Sumeet Sharma, Associate Professor and Mr. Kundan Lal, Assistant Professor, Department of Mechanical Engineering, Thapar University, Patiala. Their enthusiasm and optimism made this experience both rewarding and enjoyable. Most of the novel ideas and solutions in this work are the result of our numerous stimulating discussions. Their feedback and editorial comments were also invaluable for the writing of this thesis.

I feel very much obliged to Dr. Ajay Batish, Professor and Head of Mechanical Engineering Department, Thapar University, Patiala.

I would like to thanks to Dr. Rajeev Mehta, Head of Chemical Engineering Department, Thapar University, Patiala for giving me permission to prepare the nanofluid in MT Lab.

I would like to thanks to Dr. Madhup K. Mittal, Assistant Professor, Department of Mechanical Engineering, for providing me required measuring instruments.

I would like to thanks to Mr. Rakesh Lal, Workshop Attendant, Thapar University, Patiala for supporting me while making the tracking system.

I would also like to thanks to TEQIP for providing me fund required for thesis work.

I take pride of myself being son of ideal parents for their everlasting desire, sacrifice, affectionate blessings and help, without which it would not have been possible for me to complete my studies.

I would also like to thanks to all the faculty members and employees of Mechanical Engineering Department, Thapar University, Patiala for their everlasting support.

I would also like to thanks to all my friends and relatives for their everlasting support.

At last, I would like to thanks to God for all good deeds.

Sunil Kumar

(Sunil Kumar)

3

ABSTRACT

Literature shows that work has been done on parabolic solar collector theoretically and numerically using different nanofluids but a very limited experimental work has been reported on it. So, it has been decided to carry out an experimental investigation on parabolic solar collector using nanofluids and compares its performance with conventional fluid (water). Nanofluids used are SiO_2-water based and CuO-water based. Nanoparticles volume concentration used in the experiment are 0.01% (vol. conc.) and 0.05% (vol. conc.). The different volume flow rates taken are 20 l/h, 40 l/h and 60 l/h. Nanofluid is prepared without using any surfactant. To make the nanoparticles more stable and remain more dispersed in water, ultra bath sonicator has been used. But before this, stirring is done with the help of magnetic stirrer with hot plate system. Manual tracking mechanism has been used in the experiment to track the sun position during the day. From the results, it has been found that CuO-water based nanofluid is more efficient as compared to SiO_2-water based nanofluid and water. Instantaneous efficiency of CuO-water based and SiO_2-water based nanofluids at 0.01% (vol. conc.) is found to be upto 2.4%, 6.26%, 10.43% and 2%, 2.64% and 3.25% at volume flow rate of 20 l/h, 40 l/h and 60 l/h more as compared to water. Thermal efficiency of CuO-water based and SiO_2-water based nanofluids at 0.01% (vol. conc.) is found to be upto 3.05%, 3.36%, 4.87% and 2%, 2.39% and 1.13% at volume flow rate of 20 l/h, 40 l/h and 60 l/h more as compared to water. Instantaneous efficiency of CuO-water based and SiO_2-water based nanofluids at 0.05% (vol. conc.) is found to be upto 3.04%, 7.65%, 12.49% and 1.5%, 2.43% and 6.17% at volume flow rate of 20 l/h, 40 l/h and 60 l/h more as compared to water. Thermal efficiency of CuO-water based and SiO_2-water based nanofluids at 0.05% (vol. conc.) is found to be upto 4.34%, 4.12%, 6.6% and 1.41%, 1.78% and 4.13% at volume flow rate of 20 l/h, 40 l/h and 60 l/h more as compared to water. The maximum overall thermal efficiency obtains from water, SiO_2-water based and CuO-water based nanofluids is 6.63%, 7.83% and 9.57% respectively. The maximum value for convective heat transfer coefficient and heat removal factor is 406.85W/m^2K and 0.9579 respectively in CuO-water based nanofluid at 0.05% (vol. conc.).

Keywords: Nanofluid, Parabolic solar collector, Instantaneous efficiency, Thermal efficiency, Overall thermal efficiency, CuO, SiO_2, Properties, Performance.

CONTENT **PAGE NO.**

LIST OF FIGURES

Page No.

LIST OF TABLES

Page No.

NOMENCLATURE

Abbreviations:

MW	Megawatt
CSP	Concentrating Solar Power
PVT	Photovoltaic
SEGS	Solar Electric Generating System
PTC	Parabolic Trough Collectors
HFC	Heliostat Field Collectors
LFC	Linear Fresnel Collectors
CR	Concentration Ratio
STEP	Solar Total Energy Project
GWh	Gegawatt hour
US	United State
TEM	Transmission Electron Microscopy
KPa	Kilo Pascal
XRD	X-Ray Diffraction
SEM	Scattering Electron Microscopy
DASC	Direct Absorption Solar Collector
CNT	Carbon Nanotube
MWCNT	Multi Wall Carbon Nanotube
NCPSC	Nanofluid Based Concentrating Parabolic Solar Collectors
TPTC	Transparent Parabolic Trough Collectors
NCSWHS	Nanofluid Based Concentrating Solar Water Heating System
LPG	Liquefied Patroleum Gas
ERCUN	Energy Research Center of the University of Nyala
DSG	Direct Steam Generation
FPSC	Flat Plate Solar Collectors

Nomenclature:

R	Thermal Resistance
mV	Millivolt
m	Meter

cm	Centimeter
nm	Nanometer
T	Temperature
I	Irradiance
φ	% of Volume Fraction
V	Volume
ρ	Density
W	Weight
c	Specific Heat
N	North
E	East
G_T	Global Solar Radiation
vol.	volumetric
conc.	concentration

Subscripts:

abs	Absorption
cd	Conduction
cv	Convection
H.Ex	Heat Exchanger
eff	Nanofluid
max	Maximum
min	Minimum
f	Base Fluid
p	Nanoparticles
i	Inlet for nanofluid
o	Outlet for nanofluid
1	Inlet for water
2	Outlet for water

CHAPTER 1
INTRODUCTION

1.1 SOLAR ENERGY

Solar energy is a renewable source of energy which is limitless, immense and non- polluting. Solar energy has been used by broad variety of available power devices. It may be used directly or indirectly by converting it into another kinds of energy, like electricity and heat, which is used by man. If sunlight is utilized properly, it easily overcomes current and future electricity demand. The power of the sun coming on the earth is around 1.8×10^{11} MW which is many thousand times greater than all other energy sources. India receiving radiant energy in large amount from the sun because it is located in equatorial sun belt of the earth. So, It can complete the present and future energy needs of the world. Non-concentrating type of collectors are not used for electricity purpose and is used only for household water heating systems due to its low thermal efficiencies and low output temperatures. Concentrating type of collectors are mostly used to utilize the huge solar energy for commercial applications (like electricity generation). The focus of the report has been primarily on parabolic solar collector which is currently used for process heating and for electricity generation. Traditional parabolic solar collectors capture the astral energy by employing lengthy parabolic shaped reflector which target the sunbeams in the direction of the fluid which is flowing from the no. of tubes. For enhancing the performance of the collector, nanomaterials are mixed with base fluid (water) which is flowing through a translucent tube and due to this, roasting of the fluid might be possible directly. The basic dissimilarity amongst the nanofluid based and traditional solar collectors lies in the way of roasting of the flowing fluid. In the later case the sunbeams is occupied by the surface and is subsequently given to the flowing fluid through conduction and convection mechanisms, but in the earlier case the sunbeams is absorbed by the flowing fluid directly through radiative mechanism. A lot of investigation have been conducted in those locations where the solar energy is present in large amount i.e. at Southern Asia, Southern Europe, North Africa and Middle East to study the effect of solar potential in these lacations.

The ostensible scarcity of fossil fuels and its ecological issues will restrict the utilization of fossil fuels in coming days. So, investigators are aggravated to discover its substitutional resources of energy. The other factor for this is the continuous increament in the price of fossil fuels. Most

astral vigor relevances are financially feasible and the small devices for personal application need only some kWs of power (Sharma et al. 2011).

There are normally two types of systems used for this - concentrated solar power (CSP) system and photovoltaic system. The later uses the astral cells to produce electricity directly by photoelectric effect. The former employs various techniques for holding astral thermal energy which is then utilize in electricity generation and process heating. (David et al. 2011).

Concentrated Solar Power (CSP) systems are used for generating electricity from astral energy. Concentrated Solar Power (CSP) systems based on parabolic dish collectors, linear Fresnel reflector, power tower and parabolic trough attained the phase of ripeness. Between the different CSP systems, parabolic trough solar collector is the largest developed technology for large scale power production (Reddy et al. 2012).

Concentrating Solar Power (CSP) system has ability of supplying the high temperature steam to power the traditional Rankine cycle for electricity production. Today, the CSP system is used for solar power plants having capacity of 50 MW and have more power production capability in different sun rich areas all over the world (Roman et al. 2011).

The most technological problem of generating electricity from the solar energy is the irregular supply of solar energy which makes it inappropriate for different kinds of electrical load applications, like for household applications and industrial applications (Roman et al. 2011 & IEA 2005).

1.2 TYPES OF SOLAR COLLECTOR

A solar collector is a device for collecting solar radiation and transfer the energy to a fluid passing in contact with it. Also, we can say that a solar energy collector is a heat-exchanging device that transforms solar radiation into thermal energy that can be utilized for power generation. The heat transfer fluid links the solar collectors to the power generation system, carrying thermal energy from each collector to a central steam generator or thermal storage system as it circulates. These are general of two types:

(i) Non-concentrating or flat- plate type solar collector

(ii) Concentrating (focusing) type solar collector

1.2.(i) NON-CONCENTRATING COLLECTORS OR LOW TEMPERATURE COLLECTORS

a) Flat Plate Collector

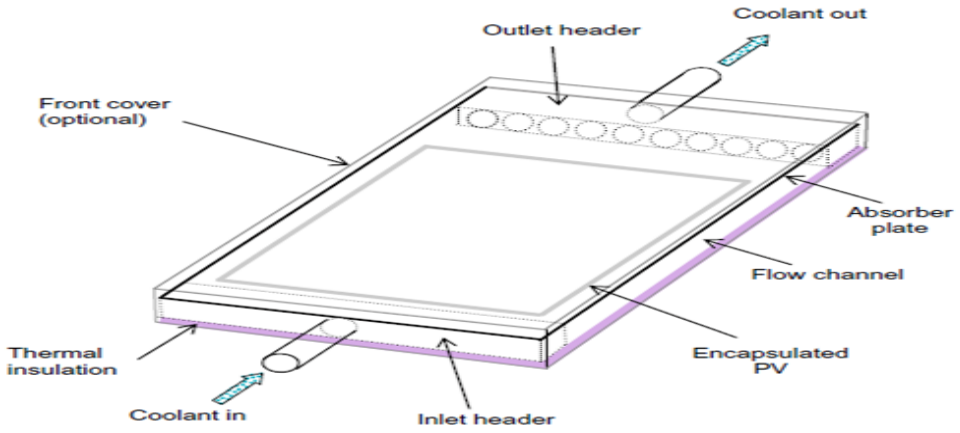

Fig.1 Flat Plate Collector (Chow T. T., 2009)

b) Hybrid PVT Collectors

Fig.2 Hybrid PVT Collector (cityu.edu.hk)

1.2.(ii) CONCENTRATING COLLECTORS OR HIGH TEMPERATURE COLLECTORS

These concentrating collectors can produce receiver temperatures above 350°C. They require accurate sun tracking by employing large number of heliostats. The concentration ratio is very

high (greater than 50). Central receiver systems employing a large number of heliostats have high values of concentration ratio (50-300) and temperature. They are most suitable for power generation. The four main types of concentrating solar collectors are:-

(1) Parabolic trough collectors

(2) Heliostat field collectors

(3) Linear Fresnel reflectors

(4) Parabolic dish collectors.

1) Parabolic Trough Collectors

Collector used in the experiment is parabolic solar collector to study its performance using nanofluids and then compare it with conventional one.

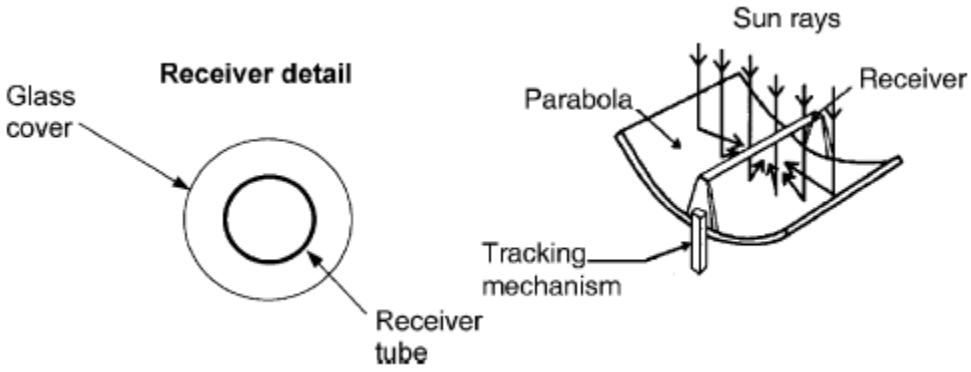

Fig.3 Parabolic Trough Collector (Kalogirou S.A., 2004)

These collectors are able to focus the solar radiation having concentration ratio 40 or more, depends upon the size of the parabolic trough. The central temperature may be from 350-400 °C. These collectors consists of group of parabolic shaped mirrors and each one has capacity to reflect the solar radiation which is equivalent to its regular axis to its ordinary central line. At this central line, a receiver tube which is painted black and wrap it with glass tube to minimize heat losses is located to capture accumulated heat. This type of collector can be altered in both directions i.e. in east to west side by trailing the sun to north-south direction, or north to south side by trailing the sun to east-west direction.

Technology based on the parabolic trench is primarily matured one. This technology is presently used by many equipped large level CSP ranches all over the world. Solar Electric Generating System (SEGS) is a compilation of entirely equipped parabolic trough collector structure situated in the California wasteland having the whole capability of 354 MW. Solar Electric Generating

System is currently the biggest parabolic trough collector based power plant all over the globe. The second PTC based power plant having the capability of 280 MW is constructed in Arizona which is planned to be equipped in 2011. Parabolic trough collector efficiently generate heat having temperature assortment as of 50-400 ^{0}C. This temperatures assortment is usually large and sufficient for industrial roasting methods and appliances, the huge part of this run underneath 300°C.

The mature area of PTC gives well-organized, comparatively cheap power manufacturing plan. A lot of improvement in the design of receiver and the design of reflector have been done in the past to improve the performance of the system and to diminishing the losses. The modeling of the compilation of heat and of the transmission methods have been done and analyzed continually to obtain maximum power output all over the day. The Parabolic trough collector system also offers simple storage idea and also, incorporation with the conventional and unconventional energy resources.

(2) Heliostat Field Collectors

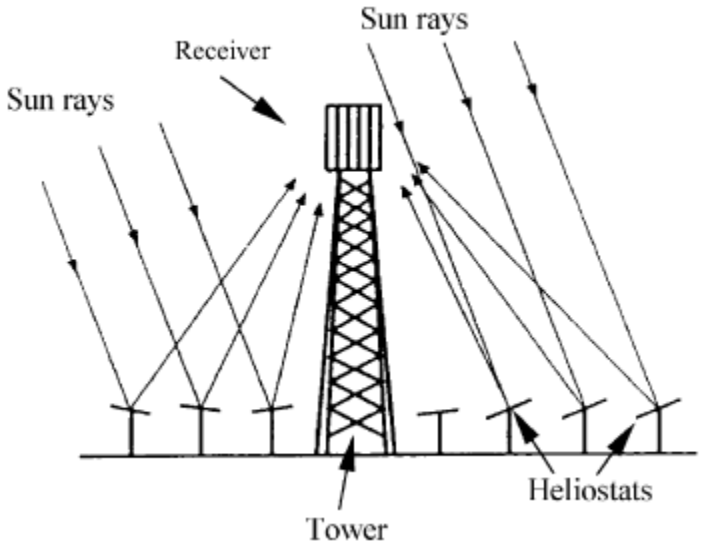

Fig.4 Heliostat Field Collector (Kalogirou S.A., 2004)

(3) Linear Fresnel Collectors

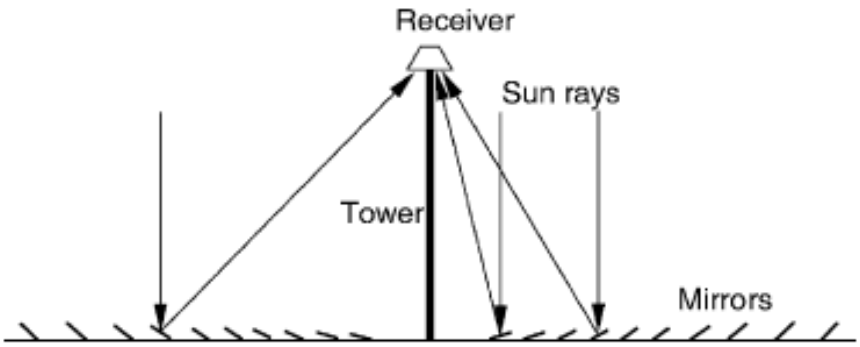

Fig.5 Linear Fresnel Reflector (Kalogirou S.A., 2004)

(4) Parabolic Dish Collectors

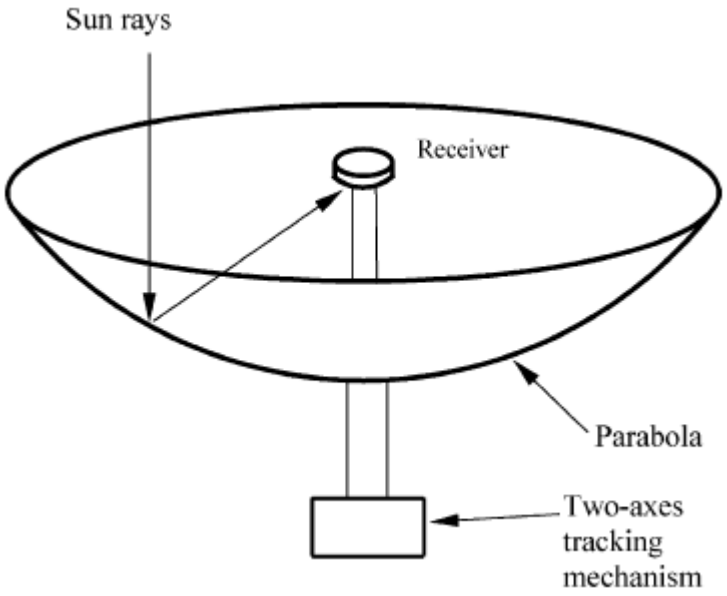

Fig.6 Parabolic Dish Collector (Kalogirou S.A., 2004)

1.4 SOLAR (STELLAR) ENERGY APPLICATIONS

Various solar energy applications are:

- Stellar locomotives for irrigate pumping.
- Stellar cookers.
- Stellar purification in small areas.
- Warming and chilling of urbanized building.

- Stellar irrigate heating.
- Foodstuff refrigeration.
- Stellar heaters.
- Stellar ventilation of farming and mammal products.
- Saline fabrication by fading of ocean irrigate.
- Stellar electrical power production.
- Stellar photovoltaic cells etc.

1.5 NANOFLUIDS

Fine nanomaterials having average size less than 100 nm poised with the conventional base fluid like heat transfer oil, water, molten salt, ethylene glycol etc. is known as nanofluid. Firstly, in 1995, this nanofluid term was invented by Choi. He represented the innovative grade nanotechnology which is based on the working fluids having excellent thermophysical properties as compared to the conventional base fluids. Due to this, it can be effectively used for cooling purposes. Pump is required for circulating the coolant in almost all the cooling devices. Proper pump choice be a big problem while selecting the coolant. The choice of pump is depend upon the viscosity of the nanofluid. Also, the viscosity of the nanofluid strongly affects the heat transfer coefficient. So, the objective of nanotechnology is to attain the excellent thermophysical properties at minimum concentration by homogeneous diffusion and the steady suspension of nanomaterials (Das et al. 2008).

The various nanomaterials employed for preparing nanofluids are, such as diamond, aluminum, silver, gold, carbon nanotubes, copper oxide, aluminum oxide etc.

Nanomaterials can be prepared mainly by two techniques. Out of them, one is physical technique and the other is chemical technique. Physical technique contains inert gas condensation and mechanical grinding while the Chemical technique contains spray pyrolysis, chemical vapour deposition, thermal spray, chemical precipitation and micro emulsions etc.

1.6 NANOFLUIDS APPLICATIONS

Various applications of nanofluids are (Wong et al. 2009):

- In industrial chilling applications for saving huge energy and secretion reduction.
- In nuclear appliances to enhance various irrigate-chilled nuclear system performance.
- Using as a smart fluid in laptops and cellphones for controlling heat flow.

- Removal of geothermal power and another energy resources by chilling the equipment and machinery working in high temperature and high friction environment.
- In automotive applications due to its better heat transfer properties.
- In computers for cooling microchips.
- In microscale fluidic applications by changing the wetting features of surface.
- In biomedical applications like nanodrug delivery, cancer theraupetics, cryopreservation, nanocryosurgery.
- In lubrication, soil remediation, oil recovery, detergency processes etc.

1.7 POTENTIAL FEATURES OF NANOFLUIDS

Potential features of nanofluids are:

I. Increase in thermal conductivity past exemption and to a large extent than hypothetical estimation.

II. Superior lubrication.

III. Superior stability than another colloids.

IV. Decreasing corrosion and obstruction in micro channels.

V. Decreasing pumping power

VI. Decreasing friction coefficient.

VII. Superior heat transfer capability.

1.8 USE OF NANOFLUID IN THE RECEIVER

Nanofluids are employed for enhancing the performance of the solar thermal systems. The geometric and experimental analysis of solar thermal collectors demonstrated that in several instances, the efficiency of the solar thermal system enhances tremendously with nanofluids. It is examined that if the nanofluid is used with high volumetric concentration, then it is always not the preeminent way. Therefore, to obtain the highest volumetric concentration, nanofluids should be examined with several volumetric concentration. Theoretical analysis provides discrete results of the influence of nanoparticles size on the system efficiency. So, it is important to do the experimental analysis on this. Several additional factors like addition of surfactant in nanofluid and the proper choice of pH value of nanofluid are helpful in system efficiency. According to economical and ecological point of view, utilization of nanofluid in collectors helps to reduce the CO_2 emissions and yearly electricity and fuel economy. In case of numerical analysis of solar devices, it is superior to employ the two phase mixture models and the temperature dependent

models for nanofluids for more accurate prophecy of solar system performance. But the main difficulties to utilize the nanofluids in solar devices are high expense of nanofluids, volatility and agglomeration hindrance, enhanced pumping power and corrosion and erosion problems etc.

1.9 THERMAL RESISTANCE NETWORK

Thermal resistance network shows the heat transfer process for a volumetric based collector and surface based collector. According to the model, to convert sunbeams into valuable heat, a volumetric receiver provides lesser resistance while keeping all other things being identical.

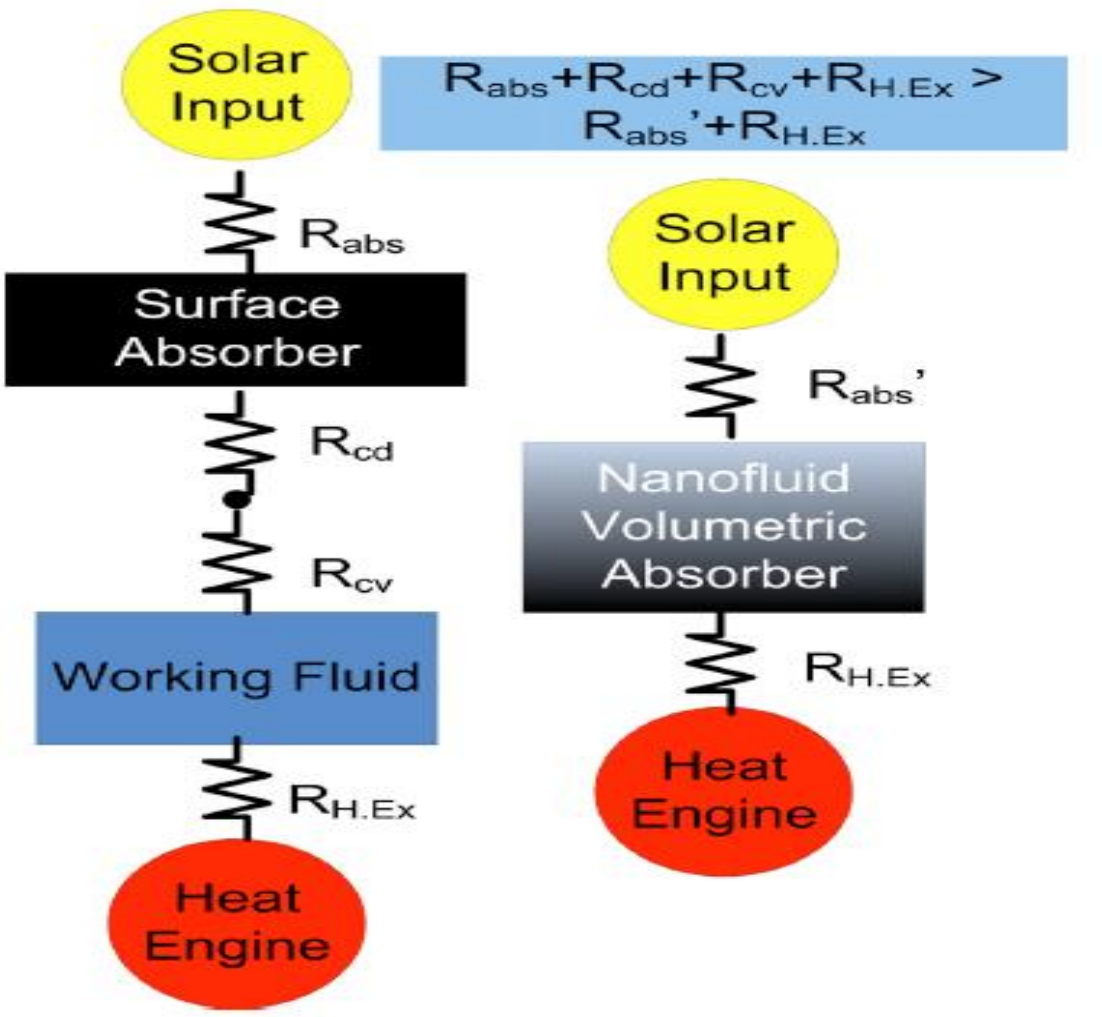

Fig.7 Thermal Resistance Network (Taylor et al. 2011)

Conventional receiver and nanofluid receiver are different from each other. Some interesting points are:

1. Translucent glazing is needed to the nanofluid receiver for holding high pressure and high temperature fluid.
2. The nanofluid can avoid certain heat loss and temperature drop by avoiding heat transfer through convection and conduction.
3. Extra maintenance is needed to the nanofluid receiver as compared to conventional receiver.
4. An identical solar collector requires extra tight proscribed optics, receiver geometry and flow states.
5. Optical and thermal properties are different.
6. Receiver efficiency also different.
7. High capital costs in case of nanofluid receiver than conventional receiver.

1.10 ADVANTAGES OF CONCENTRATING COLLECTORS

The main advantages of concentrator systems over flat-plate type collectors are:

1. High insolation strength because concentrating collectors have less absorber area as compared to flat plate type collectors for identical astral radiation collection.
2. Concentrating collectors are simple in design and material required for reflecting surfaces is in lesser amount as compared to flat plate type collectors.
3. The expenditure / area of astral accumulating surface for concentrating collectors is low as compared to flat plate type collectors.
4. For the identical astral radiation accumulating surface, liquid flow in concentrating collectors is capable of achieving high temperature as compared to flat plate type collector because it losses less heat to the environment and also, the lagging to the absorber is highly intense.
5. To defend the absorber, small or zero unfreeze is needed to concentrated collectors but in flat plate type collectors unfreeze is needed.
6. The quantity of storage of heat / volume is high in concentrating collectors because the working fluid achieves high temperature.
7. Choosy surface handling and vacuity lagging to decrease the heat sufferers and to enhance the collector performance are efficiently possible because of the less absorber area / astral radiation accumulating area.

8. Concentrating systems may also be employed for electricity production when not employed neither chilling purpose nor cooling purpose.
9. Total effective working period / year for concentrating system is large as compared to flat plate collector based system and the primary installation expense of the concentrated system is recovered by conserving the energy in the small time.
10. Heat collection expenses for concentrated collectors are low as compared to flat plate type collectors.
11. For astral chilling and heating purposes, it is feasible to obtain high efficiency because the flowing liquid in concentrated collectors achieves high temperature in the cooling sequence and less expenses for conditioning of air in concentrated system.

1.11 DISADVANTAGES OF CONCENTRATING COLLECTORS

1. Merely beam element is accumulated in concentrated collectors because it is unable to collect diffuse element and is mislaid.
2. Primary cost is high.
3. Expensive orienting structure employed to trace the sun.
4. Extra continuance particular is required to protect the mirrors from dust, climate, corrosion etc.
5. Flux in concentrating collector is not uniform.
6. Extra ocular sufferers like reflectance sufferers and the interrupt sufferers, thus establish extra aspects for energy stability.

CHAPTER 2
LITERATURE REVIEW

This chapter contains the method of preparation of nanofluids, characterization of nanofluids and an extensive literature review of several research papers on nanofluids.

2.1 NANOFLUIDS PREPARATION TECHNIQUES

There are mainly two techniques used to produce nanofluids:

1. Single step method.
2. Two step method.

Single Step Method

Akoh et al. (1978) developed one step physical vapour condensation method. It is used to reduce the agglomeration of nanoparticles. This method combines the synthesis of nanofluids with the preparation of nanoparticles in which nanoparticles are prepared directly by either liquid chemical method or by using physical vapour deposition technique. In this method, nanoparticles simultaneously making and dispersing in the base fluid. In this method, in order to decrease the agglomeration of nanoparticles and increase the stability, the processes of drying, storage transportation and dispersion of nanoparticles are avoided. One step physical method is unable to produce nanoparticles in large scale (Yu et al. 2011). For this, one step chemical method is used (Zhu et al. 2004) in which by chemical reaction of two reactants produces well dispersed nanofluid.

Two Step Method

It is mostly used technique for preparing the nanofluids. In this method, nanoparticles used are first produced as dry powder by using physical or chemical method. After that, in the second step, dry nanoparticles are dispersed into base fluid like water, ethylene glycol etc. using ultrasonic agitation, high shear mixing or by using ball milling or magnetic force agitation etc. C.G. Granqvist, and R.A. Buhrman (1976) found the two- step process. Two step method is widely used because it is most economical method and due to this nanofluids can be produced in large scale because According to Romano et al. (1997), nanopowder synthesis technique have been already set up to industrial production levels. Nanofluids have the problem of aggregation because of its high surface area and surface activity. Surfactants or other surface stable additives

can be used to increase the stability of nanoparticles in the base fluid. In addition to mechanical mixing, ultra-sonic mixers can be used to break up agglomerates and give more uniform dispersions.

2.2 CHARACTERIZATION TECHNIQUES

Nanoparticles Characterization is required for better understanding and control of nanoparticles synthesis and application. Commonly used techniques for the characterization of nanoparticles are as follows:

(1) X- Ray Diffraction (XRD)

XRD is a fast logical method which is mostly used in phase recognition of a crystalline matter. The analyzed matter which is delicately crushed, homogenized and then regular size structure is determined. XRD is based on the positive intervention of monochromatic X-rays and a crystalline taster. X- rays are conceded to this crystalline taster and then the diffracted rays are detected, processed and counted. Crystalline taster is scanned during a variety of 2θ angles, all feasible diffraction information can be achieved because of the unsystematic direction of the crushed matter of the pattern. By the exchange of the diffraction crests to d-spacing, it permits the mineral detection because of single d-spacing of each mineral. Usually, this can be attained by the judgement of d-spacing with a normal orientation prototype.

(2) Transmission Electron Microscopy (TEM)

It is employed to illustrating the microstructure of matter with peak spatial perseverance. Information can be gained for nanoparticles about the gemstone stages, morphology, gemstone configuration and imperfections, constitution and fascinating microstructure by the mixture of electron diffraction, electro-optical imaging and tiny probe abilities.

TEM utilizes a high power electron rays which is spreaded in a extremely lean sample to picture and examine the microstructure of elements with infinitesimal level perseverance. The electrons are concentrated by using electromagnetic lenses and the resulting image can be detected on a luminous display, or can be evidenced on film or by using digital camera. The whole assembly, including the sample then put in peak vacuum to prevent absorption and spreading of electrons from air. According to Shah et al. 2010, normally the pressure preserved in the chamber is in between 10^{-4} to 10^{-8} kPa .

(3) Scattering Electron Microscopy (SEM)

It is employed to the nanoparticles for investigation of the chemical composition and microstructure morphology. According to Shah et al. 2010, for producing diversity of signals at sturdy specimens surface, SEM employs a concentrated rays of excessive power electrons. The signals which are obtained from electron-sample contacts gives the information of the sample involving chemical composition, exterior morphology, gemstone arrangement and orientation of objects constructing the sample. SEM generates an electronic plot of the sample which is presented on the cathode beam tube. It is also helpful to operate the investigation of the preferred point positions on the taster. This tactic is useful in semi-quantitatively or qualitatively establish the chemical composition.

2.3 EXPERIMENTAL INVESTIGATIONS

Tyagi et al. (2009) investigated the performance of non-concentrating and nanofluid based direct absorption solar collector (DASC) theoretically by using different parameters. After that, its performance is compared with flat- plate collector where nanofluid is used as a working fluid which is the mixture of water with aluminum nanoparticles. The model of heat transfer in two dimension was utilized and after that, it was numerically solved. In this model, the incidence of sunlight was directly on the flowing nanofluid having thin film. The heat transport equation was used for the evaluation of intensity distribution within the nanofluid. The energy balance equation was used for obtaining the temperature profile within the nanofluid. Through this, It was found that incident solar radiation absorption is high in case of nanoparticles by nine times compared to pure water. The results showed that the efficiency of DAC is 10% higher than flat-plate collector. The various parameters showed that collector efficiency increases with particle volume fraction, glass cover transmissivity and collector height but the particle size and the collector length had unsignificant effect on the collector efficiency as shown in fig. below.

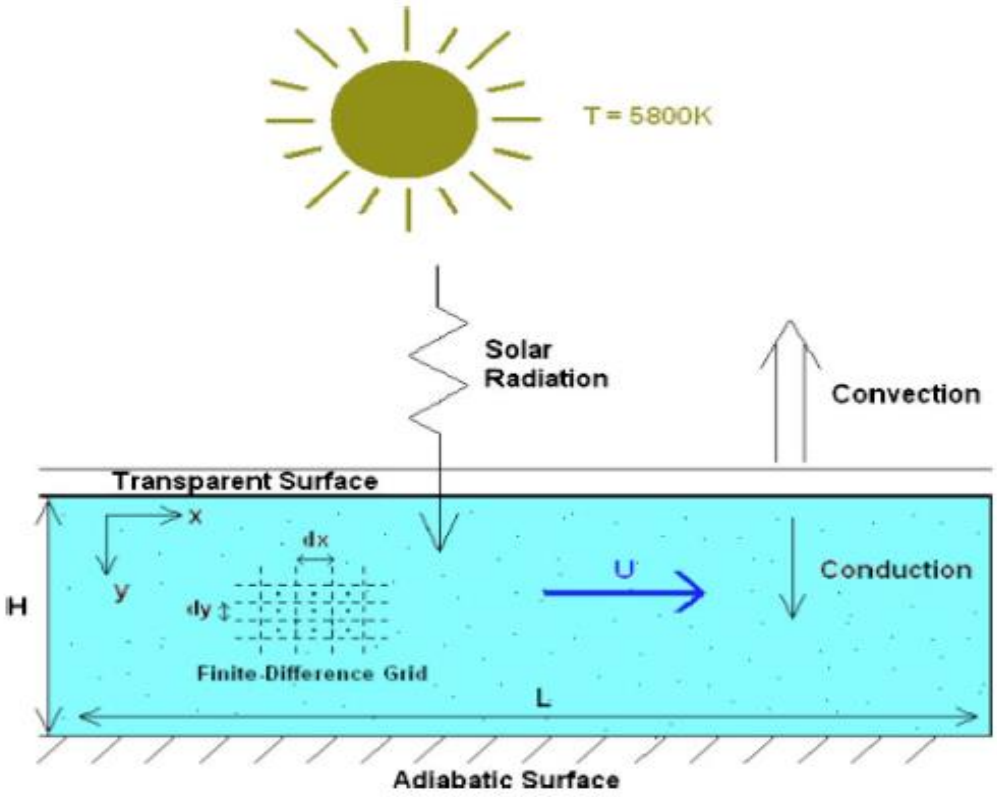

Fig.8 Schematic of the nanofluid-based direct absorption solar collector (Tyagi et al. 2009)

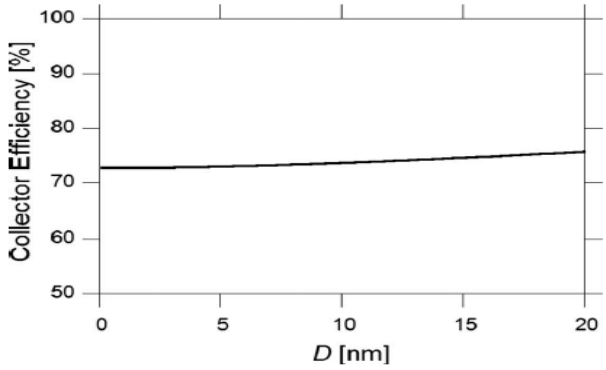

Fig.9 Effect of nanoparticle size on collector having volume fraction 0.8% (Tyagi et al. 2009)

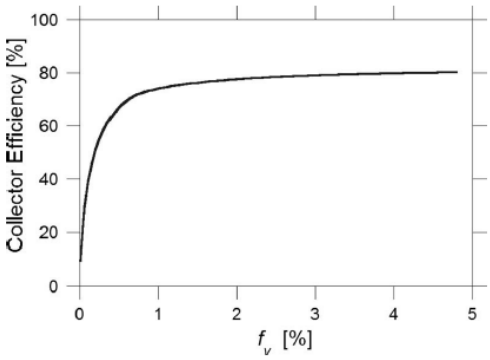

Fig.10. Effect of particle volume fraction on collector efficiency having D = 5nm (Tyagi et al. 2009)

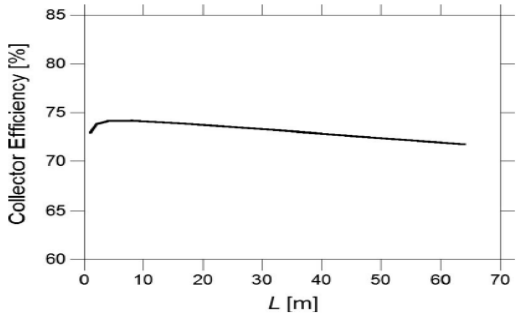

Fig.11 Effect of collector length on collector efficiency (Tyagi et al. 2009)

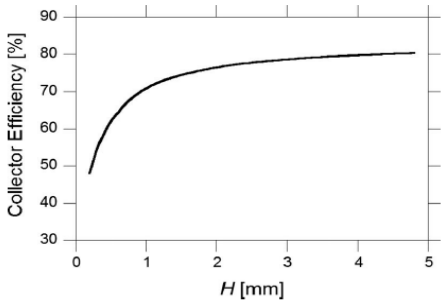

Fig.12 Effect of collector height on collector efficiency (Tyagi et al. 2009)

Taylor et al. (2011) investigated the performance of concentrated solar thermal power system taking nanofluid as a working fluid. After that, its performance was compared with traditional solar thermal power system where base fluid used was oil. Some conceptual designs were also presented of the traditional concentrated solar collector and nanofluid based concentrated solar collector. From the results, it was found that efficiency can increased upto 10% using nanofluid as a working fluid. For this, concentration ratio was in between 100-1000. It was also found that using graphite as nanofluid having volume concentration upto 0.001% were better for small scale power plants. It was also found that if nanofluid based receiver was used in small scale concentrated solar thermal power plant, then it generated more than $ 3.5 million per year. At last, it also compared electricity generation per year for 10 MW traditional and nanofluid based concentrated solar power plant and estimated yearly revenue for commercial level plant having capacity 100 MW.

He et al. (2011) examined experimentally the light to heat conversion attributes of carbon nanotube-water based and TiO_2-water based nanofluids in the vacuity tube astral collector underneath sunlit & overcast climate. From the results, it was found that carbon nanotube-water based nanofluid demonstrated superior light to heat conversion attributes as compared to TiO_2-water based nanofluid having 0.5% weight fraction. Also, the temperature of carbon nanotube-water based nanofluid was larger than TiO_2-water based nanofluid due to superior light to heat conversion attributes of carbon nanotube-water based nanofluid. This denoted that the stability of carbon nanotube-water based nanofluid was more than TiO_2-water based nanofluid when used in the vacuity tube astral collector.

Yousefi et al. (2012) examined experimentally the performance of flat plate solar collector where working fluid was Al_2O_3-water based nanofluid. Then, its performance was compared

with traditional flat plate solar collector where water was used as working fluid. Parameters used were mass flow rate, volumetric concentration of nanomaterials in water, use of surfactant and without surfactant. ASHARE standard was taken for calculating the thermal performance of flat plate solar collector. From the results, it was found that efficiency of flat plate solar collector increased by 28.3% by using 0.2 wt.% Al_2O_3 in water for making nanofluid as compared to water. It was also found that addition of surfactant increased the efficiency upto 15.63%. Also, If $(T_i - T_a / G_T) > 0.0015$, then efficiency of flat plate solar collector increased by increasing mass flow rate.

Yousefi et al. (2012) used similar set up for examined the performance of flat plate solar collector using MWCNT-water based nanofluid as working fluid. Parameters used were mass flow rate, volumetric concentration of nanomaterials in water, use of surfactant and without surfactant. Different mass flow rate were taken as 0.0167 Kg/s, 0.033 Kg/s and 0.05 Kg/s. Nanoparticles concentration taken were 0.2 wt.% and 0.4 wt.%. From the results, it was found that nanofluid with surfactant increased the efficiency of flat plate solar collector as compared to nanofluid without surfactant. It was also found that nanofluid at 0.2 wt.% without surfactant decreased the efficiency of flat plate solar collector as compared to 0.4 wt.% nanofluid without surfactant. At last, it was found that the effect of mass flow rate on the efficiency of flat plate solar collector depended on reduced temperature parameter i.e. $(T_i - T_a / G_T)$. ASHARE standard was used for calculating the performance of flat plate solar collector.

Taylor et al. (2011) used experimental and modeling approach to determined the nanofluid's optical properties. For this, they compared the experimental and modeling results to measure the extinction coefficient vs wavelength having range of 0.25-2.5 μm. Nanofluid extinction coefficient was found by adding the extinction coefficient of nanomaterials and base fluid for approximation. It was also found by the comparison that approximation for graphite-water based nanofluid and aluminium-water based nanofluid showed good response but other metals and base fluid i.e. oil showed less well response. It was also indicated that mostly absorption was due to smaller wavelength of nanoparticles and longer wavelength of base fluid.

Khullar et al. (2012) theoretically examined the performance of concentrated parabolic solar collector using Al-therminol VP-1 based nanofluid. Finite difference technique was used for this. Then, its performance was compared with experimental result of traditional concentrated parabolic solar collector. It was found that nanofluid based concentrated parabolic solar collector

was 5-10% more efficient as compared to the conventional one in terms of efficiency having same external condition for both. Various parameters angle of incidence, solar intensity and convective heat transfer coefficient were also studied to find its effect on the performance of solar collector as shown below.

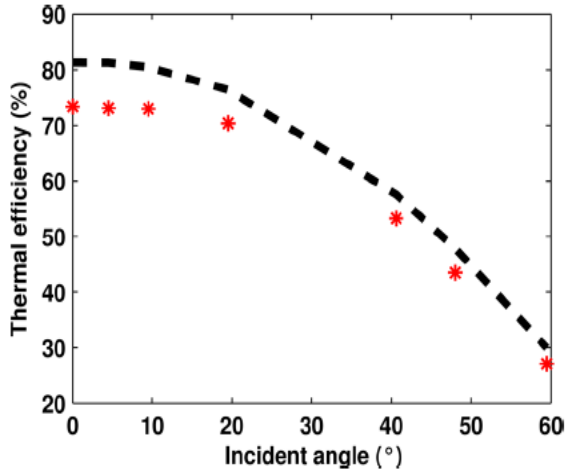

Fig.13 Thermal efficiency as a function of incident angle (Khullar et al. 2012)

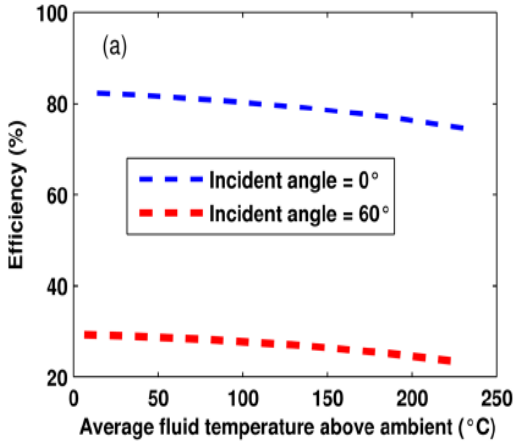

Fig.14 Effect of solar incident angle on thermal efficiency (Khullar et al. 2012)

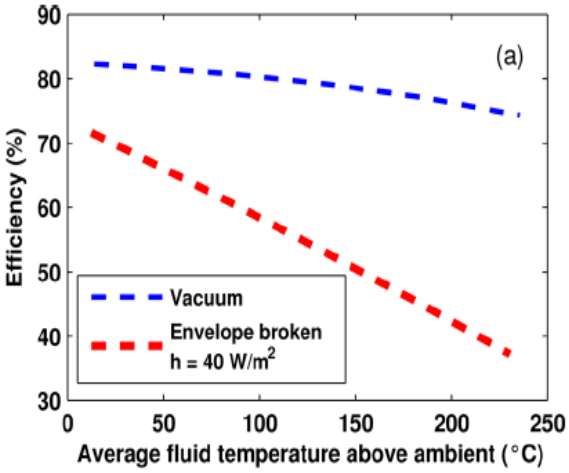

Fig.15 Effect of convective heat transfer coefficient on thermal efficiency (Khullar et al. 2012)

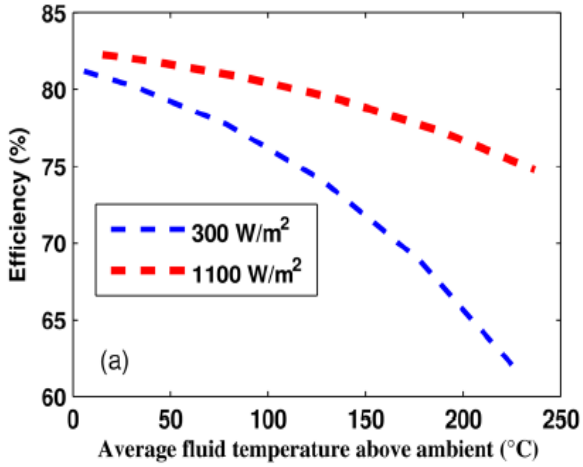

Fig.16 Effect of solar irradiance on thermal efficiency (Khullar et al. 2012)

Otanicar et al. (2010) experimentally examined the influence of nanofluids on direct absorption solar collector and compared it with the help of numerical modeling of direct absorption solar collector. The nanofluids used were silver, carbon nanotube and graphite based. The parameters used were different nanoparticle size and different volumetric concentration of nanoparticles. It

was found that 5% improvement in efficiency can be obtained using nanofluid as working fluid in solar collector of direct absorption type. It was also found that efficiency increased by increasing the volumetric concentration of nanoparticles. At last, it was also showed the increament in the efficiency when the size of silver nanoparticle reduced from 40 to 20 nm because optical properties depended on nanoparticle size.

Saidur et al. (2012) examined the influence of nanofluid on direct solar collector. Al_2O_3-water based nanofluid was used for this. The extinction coefficient of nanofluid was evaluated at different nanomaterials size and concentration. It was found that the maximum extinction coefficient of aluminium nanoparticles was at 0.3μm wavelength and after that it decreased sharply. The extinction coefficient was found to be directly related to the nanopaticles concentration. It was also found that extinction coefficient was not depend on nanoparticle size because it was directly related to the optical properties of nanofluid and the size of nanoparticles did not showed significant effect on optical properties.

Risi et al. (2013) examined the effect of gas based nanofluid on translucent parabolic trough collector. For this, mathematical model was used and also genetic algorithm was proposed. The purpose of this was to improve and optimized the performance of translucent parabolic trough collector. Nanofluid used was the mixture of 0.25% CuO and 0.05% Ni. Soalr to thermal efficiency was plotted with respect to different nanoparticles concentrations, mass flow rates and solar radiation as shown below. From the simulation results, it was found that solar to thermal efficiency was 62.5% at the outlet temperature of nanofluid which was 650^0 C having volume fraction of 0.3%.

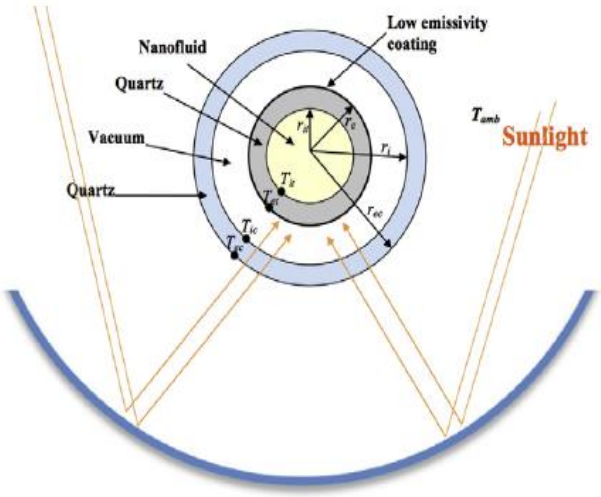

Fig.17 Schematic of Solar PTC (Risi et al. 2013)

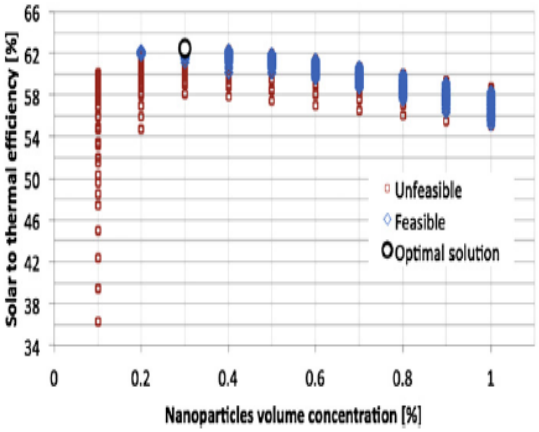

Fig.18 Solar to thermal efficiency as a function of particle concentration (Risi et al. 2013)

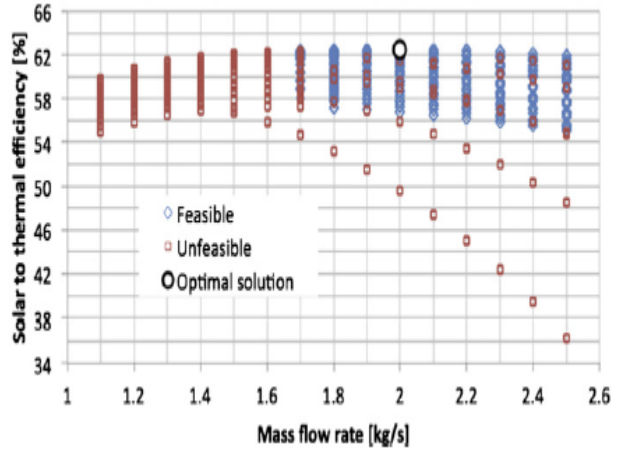

Fig.19 Solar to thermal efficiency as a function of mass flow rate (Risi et al. 2013)

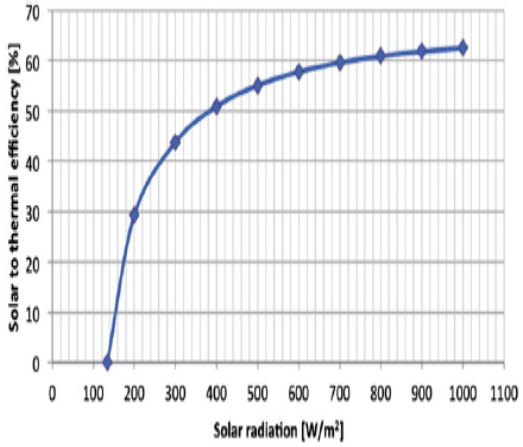

Fig.20Solar to thermal efficiency as a function of solar radiation (Risi et al. 2013)

Khullar et al. (2012) investigated the environmental impact of concentrated solar water heating system where nanofluid was used as working fluid and compared it with flat plate solar water heating system. It was found that concentrated solar water heating system got high output temperature. It was also found that greenhouse gas emission of about 2.2 * 10^3 Kg of CO_2/household/year can be reduced through the use of nanofluid based concentrated solar water

heating system. It was also found that the fuel saving of about 206 Kg/household/year and electricity saving of about 1716 kWh/household/year possible through the use of nanofluid based concentrated solar water heating system.

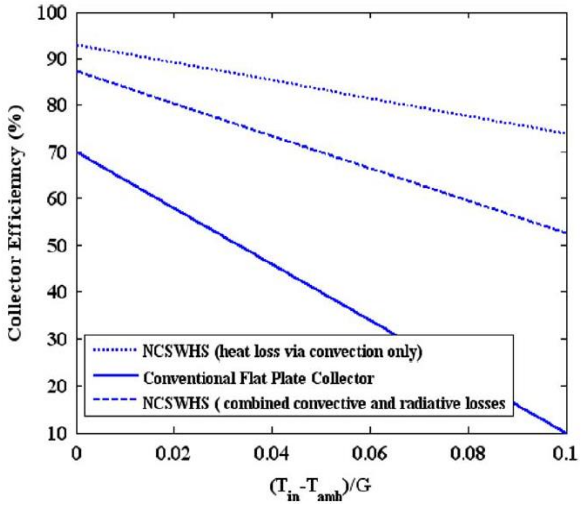

Fig.21 Collector efficiency as a function of normalized fluid inlet temperature (Khullar et al. 2012)

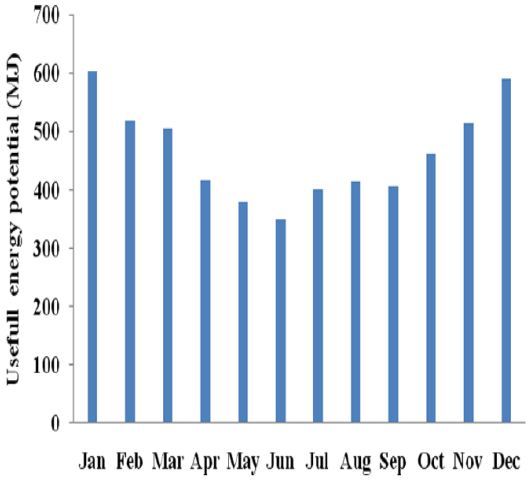

Fig.22 Useful energy potential per month per household (Khullar et al. 2012)

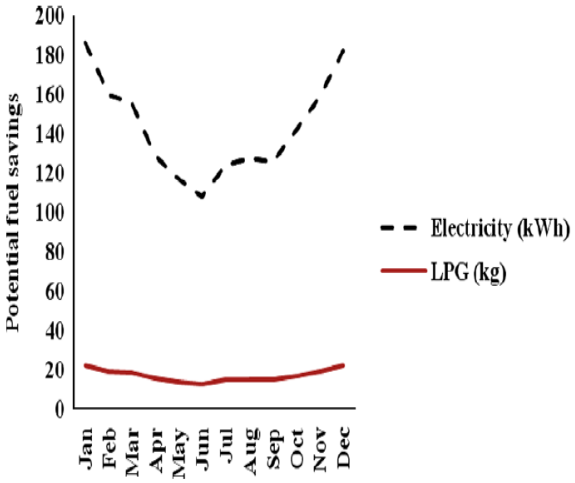

Fig.23 Potential fuel saving per month (Khullar et al. 2012)

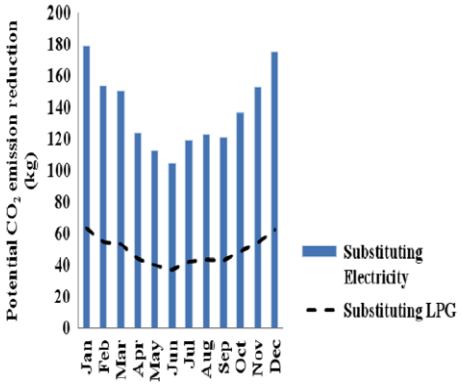

Fig.24 Potential CO_2 emmision reduction per year (Khullar et al. 2012)

Javadi et al. (2013) examined analytically the consequences of Al_2O_3-liquid nitrogen, TiO_2-liquid nitrogen and SiO_2-liquid nitrogen based nanofluids on the plate fin heat exchanger. After that, its results were compared with liquid nitrogen results which was used as a base fluid. The effect of nanofluids on the entropy generation & the pressure drop were also examined. From the results, It was found that the thermal conductivity, heat transfer rate and the heat transfer

coefficient of the base fluid were enhanced by mixing the nanomaterials in it. The thermophysical properties of Al_2O_3 and TiO_2 were higher as compared to SiO_2. The overall heat transfer coefficient found to be maximum in Al_2O_3-liquid nitrogen based nanofluid, that was 308.69 $W/m^2.K$ at 0.2% nanoparticle volumetric concentration. Associated heat transfer rate was 30% more in comparison to SiO_2-liquid nitrogen based nanofluid. But the pressure drop per length of SiO_2 was 50% lower than Al_2O_3 and TiO_2.

Kalogirou et al. (2004) illustrated the review of the different astral collectors and their applications in various fields. Firstly, the psychiatry of ecological drawback associated to the utilization of non renewable energy sources were illustrated and then the advantages from the use of non conventional energy sources were delineated. A prior foreword of astral energy was stabbed and then explained different astral collectors consisting flat plate astral collector, parabolic astral collector, parabolic dish astral collector, compound parabolic astral collector, Fresnel lens astral collector, evacuated tube astral collector and heliostat field astral collector. Then, thermodynamic, optical and thermal psychiatry of the astral collectors and delineation of the processes utilized to estimate their performance. After that, some appliances of different astral collectors were offered like in astral irrigate heating devices, astral space roasting and chilling, astral refrigeration devices, industrial process heating, astral desalination devices, astral thermal power devices, astral furnaces and in astral chemistry purposes.

Mahian et al. (2013) investigated different applications of nanofluids in solar thermal system like in solar water heaters, different solar collectors, for thermal energy storage, in solar stills and in solar cells etc. It also mentioned different solar system in which work can be possible in future using different nanofluids. The other solar devices like solar cooling devices, solar refrigerating device or different solar system combination in which nanofluids can be used in future. It also mentioned the different types of problems regarding the use of nanofluids like agglomeration, high nanofluid cost, stability of nanoparticles, corrosion and erosion of thermal system and pumping problems etc. It also suggested the use of nanofluids having different volumetric concentration for finding the optimum volumetric concentration of nanoparticles, work on particle size and surfactant used for providing stability to nanofluids.

Reddy et al. (2012) investigated experimentally the strictures of parabolic solar collector in frost circumstances and to attain optimal process strictures by using grey relational analysis. The experimentation was designed by Taguchi's L_9 orthogonal array. Through this investigation,

parabolic solar collector strictures like absorber tube location, reflector material, absorber tube angles and absorber material were optimized by taken into account the multiple responses like optical efficiency, temperature, thermal efficiency and enthalpy. A grey relational grade was achieved from grey relational analysis. Using grey relational grade, high level strictures were recognized. At last, conformation analysis was carried out to confirm the experimental result. From the results, it was found that vacuity glass tube when used as absorber provided excellent result.

Gunge et al. (2012) constructed the parabolic solar collector which has efficient irrigate heating in comparison with flat plate solar collector. Step tube receiver was used for this. Thermal psychiatry process of the parabolic solar collector model begins with the assortment of several strictures like receiver diameter and aperture area to get the arithmetical concentration. The experiment was based on changeable concentration ratio by changing the diameter of step tube receiver. It was found that the reduction in receiver diameter reduced the losses from receiver. It also proposed the parabolic profile and the step tube receiver for best recital. Parabolic solar collector having focal length 0.15 m, aperture area 0.6 m and length 0.9 m was built.The step tube of copper havig diameter 1.2 cm, 1.4 cm, 1.6 cm was located on the central axis which was utilized as receiver. It was also found that the parabolic solar collector having step tube of copper as receiver obtained 80^0 C temperature which was higher than the temperature obtained from the uniform tube based receiver.

Maddah et al. (2013) experimentally examined the influence of Al_2O_3 and Ag nanomaterials on electrical conductivity, thermal conductivity and viscosity. The average diameters of Al_2O_3 and Ag nanomaterials were taken as 40nm and 20 nm. The different volumetric concentrations were taken as 0.25%, 0.5%, 1%, 2%, 3%, 4%, and 5% at 15°C temperature. The nanofluids were primed by producing firstly Ag and Al_2O_3 nanomaterials using microwave-assisted chemical precipitation method and after that, these were suspended in distilled water with the help of sonicator. From the results, it was found that the thermal conductivity and viscosity of nanofluids enhanced when enhanced the volumetric concentration of nanomaterials and the electrical conductivity of nanofluids enhanced linearly when enhanced the volumetric concentration of the Ag and Al_2O_3 nanomaterials. It was also found that at the high volumetric concentration of nanofluids, viscosity was also high and the electrical conductivity of silver and alumina based nanofluids were much higher than the base fluid.

Natarajan et al. (2009) examined the influence of nanofluids in astral irrigate heater. The objective of the investigation was to distinguished the heat transfer characteristics of the nanofluids with traditional one. Multiwall carbon nanotubes-water based nanofluid having volume concentration 0.2-1.2% was used. For preparing nanofluid, sodium dodecyl sulphate (SDS) was added as surfactant to enhanced the stability. Transient hot-wire method was employed for determining thermal conductivity. From the results, it was found that the thermal conductivity of MWCNT-water based nanofluid enhanced by increasing the volumetric concentration of MWCNTs. It was increased up to 41% at the volumetric concentration of 1. Also, the values calculated from Hamilton–Crosser model was compared with experimental values of MWCNT in base fluid and it was concluded that thermal conductivities measured experimentally were higher than the values obtained from Hamilton–Crosser model. Also, found that if nanofluids were employed for heating purposes, then it enhanced the performance of the conventional astral irrigate heater.

Chougule et al. (2012) examined the effect of nanofluid in astral irrigate heater employing astral tracker device. For that, two similar flat plate collectors of identical dimensions using roast pipes were constructed. In one, pure water was used and in second, carbon nanotube-water based nanofluid was used. The diameter of carbon nanotube nanomaterials were10-12 nm and length 0.1-10 μ and volumetric concentration of 0.15% in water. Functionalization process was used for dispersing the nanomaterials in water. These systems were firstly examined at Indian normal tip angle of 31.5°and greatest recital angle 50°. At the identical angles these systems were examined by employing the astral tracker device. From the results, it was found that both systems attained high instantaneous efficiency without and with the help of tracker at the 50°. The nanofluid based collectors have superior recital in all situations. For both water and nanofluid, astral tracker device was useful and the variation in their instantaneous efficiencies were firstly high, then low, then almost same and then again high. Enhanced average efficiency was 11% for nanofluid and 12% for water at 31.5° and 4% for nanofluid and 7% for water at 50° utilizing astral tracker device.

Tiwari et al. (2013) investigated the effect of Al_2O_3-H_2O based nanofluid on the efficiency of flate plate solar collector. Parameters taken were mass flow rate 0.5 Lit/min, 1 Lit/min, 1.5 Lit/min, 2 Lit/min and volume concentration of nanoparticles 0.5%, 1%, 1.5% and 2% respectively. From the results, it was found that efficiency of flat plate solar collector using

nanofluid as a working fluid having nanoparticles volumetric concentration of 1.5% was 31.64% more as compared to water. Also, it was concluded that at this concentration, 31% kgCO_2/kWh more saving as compared to water used as a working fluid.

Sani et al. (2010) examined the thermal and ocular properties of single wall carbon nanohorns-water based nanofluid with respect to the nanomaterials concentration. The nanofluid features were estimated for using it as sunbeams soak up fluid in different solar systems. It was examined that nanofluid has high thermal conductivity as compared to untainted water. From the spectral transmission measurement, it was found that single wall carbon nanohorns were very helpful for enriched the photonic possessions of the base fluid, considerably raised the luminosity extermination echelon yet at extremely small concentrations. At inspected concentrations thermal conductivity was enhanced upto 10%. The awareness about the thermal and ocular properties of nanofluid gives helpful information to sunbeams collector maker for the device dimensioning and the improvement in roast transfer efficacy. At last, it was found that single wall carbon nanohorns-water based nanofluid in solar systems were very helpful for improving efficiency and for more efficient and incorporated designs.

Chaji et al. (2013) experimentally investigated the performance of flat plate solar collector using TiO_2-water based nanofluid. Nanofluid was prepared without using any surfactant. Mass flow rate taken were 36 lit/m^2.hr, 72 lit/m^2.hr and 108 lit/m^2.hr. The volumetric concentration of nanoparticle taken were 0.1%, 0.2% and 0.3%. After that, its results were compared with water. From the results, it was found that enhancing the mass flow rates of water interior to the flat plate solar collector enhanced the index of total collector efficiency area under the curves up to 15.7%. It was also found that by mixing the nanoparticles in water enhanced the index of total collector efficiency area under the curve upto 2.6% to 7% relative to base fluid at the same flow rate.

Khullar et al. (2010) investigated the influence of Al-water based nanofluid on concentrated parabolic solar collectors by modeling its roast transfer and flow characteristics mathematically. The collector was modeled in two dimensions and was in steady state and then finite difference technique was employed to solve the equations numerically. The 2-dimensional temperature field, mean outlet temperatures, thermal and ocular efficiencies was quantitatively calculated and then compared the performance of nanofluid based parabolic solar collectors with the conventional one. Also, the influence of different strictures like fluid velocity, receiver length,

concentration ratio, volume fraction of nanoparticles was studied. The entire investigation discovered that the solar collectors based on nanofluids were more efficient as compared to the conventional one under identical working environment.

Yousefi et al. (2012) examined experimentally the influence of pH variation of multi wall carbon nanotube-water based nanofluid on the performance of flat plate solar collector. For this, nanoparticles concentration was taken as 0.2 wt.% and the mass flow rate was taken as 0.0333 kg/s. The different pH values were taken as 3.5, 6.5 and 9.5. Triton X-100 was used as a surfactant for providing the stability to the nanofluid. The ASHARE standard was employed for calculating the thermal efficiency of flat plate solar collector. From the results, it was found that if the variation in pH value of isoelctric point and the nanofluid was high, then the performance of flat plate solar collector was better.

CHAPTER 3
GAP STUDY AND PROPOSED WORK

3.1 GAP STUDY

Natarajan & Sathish (2009), Role of nanofluids in solar water heater

- A very limited work on mathematical or numerical modelling of the collector has been done.

Risi et al. (2013), Modelling and optimization of transparent parabolic trough collector based on gas-phase nanofluids

- Mathematical modeling has been employed for the optimization of nanofluid based transparent parabolic trough solar collector (TPTSC).
- Genetic algorithm has been used for enhancing the performance of parabolic trough solar collector.

Tyagi et al. (2009), Predicted Efficiency of a Low-Temperature Nanofluid- Based Direct Absorption Solar Collector

- Theoretically examined the possibility of employing a non-concentrating direct absorption solar collector.
- Not related to experimental work on the non-concentrating direct absorption collector.

Otanicar et al. (2010), Nanofluid-Based Direct Absorption Solar Collector

- Experimental, theoretical &numerical investigations have been carried out to study the performance of a nanofluid based micro scale direct absorption solar collector (DASC).

Taylor et al. (2011b),Nanofluid optical property characterization: towards efficient direct absorption solar collectors

- Theoretical and experimental investigations have been employed to study the optical property characterization of various nanoparticles.
- The study mainly deals with the direct absorption solar collector.

Taylor et al. (2011), Applicability of Nanofluids in High Flux Solar Collectors

- Experimental and theoretical examinations have been done for the comparison between nanofluid-based parabolic dish type concentrating collector and the conventional one.
- Very limited mathematical modeling has been done on this type of collector.

Yousefi et al. (2012), An experimental investigation on the effect of Al_2O_3-H_2O nanofluid on the efficiency of flat-plate solar collectors

- The performance of flat plate type solar collector using Al_2O_3-water based nanofluid has been investigated experimentally .
- A very limited mathematical modeling of flat plate type solar collector has been done.

Yousefi et al. (2012), An experimental investigation on the effect of MWCNT-H_2O nanofluid on the efficiency of flat-plate solar collectors

- Experimental examination has been employed to study the performance of flat plate type solar collector using MWCNT-H_2O based nanofluid.
- A very limited mathematical modeling of flat plate type solar collector has been done.

Yousefi et al. (2012c),An experimental investigation on the effect of pH variation of MWCNT–H_2O nanofluid on the efficiency of a flat-plate solar collector

- Experimental investigation has been employed to study the effect of pH variation of MWCNT–H_2O nanofluid on the efficiency of a flat-plate solar collector.
- A very limited mathematical or numerical modelling of the collector has been done.

Saidur et al. (2012), Evaluation of the effect of nanofluid-based absorbers on direct solar collector

- Experimental investigation has been employed for analyzing the performance of nanofluid based direct absorption type solar collector.

Khullar et al. (2010) Application of nanofluids as the working fluid in concentrating parabolic solar collectors

- Theoretical & numerical investigations have been employed for the application of nanaofluids as the working fluid in concentrating parabolic solar collectors.
- Mathematical modelling of heat transfer and flow aspects of the linear parabolic solar collectors has been done.
- FDM (finite difference method) technique has been used to solve the equations numerically.
- No experimental work has been done using nanofluids on the concentrating type parabolic solar collectors.

Khullar et al. (2012), A study on environmental impact of nanofluid based concentrating solar water heating system

- Theoretical investigation has been employed for studying the environmental effect on nanofluid based concentrated solar water heating system.
- A very limited mathematical modeling has been done.

Khullar et al. (2012), Solar Energy Harvesting Using Nanofluids-Based Concentrating Solar Collector

- Theoretical examination has been employed for studying the concentrating type parabolic solar collectors.
- Nanofluid-based concentrating parabolic solar collectors (NCPSC) has been mathematically modelled using FDM technique.
- No experimental work has been done on the concentrating type parabolic solar collectors.

Chaji et al. (2013), Experimental Study on Thermal Efficiency of Flat Plate Solar Collector Using TiO_2/Water Nanofluid

- Experimental examination has been employed for checking the thermal efficiency of nanofluid based flat plate solar collector (FPSC).
- A very limited mathematical modelling has been employed.
- Experimental results are not compared with conventional flat plate solar collector.

Tiwari et al. (2013), Experimental Study on Thermal Efficiency of Flat Plate Solar Collector Using TiO_2/Water Nanofluid

- A very limited mathematical modelling has been done on the flat plate type solar collector
- No comparisons are carried out to compare the result with the conventional type collectors.

Chougule et al. (2012), Performance of nanofluid-charged solar water heater by solar tracking system

- Experimental examination has been employed for studying the performance of nanofluid charged solar water heater using solar tracking system.
- A very limited mathematical modeling has been employed.

3.2 PROPOSED WORK

From the experimental results, it is found that nanofluids improves the performance of solar collectors due to its superior thermophysical properties as compared to the water depends upon the type of nanofluid used. But the experimentation is done only on low temperature based solar

collector i.e. flat plate type solar collector and till now only theoretical and numerical investigation is done on high temperature based concentrated solar collector. Based on the gap study it is found that a lot of research can be done on high temperature based concentrated solar collector using nanofluids by taking different parameters into account because nanofluids improves the performance of high temperature based concentrated solar collector more as compared to low temperature based flat plate solar collector. Papers also represent studies on direct solar collector, micro-scale direct absorption type collector. A lot of theoretical and experimental work were done by the various authors on the flat plate type solar collectors.

As literature cited in chapter 2, few papers deal with concentrating type collectors. Khullar & Tyagi continuously doing work on concentrating parabolic solar collector. Till now, they have been done lot of theoretical and mathematical modeling of it and no experimentation is done on the concentrated parabolic solar collector. In future, they can do experimental work on it as they already says that.

So, based on the above cited gap study our main aim is to do the experimental work on the concentrated parabolic solar collector. During experimentation we check the performance of concentrated parabolic solar collector in which nanofluid is used as a working fluid and then compares its performance with conventional fluid.

CHAPTER 4
OBJECTIVES STUDY

A lot of research has been done on the flat-plate collector by using different nanofluids. These nanofluids are the mixture of nanoparticles with one or more base fluid. Its results are compared with conventional base fluid. It has been found out that conventional fluids can absorb heat upto a certain limit which limits the efficiency of solar collector. Also, flat plate types of collectors (due to inherent limitations of relatively low thermal efficiencies and low output temperatures) are limited to household water heating systems. On the parabolic trough collector, experimental investigation has been done by using conventional fluid and nanofluid based parabolic trough collector is theoretically analyzed by using mathematical modelling and governing equations have been solved by using numerical techniques. As we know, the efficiency of solar collector mainly depends on the fluid that is absorbing the heat. So it has been found that the thermal properties (Specific heat, Heat capacity, viscosity, density etc.) of the fluid that is passing through the collector plays an important role to make the system more effective. "Nanofluids" possesses very good thermal properties. So it can be used in solar collectors in order to improve its performance. So, In this thesis we are going to evaluate the performance of parabolic trough collectors experimentally by using SiO_2-water based and CuO-water based nanofluids.

The main objectives of this experimental work are as follows:

1. To investigate the variation of parabolic solar collector efficiency by using nanofluids (average size 20-40nm).
2. To investigate the variation of parabolic solar collector efficiency by using water.
3. To investigate the variation of parabolic solar collector efficiency with varying volume fraction of nanoparticles.
4. To investigate the variation of parabolic solar collector efficiency at different volume flow rates of nanofluids and water.
5. To carry out the temperature variation study throughout the day.
6. Comparison of performance of parabolic solar collector for nanofluids and water.

CHAPTER 5
METHODOLOGY

5.1 PREPARATION OF NANOFLUIDS

5.1.1 SYNTHESIS OF SiO_2 NANOPARTICLES (Gorji et al. 2012)

Firstly, Tetraethylorthosilicate $Si(OC_2H_5)_4$ combines with water using ammonium hydroxide (NH_4OH) as catalyst which produces silicon hydroxides. In this, ethoxy groups are replaced with OH groups.

$$Si(OC_2H_5)_4 + 4H_2O \longrightarrow Si(OH)_4 + 4C_2H_5OH$$

After that, silicon hydroxides are condensed which produces silicon oxide.

$$Si(OH)_4 \longrightarrow SiO_2 + 2H_2O$$

5.1.2 SYNTHESIS OF CuO NANOPARTICLES (Chang et al. 2011)

Firstly, copper sulphate reacts with sodium carbonate and water which produces precursor i.e. $Cu_2(OH)_2CO_3$.

$$2CuSO_4 + 2Na_2CO_3 + H_2O \longrightarrow Cu_2(OH)_2CO_3 + 2Na_2SO_4 + CO_2 \uparrow$$

After that, precursor decomposes to produce copper oxide.

$$Cu_2(OH)_2CO_{3(s)} \xrightarrow{\Delta} 2CuO_{(s)} + CO_2 \uparrow + H_2O$$

5.1.3 STRUCTRUAL CHARACTERIZATION

XRD of Purchased SiO_2 Nanoparticles

Specifications

Company Name	:	Intelligent Materials Pvt. Ltd.
Nanopowder	:	Silicon Oxide (SiO_2)
Type	:	Amorphous
Purity	:	99%
APS	:	20-30 nm
SSA	:	110-120 m^2/gm
Color	:	White
Bulk Density	:	< 0.10 g/cm^3
True Density	:	2.4 gm/cm^3

Ultraviolet Reflectivity	:	>75%
pH Value	:	7
Flash Point	:	1300 degree
Boiling Point	:	2500 degree
Melting Point	:	3900 degree

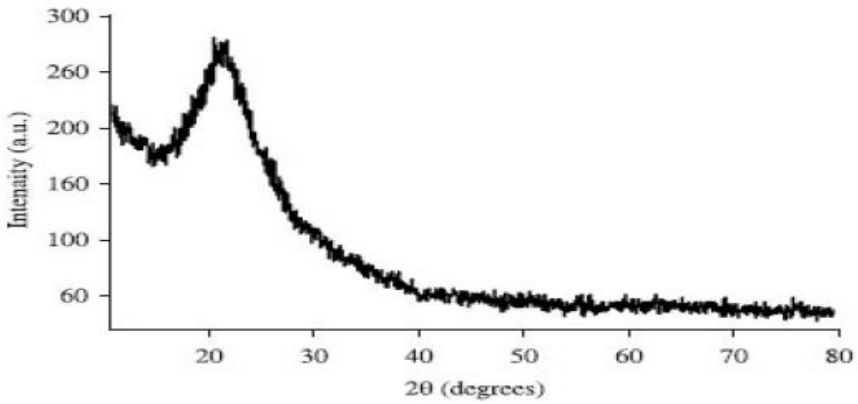

Fig.25 XRD of Purchased SiO_2 Nanoparticles

XRD in SAI Lab of Purchased SiO_2 Nanoparticles

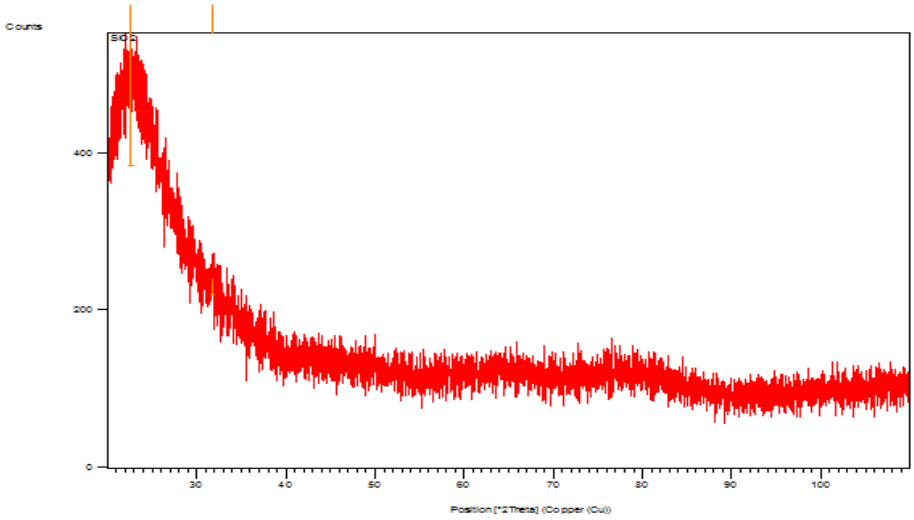

Fig.26 XRD in SAI Lab of Purchased SiO_2 Nanoparticles

TEM of Purchased SiO_2 Nanoparticles

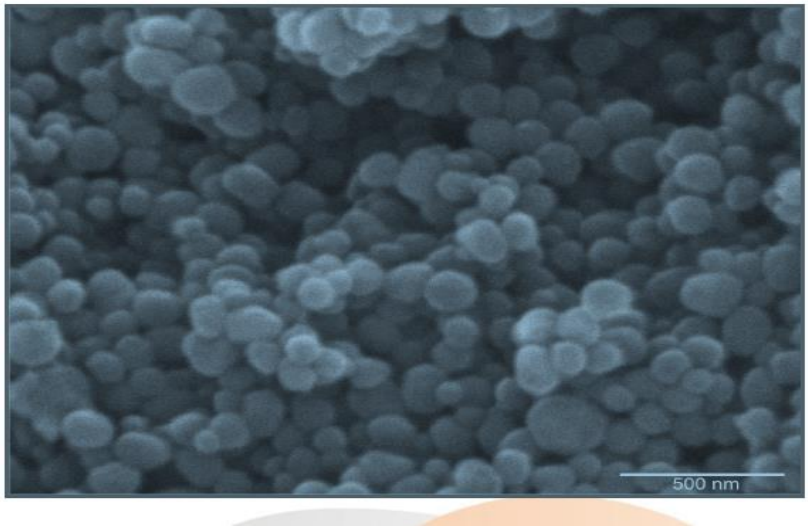

Fig.27 TEM of Purchased SiO_2 Nanoparticles

XRD of Purchased Sample CuO Nanoparticles

Specifications

Company Name	:	Intelligent Materials Pvt. Ltd.
Nanopowder	:	copper Oxide (CuO)
pH Value	:	7
Purity	:	>99%
APS	:	40 nm
BET Specific Surface Area	:	>13 m^2/gm
Color	:	Black
True Density	:	6.4 gm/cm^3
Content of CuO	:	>99%

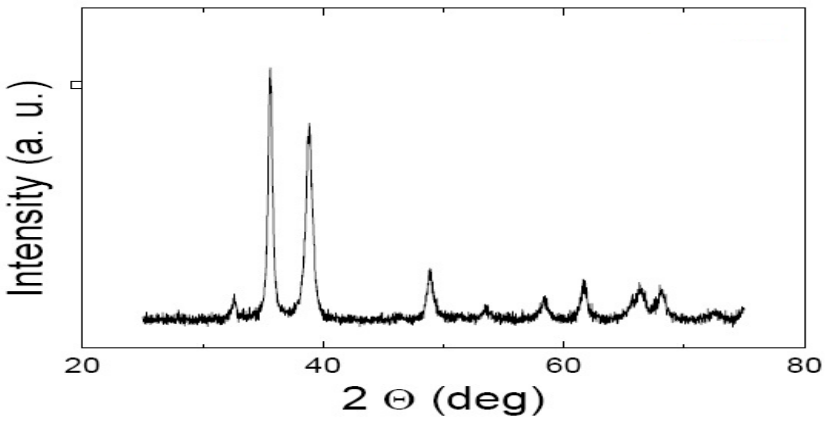

Fig.28 XRD of Purchased CuO nanoparticles

XRD in SAI Lab of purchased CuO Nanoparticles

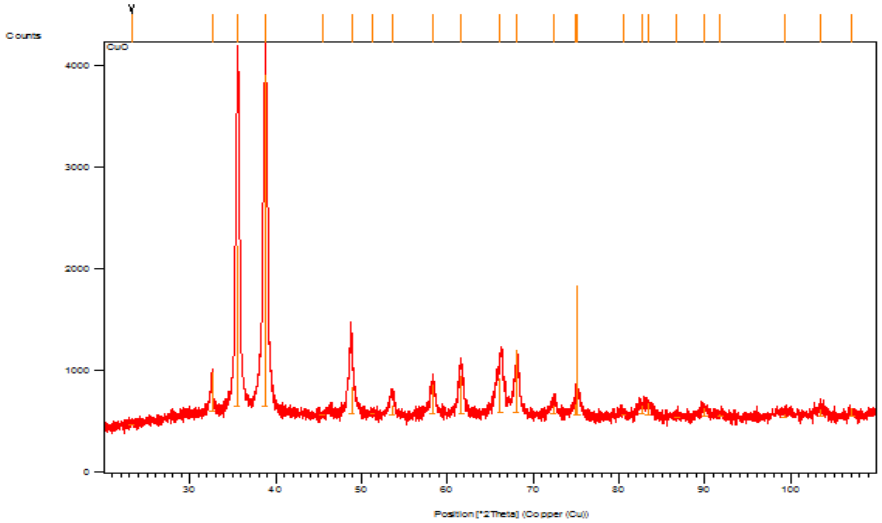

Fig.29 XRD in SAI Lab of Purchased CuO Nanoparticles

5.1.4 SONICATION

In this experiment, two types of nanofluids are used. First is SiO_2-water based nanofluid which is prepared by mixing SiO_2 nanoparticles with water and the other is CuO-water based nanofluid which is prepared by mixing CuO nanoparticles with water. But before preparing the nanofluids, it is very necessary to measure the weight of SiO_2 and CuO nanoparticles required in water for varying concentrations. This is done by employing the typical expression (Chang et al., 2011):

$$\varphi = V_p / V_{eff}$$

Where,

$V_{eff} = V_p + V_f$,

$V_p = W_p / \rho_p$

and

$V_f = W_f / \rho_f$

Total volume of Base fluid (Water), V_w = 10 litre

Density of CuO nanoparticles, ρ_{CuO} = 6.4 gm/cm^3

Density of SiO_2 particles, ρ_{SiO2} = 2.4 gm/cm^3

Density of water, ρ_w = 1000 kg/m^3

Table 1: Following table illustrate the weight of SiO_2 nanoparticles and CuO nanoparticles to make the nanofluid at varying concentrations.

φ	W_p for SiO_2 nanoparticles per litre of water in gm	W_p for CuO nanoparticles per litre of water in gm
0.01	0.24	0.64
0.05	1.20	3.20

Make the volumetric concentration of 0.01 % and 0.05 % by mixing 0.24 gm and 1.20 gm of SiO_2 nanoparticles in 1000 ml of distilled water. In case of CuO-water based nanofluid, 0.64 gm and 3.20 gm of CuO nanoparticles are required in 1000 ml of distilled water for the volumetric concentration of 0.01 % and 0.05 %.

Fig.30 Weighing Machine

The weight of nanoparticles are measured in grams by using weighing machine in fig. 30 as shown above. Now, stirring is done by putting small amount of SiO_2 nanoparticles in water continuously for about 30 minutes on the magnetic stirrer with hot plate system. For preparing CuO-water based nanofluid, stirring is done by putting small amount of CuO nanoparticles in water continuously for about 60 minutes on the magnetic stirrer with hot plate system as shown in fig.31.

Fig.31 Magnetic stirrer with hot plate

To make the nanoparticles more stable and remain more dispersed in water, ultra sonicator is used. The solution then put on the sonicator and sonication is done for two and a half hours. By this nanoparticles become more evenly dispersed in distilled water. After sonication the required nanofluid solution is ready for the application. The sonicator is used shown in fig. 32 is a ultra bath sonicator.

Fig.32 Ultra bath sonicator

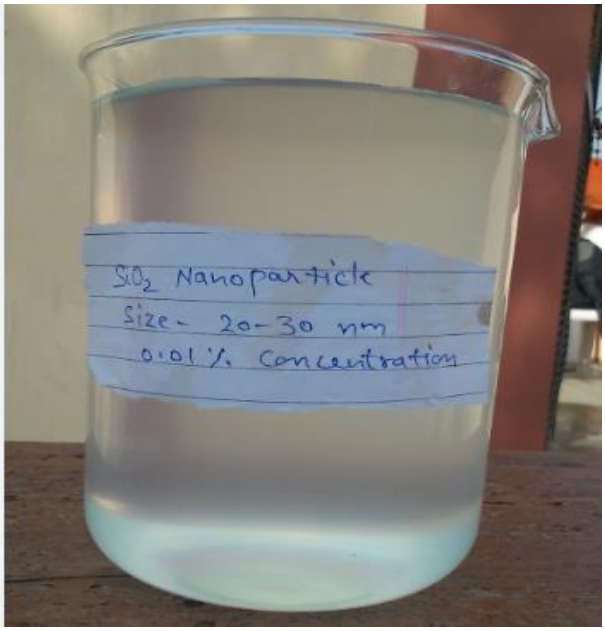

Fig.33 (a)

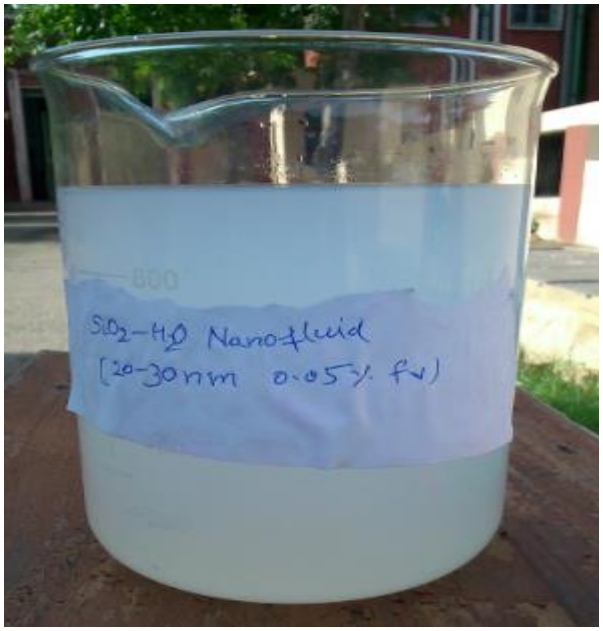

Fig.33 (b)

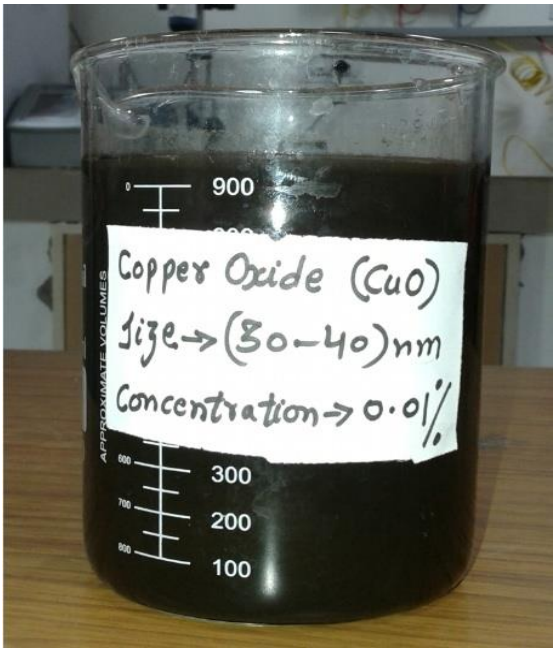

Fig.33 (c)

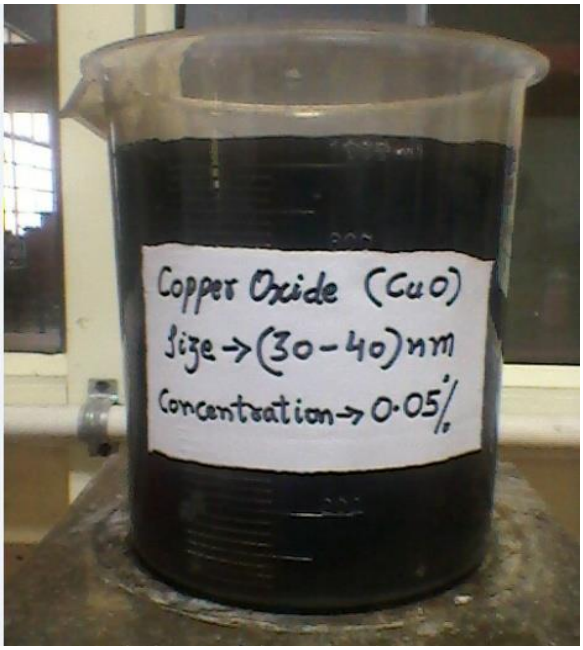

Fig.33 (d)

Fig.33 (a) SiO_2-water based nanofluid having volumetric concentration of 0.01%

Fig.33 (b) SiO_2-water based nanofluid having volumetric concentration of 0.05%

Fig.33 (c) CuO- water based nanofluid having volumetric concentration of 0.01%

Fig.33 (d) CuO- water based nanofluid having volumetric concentration of 0.05%

5.2 THERMOPHYSICAL PROPERTIES MEASUREMENT

5.2.1 Thermal Conductivity

Thermal conductivity of the nanofluid is determined by applying equation as shown below (Javadi et al. 2013):

$$\mathbf{k_{eff} = k_f [k_p + 2\, k_f + 2\, \varphi_p\, (k_p - k_f)] / [k_p + 2\, k_f - \varphi_p\, (k_p - k_f)]}$$

Where

k_{eff} = thermal conductivity of nanofluid

k_p = thermal conductivity of nanoparticles

k_f = thermal conductivity of base fluid

φ_p = concentration of nanoparticle

5.2.2 Viscosity

Viscosity of the nanofluid is determined by applying equation as shown below (Javadi et al. 2013):

$$\mathbf{\mu_{eff} = \mu_f / (1 - \varphi_p)^{2.5}}$$

Where

μ_{eff} = viscosity of the nanofluid

μ_f = viscosity of the base fluid

φ_p = concentration of nanoparticle

5.2.3 Density

Density of nanofluid is determined by applying equation as shown below (Yousefi et al., 2012):

$$\mathbf{\rho_{eff} = (1 - \varphi_p)\, \rho_f + \varphi_p\, \rho_p}$$

Where

ρ_{eff} = density of nanofluid

ρ_p = density of nanoparticle

ρ_f = density of base fluid

φ_p = concentration of nanoparticle

5.2.4 Specific Heat

Specific heat of nanofluid is determined by applying equation as shown below (Yousefi et al., 2012):

$$c_{eff} = \{(1 - \varphi_p)\ \rho_f\ c_f + \varphi_p\ \rho_p\ c_p\} / \rho_{eff}$$

Where

c_{eff} = specific heat of nanofluid

ρ_{eff} = density of nanofluid

ρ_p = density of nanoparticle

ρ_f = density of base fluid

φ_p = concentration of nanoparticle

c_f = specific heat of base fluid

c_p = specific heat of nanoparticle

5.3 EXPERIMENTAL SET UP

Fig.34 Experimental set up

Table 2: Different parameters and their values for the fabricated PTSC

Collector length	1.20 m
Collector breadth	0.915 m
End Plate thickness	2 mm
Aperture area	1.0188 m^2
Rim angle	90^0
Focal length	0.30 m
Receiver inside diameter	0.027 m
Receiver outside diameter	0.028 m
Receiver length	1000 mm
Glass envelope inside diameter	0.064 m
Glass envelope outside diameter	0.066 m
Insulation on pipes	Aluminium foil , Superlon
Concentration ratio	11.30
Tank material	Plastic
Tank insulation material	Glass wool
Circulating pump	18 W
Water flow rate	20 lt/h, 40 lt/h, 60 lt/h
Nanoparticle	SiO_2, CuO
Base fluid	Distilled water
Nanofluid flow rate	20 lt/h, 40 lt/h, 60 lt/h

5.4 DIFFERENT CONSTITUENTS OF THE PARABOLIC SOLAR SYSTEM: The different constituents of the parabolic solar system are described as:

1) Reflector

A Stainless steel sheet having 1.2m collector length and 0.91m collector aperture is employed to develop the parabolic structure. The reason behind the use of stainless steel sheet is that it gives mechanical strength to the parabolic structure. Then, glass mirror strips are sticked on the parabolic sheet with the help of fevetite raped. Total 26 glass mirror strips are used which are 5mm thick and 90 cm length of each.

Fig.35 Reflector

These glass mirror strips are sticked in such a manner that it does not make any impact to the parabolic structure. Glass mirror strips are employed due to its high reflectivity of about 96%.The reflector which is prepared by the use of glass mirror strips sticked on the parabolic stainless steel sheet is shown in fig.35.

2) Receiver Tube

A copper tube having inside diameter 27mm and outside diameter 28mm and 120cm length is employed as receiver tube. Its outside surface is painted black to absorb maximum solar radiation and is covered with glass tube having inside diameter 64mm and outside diameter 66mm and length 90cm which is tied by the glass to metal seals on both sides of the copper tube.

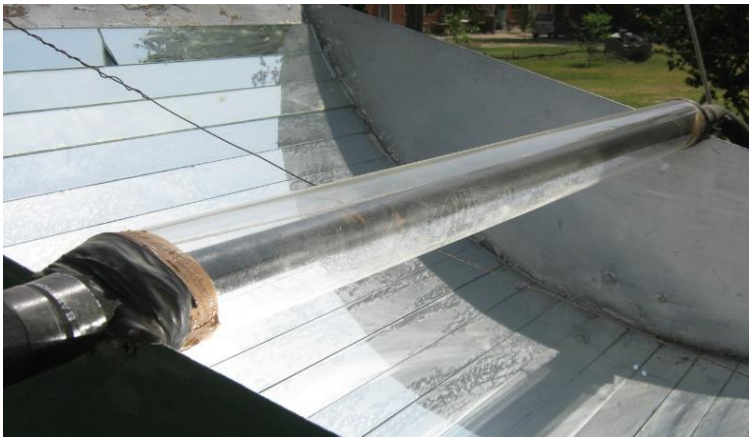

Fig.36 Receiver tube

The cover of glass tube on the copper tube is employed to reduce the losses which are due to conduction, convection and radiation mechanism. The receiver tube is shown in fig.36.

3) Storage Tank

Storage tank is made up of plastic having capability of 10 ltr. Firstly, experiment is done by using distilled water in the storage tank and then, experiment is done by using SiO_2-water based nanofluid and CuO-water based nanofluid in this storage tank. The distilled water and nanofluids both are circulated from the storage tank by using pump having 18 W capacity.

Fig.37 Storage tank

Pump is placed inside the storage tank. The working fluid used is circulated from the storage tank to the inlet of the receiver tube and after absorbing heat from the receiver tube,it goes in the same tank and is re-circulated again and again. The inlet of the storage tank is connected to the inlet of the receiver tube and outlet of the storage tank is connected to the outlet of the ball valve. Glass wool insulation is used on the storage tank to protect it from heat loss. Storage tank used is shown in fig.37.

Fig.38 Pump

Specifications of Pump

Pump Type: Universal Submersible Pump

Voltage: 165-240V/50Hz

H-max: 1.750 (5 Feet)

Output: 1100 L/h

Power: 18W

4) Support Structure

The support structure is made up of cast iron for parabolic solar collector system. The support structure is made up of cast iron because it overcomes the limitation of wood material. The cast iron support structure is green painted. It is constructed in such a manner that it holds easily stress loads, wind loads etc. Also, not make any impact on the parabolic structure and also for the alignment errors minimization. The manual tracking system is also attached to the support structure. Support structure used for this experiment is shown below in fig.39.

Fig.39 Support structure

5) Insulation

Firstly, pipes are insulated with the help of aluminium foils and are further insulated with the help of Superlon insulation.This is done for reducing the heat losses as much as possible during the flow of liquid from piping system.

Fig.40 Insulation on pipes

The insulation used on the storage tank is glass wool type which have very low thermal conductivity. These insulations are easily obtained from the Air Conditioners and Refrigerators spare parts shop. Thermocol sheets are also used for wrapping the glass wool insulation. Insulations used on the storage tank and piping system are shown in fig.40 and 41.

Fig.41 Insulation around the storage tank

6) Tracking Mechanism

In the experiment, manual tracking mechanism is used because it is simple, cheaper and easy to use. Automatic tracking system employs gear-motor mechanism which makes the system costly, not easy to use and difficult in design. Mainly, it consists of bicycle hub, rectangular support structure of cast iron, handle, stopper and clutch wire. One end of clutch wire is wounded on bicycle hub and other end is connected to the back side of the reflector. The hub is inserted in support structure and a handle is attached to the hub to rotate it manually. Stopper is provided to maintain the reflector at required angle. So, parabolic solar collector is rotated manually in north-

south direction to focus the maximum solar radiation on the receiver tube which is reflected by the reflector. One axis tracking mechanism can also be used for this. Manual tracking system used for this experiment is shown in fig.42.

Fig.42 Tracking Mechanism

7) Ball Valve

Ball valve is used to vary the mass flow rate of water and nanofluid which is used as a working fluid in the system. Its one side is connected to the outlet of the receiver tube and other side is connected to the outlet of the storage tank.

Fig.43 Ball valve

Ball valve is opened according to the required mass flow rate. The mass flow rate of working fluid is taken as 20 l/h, 40 l/h and 60 l/h. Ball valve is attached to the system with the help of fevetite raped. Ball valve is shown in fig.43.

5.5 WORKING PRINCIPLE OF PARABOLIC SOLAR SYSTEM

The working principle of parabolic solar collector is explained by using line diagram. The line diagram is shown in fig.44. The working fluid from the storage tank is circulated to the receiver tube by using pump of 18 W. The pump is placed inside the tank. The different volume flow rate of working fluid taken is 20lt/h, 40lt/h and 60lt/h. The volume flow rate is varied with the help of ball valve. In the receiver tube, working fluid absorbs heat and goes back to the storage tank. The working fluid is then recirculated again and again from the receiver tube till 3 pm. The receiver tube is covered with glass tube to decreases the losses from it as much as possible which is due to conduction, convection and radiation mechanism.

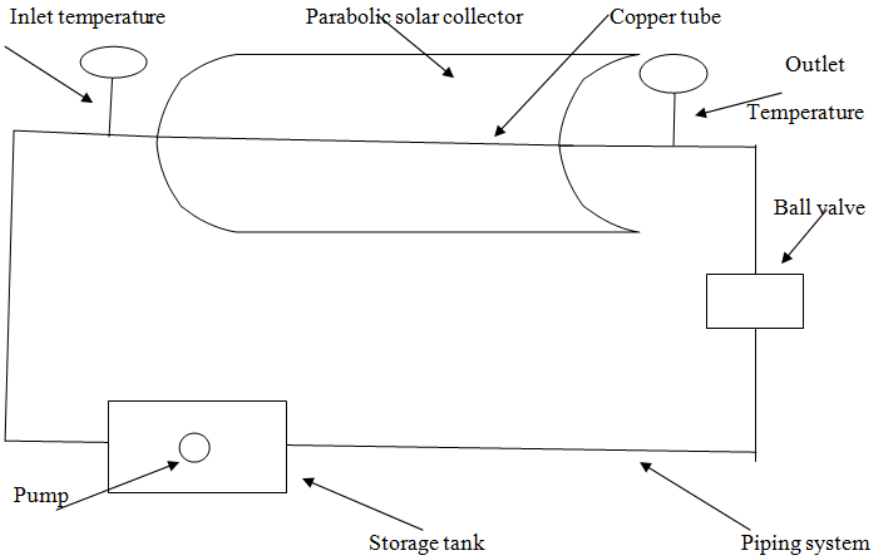

Fig.44 Line diagram of parabolic solar system

Piping system which is well insulated is used to take the working fluid from inlet of the storage tank to the inlet of the receiver tube, outlet of the receiver tube to the inlet of the ball valve and the outlet of the ball valve to the outlet of the storage tank. It is observed from the experiment that the maximum temperature obtained is at 3 pm. The inlet and outlet temperature of the receiver tube is measured by using thermometers. The solar intensity is measured by using solar power meter.

5.6 MEASURING INSTRUMENTS

Various instruments used during the experiment are as follows:

1) Solar power meter
2) Thermometer
3) Magnetic based angular measurement device
4) Stopwatch system
5) Anemometer

1) Solar Power Meter

Solar power meter is employed to determine the solar intensity of the sun which falls on the system. It is determined in W/m^2. It contains a sensor which measures the solar intensity and displayed it on the screen. It is calibrated with the actual pyranometer and the following relation is used to measure the actual solar intensity.

$$Y = 0.745\ x + 1.839$$

Where

Y = actual solar intensity

x = intensity measured from solar power meter.

Solar power meter used is shown in fig.45.

Fig.45 Solar power meter

Specifications of Solar Power Meter

Display: 3.5 digits, 2000 readings

Range: 2000 W/m^2, 634 BTU/(ft2xh)

Resolution: 0.1 W/m^2, 0.1 BTU/ (ft2xh)

Accuracy: Typically within +/- 10W/m^2 [+/-3 BTU/ (ft2xh)] or +/- 5% whichever is greater in sunlight. Temperature included error +/- 0.38 W/m^2 / ºC [+/-0.12 BTU/ (ft2xh)] / ºC] deviation from 25 ºC.

Angular accuracy: Cosine corrected

Drift: < +/- 2% per year

Over-input: Display "OL"

Sampling time: 0.25 second

Operating temperature: 0C ~ 50ºC

Humidity: below 80% RH

Power supply: 9V battery x1

2) Thermometer

Thermometer is employed to measure the temperature of the working fluid. In the experiment, three thermometers are used in which one is used to measure the inlet temperature of the working fluid and other two are used for measuring the outlet temperature and the working fluid inside the storage tank. It consists of a red mercury line which shows the temperature and the range is -10^0-110^0 C. Thermometer used is shown in fig.46.

Fig.46 Thermometer

3) Magnetic Based Angular Measurement Device

This device is used for measuring the varying tracking angles to focus the maximum sun rays on the receiver tube which are reflected by the reflector. The angular measurement device used for this is magnetic based. It consists of a flexible red needle which tells the required angle. This angle is in between the reflector and the earth for trapping maximum solar radiation.

Fig.47 Magnetic based angular measurement device

Specifications

- 4-1/8" angle finder with magnetic base.
- Measures any angle accurately and quickly from 0-90 degrees in any quadrant.
- Accurate to within 1/2 of 1 degree.
- Magnetic base for mounting on steel framing or pipes.

4) Stopwatch System

Stopwatch system is used for measuring the varying mass flow rate of the working fluid in the system. In this, a beaker which collects working fluid and correspondingly time is noted by using stopwatch system. This is done for 10 seconds. Now, the mass flow rate is in l/s and to convert it into l/h, it is multiplied by 3600. For example

Let us assume in 10 seconds, beaker collects 0.3l working fluid. Then, in one second it will be 0.03 l/s. For measuring it in terms of l/h, then 0.03 is multiplied by 3600.

5) Anemometer

Anemometer is used to measure the wind speed which also affects the system performance depends upon the direction in which it flows. It consists of a small fan which rotates continuously when put it in the direction of wind flow and a sensor which sense the wind speed and displayed on the screen as shown in fig 48.

Fig. 48 Anemometer

General Specifications:

Digital Anemometer Model: AM-4201

Display: 18mm (0.7") LCD (Liquid Crystal Display), 3 1/2 digits.

Measurements: m/s (meters per second), km/h (kilometers per hour), ft/min (feet/per minute), knots (nautical miles per hour).

Operating temperature: 0^0 C to 50^0 C (32 ^{0}F to 122 ^{0}F).

Operating humidity: Less than 80% RH.

Air velocity sensor structure: Conventional twisted vane arms and low-friction ball-bearing design.

Temperature sensor: Naked-bead type k thermocouple probe.

Power supply: DC 9V 006P, MN1604(PP3) battery (Heavy Duty Type) or equivalent.

Power consumption: Approx. DC 9 mA.

Weight: 325 g/0.72 LB (including battery).

Instrument dimension: 168 x 80 x 35mm (6.6 x 3.2 x 1.2 inch).

Sensor head dimension: Round, 72 mm Dia.

Standard accessories: Instruction Manual.....1 PC., Sensor probe.....1 PC., Carrying case.....1 PC.

Electrical Specifications: (23 ±5 ^{0}C)

Measurements: m/s, km/h, ft/min, knots.

Range: 0.4-30.0 m/s, 1.4-108.0 km/h, 80-5910 ft/min., 0.8-58.3 knots

Resolution: 0.1 m/s, 0.1 km/h, 10 ft/min., 0.1 knots

Accuracy: ± (2 % + 1 d), ± (2 % + 3 d), ± (2 % + 2 d), ± (2 % + 2 d)

5.7 FORMULAE USED

To study the performance of nanofluid using parabolic solar collector, following formulae are used (Sukhatme S. P., 1984):

1) Useful Heat Gain

Useful heat gain under steady state condition can be obtained by the equation:

$$q_u = \dot{m}_{eff}\, c_{eff}\, (T_0 - T_i)$$

$$q_u = \dot{m}_w\, c_{pw}\, (T_2 - T_1)$$

Where

q_u = useful heat gain in watt

c_{eff} = specific heat of nanofluid in J / kg K

$\dot{m}_{eff}$ = mass flow rate of nanofluid in kg / s

T_0 = outlet temperature of nanofluid in K

T_i = inlet temperature of nanofluid in K

$\dot{m}_w$= mass flow rate of water in kg/s

c_{pw} = specific heat of water

T_2 = temperature of water at outlet

T_1 = temperature of water at inlet

2) Thermal Efficiency (per half an hour)

Thermal efficiency under steady state condition is obtained by equation:

$$\eta_{th} = m_{eff}\, c_{eff}\, (T_0 - T_i) / A_{aper}\, G_T\, t$$

$$\eta_{th} = m_w\, c_{pw}\, (T_2 - T_1) / A_{aper}\, G_T\, t$$

Where,

η_{th} = thermal efficiency

A_{aper} = aperture area in m^2

G_T = incident solar flux in W/m^2

m_w = mass of water in storage tank in kg

3) Overall Thermal Efficiency (average)

Thermal efficiency under steady state condition is obtained by equation:

$$\eta = m_{eff}\, c_{eff}\, (T_{max} - T_{min}) / A_{aper}\, G_{av}\, t$$

$$\eta = m_{w}\, c_{pw}\, (T_{max} - T_{min}) / A_{aper}\, G_{av}\, t$$

where

η = Overall thermal efficiency

A_{aper} = aperture area in m^2

G_{av} = average incident solar flux in W/m^2

m_{eff} = mass of nanofluid in storage tank in kg

4) Instantaneous Efficiency

$$\eta_i = q_u / G_T\, R_b\, W\, L$$

5) Optical Efficiency

$$\eta_o = \rho\, \Upsilon\, (\tau\alpha)\, (W - d_{co}) / W + (\tau\alpha)\, d_{co} / W$$

6) Absorbed Flux

$$S = G_T\, R_b\, (\alpha\tau)\, \rho\Upsilon$$

Where

R_b = bond resistance

Υ = Intercept factor

α = Absorptivity of absorber tube

τ = Glass cover transmitivity

ρ = Specular reflectivity of the concentrated surface

7) Convective Heat Transfer Coefficient

$$h_f = N_u \times k / D_i$$

Where

N_u = Nusselt number = $0.023 \times R_e^{0.8} \times P_r^{0.4}$

R_e = Reynold number = $V\, D_i / \nu$

V = Average velocity = $4\, \dot{m} / \pi\, D_i^2\, \rho$

P_r = Prandtl number = $c_p\, \nu\, \rho / k$

8) Collector Heat Removal Factor

$$F_R = \dot{m}\, c_p / \pi\, L\, D_o\, U_L\, [1 - \exp(-\pi\, D_o\, U_L\, L\, F' / \dot{m}\, c_p)]$$

$$F' = D_i h_f / (D_i h_f + D_o U_L)$$

9) Concentration Ratio

$$C_R = \text{Aperture area / Absorber area} = (W - d_{co}) L / \pi D_0 L = (W - d_{co}) / \pi D_0$$

Where,

C_R = concentration ratio

W = width of the reflector

d_{co} = diameter of glass cover tube

D_0 = diameter of receiver tube

L = length of receiver tube

CHAPTER 6
RESULTS AND DISSCUSSIONS

This chapter contains results which are obtained by doing experimental work on parabolic solar collector using SiO_2-water and CuO-water based nanofluids and its performance is compared with conventional fluid and also containing detailed description of obtaining results. Firstly, efficiency calculation of parabolic solar collector has been done for water at 20 l/h. Then, results are plotted of water (working fluid) at different volume flow rate and after that, results are plotted of SiO_2-water and CuO-water based nanofluids (working fluid) at different volume flow rate and at different particle concentration using graphs as shown below.

6.1 EFFICIENCY CALCULATION OF PARABOLIC SOLAR COLLECTOR

For Water at 20 L/h

1) Absorbed Flux

$$S = G_T R_b (\alpha\tau) \rho\Upsilon$$
$$= 778\times1\times(0.9\times0.88)\times0.93\times0.95$$
$$= 544.39 \text{ W/m}^2$$

2) Convective Heat Transfer Coefficient

Thermophysical properties of water are

Density, ρ = 1000 kg/m^3

Specific heat, c_{pw} = 4.187 KJ/kg K

Thermal conductivity, k = 0.667 W/m-K

Viscosity, ν = 0.415×10^{-6} m^2/s

Average velocity, $V = 4\dot{m}_w / \pi D_i^2 \rho$ = $4\times0.00555 / 3.14\times(0.027)^2\times1000 = 0.0097$ m/s

Reynold number, $R_e = V D_i / \nu$ = $0.0097\times0.027 / 0.415\times10^{-6} = 631.084$

Prandtl number, $P_r = c_{pw} \nu \rho / k$ = $4187\times0.415\times10^{-6}\times1000 / 0.667 = 2.605$

Nusselt number, $N_u = 0.023 \times R_e^{0.8} \times P_r^{0.4}$ = $0.023\times(631.084)^{0.8}\times(2.605)^{0.4} = 5.863$

Convective heat transfer coefficient, $h_f = N_u \times k / D_i$ = $5.863\times0.667/0.027 = 144.84$ W/m^{2}K

3) Collector Heat Removal Factor

Assume U_l = 13.28 W/m^{2}K

Collector efficiency factor, $F' = D_i h_f / (D_i h_f + D_o U_l)$

$= 0.027 \times 144.84 / ((0.027 \times 144.84) + (0.028 \times 13.28))$

$= 0.9132$

$\dot{m}_w c_{pw} / \pi L D_o U_l = 0.00555 \times 4187 / 3.14 \times 1.2 \times 0.028 \times 13.28 = 16.585$

Heat removal factor, $F_R = \dot{m}_w c_{pw} / \pi L D_o U_L [1 - \exp(-\pi D_o U_L L F' / \dot{m}_w c_{pw})]$

$= 16.585 [1-\exp(-0.913/16.585)] = 0.8885$

4) Concentration Ratio

Concentration Ratio C_R **= Aperture area / Absorber area =** $(W - d_{co}) / \pi D_0$

$= (0.915-0.066) / 3.14 \times 0.028 = 9.66$

5) Optical Efficiency

$\eta_o = \rho \Upsilon (\tau\alpha) (W - d_{co}) / W + ((\tau\alpha) d_{co} / W)$

$= 0.93 \times 0.95 \times (0.88 \times 0.9) \times (0.915-0.066) / 0.915 + ((0.88 \times 0.9) \times 0.066/0.915)$

$= 0.706 = 70.6\%$

6) Useful Heat Gain

$q_u = \dot{m}_w c_{pw} (T_2 - T_1)$

$= 0.00555 \times 4187 \times (35.6-32) = 83.66$ W

7) Instantaneous Efficiency

$\eta_{th} = \dot{m}_w c_{pw} (T_2 - T_1) / G_T R_b W L$

$= 83.66 / (778 \times 1 \times 0.915 \times 1.2) = 0.0979 = 9.79\%$

8) Thermal Efficiency (per half an hour)

$\eta_{th} = m_w c_{pw} (T_2 - T_1) / A_{aper} G_T t$

$= 10 \times 4187 \times (35.6-32) / (1.0188 \times 778 \times 30 \times 60)$

$= 0.1056 = 10.56\%$

9) Overall Thermal Efficiency (average)

$\eta_{overall} = m_w c_{pw} (T_{max} - T_{min}) / A_{aper} G_{av} t$

$= 10 \times 4187 \times (60.3-32) / 1.0188 \times 851 \times 5.5 \times 3600$

$= 0.0663 = 6.63\%$

Similarly for water at other volume flow rates and nanofluids at different volume flow rates can be calculated using these relations.

6.2 PERFORMANCE OF PARABOLIC SOLAR COLLECTOR USING WATER

1) Variation in solar intensity and temperature with time

a) For Water at volume flow rate of 20 l/h

Fig.49 shows variation in solar intensity and temperature with time. The reading has been taken on 26 April, 2014 from 9:30 am to 3:00 pm. In this, the solar intensity is continuously increases upto 12:30 pm and after that, it starts decreases. The maximum solar intensity is 955 W/m^2 which is at 12:30 pm. Also, the inlet and outlet temperatures of water are increases continuously upto 3:00 pm because the system is placed in closed circuit and the losses from the pipes are negligible. The initial and maximum outlet temperatures are 32^0 C and 60.3^0 C respectively.

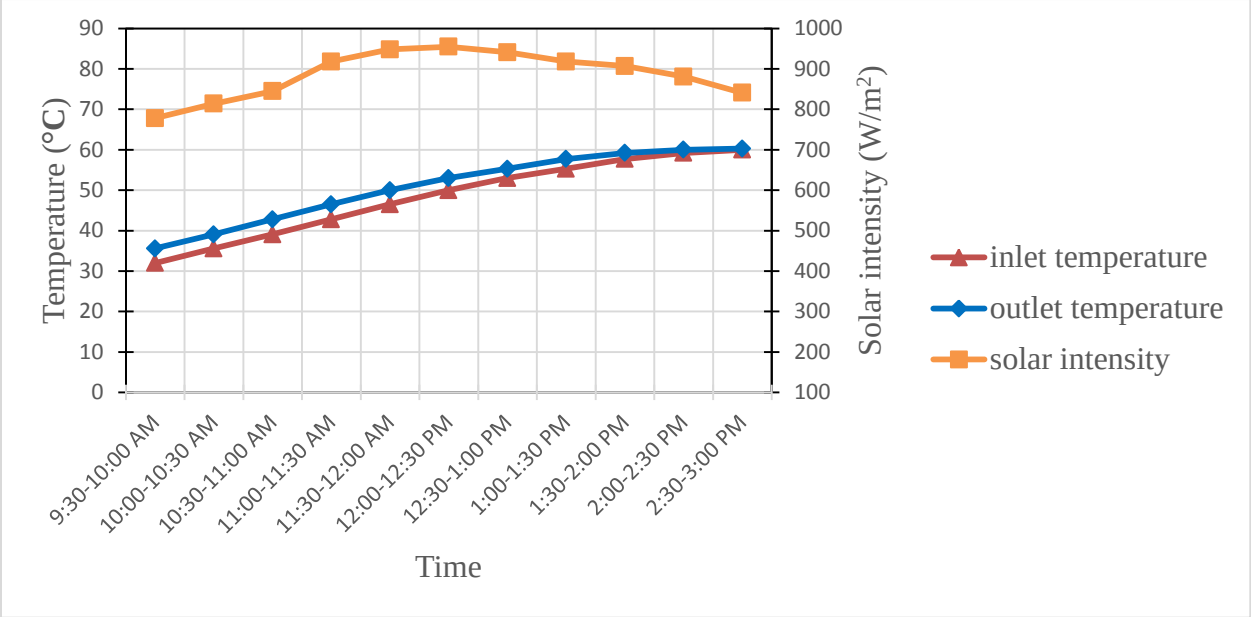

Fig.49 Variation in solar intensity and temp.with time for water at volume flow rate of 20 l/h

b) For Water at volume flow rate of 40 l/h

The reading has been taken on 28 April, 2014 from 9:30 am to 3:00 pm. In this case also, solar intensity is continuously increases upto 12:30 pm and after that, it starts decreases as shown in fig.50. The maximum solar intensity is 978 W/m^2 at 12:30 pm. Also, the inlet and outlet temperatures of water are increases continuously upto 3:00 pm. In this case, the initial and maximum outlet temperatures are 32.5^0 C and 61^0 C respectively.

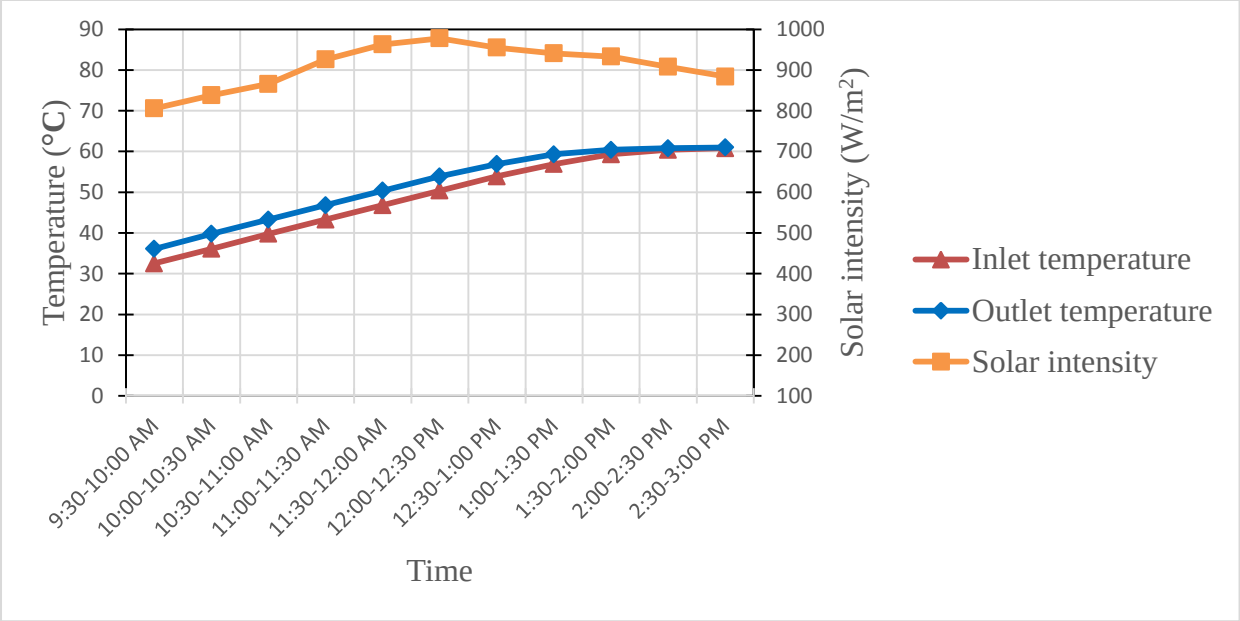

Fig.50 Variation in solar intensity and temp.with time for water at vol. flow rate of 40 l/h

c) For water at volume flow rate of 60 l/h

The maximum solar intensity in this case is 966 W/m^2 at 12:30 pm as shown in fig.51. In this case, the initial and maximum outlet temperatures of water are 33^0 C and 59.7^0 C respectively. The reading has been taken on 29 April, 2014 from 9:30 am to 3:00 pm. It also follows same trend as in fig.49 and fig. 50 for variation in solar intensity and temperature with time.

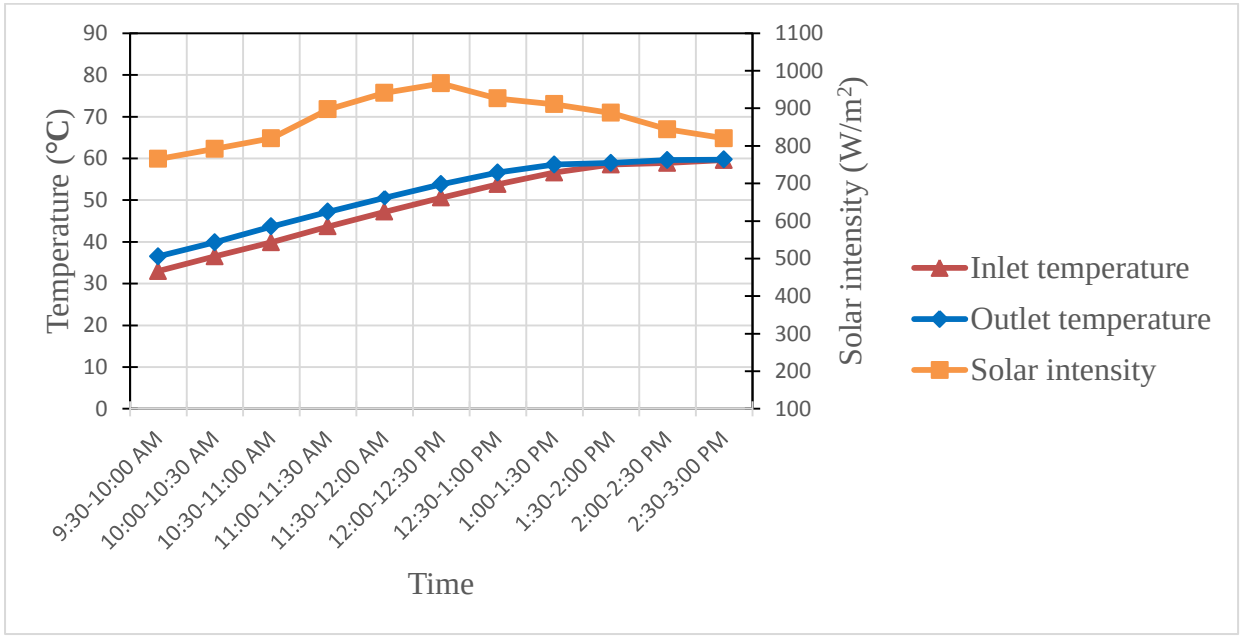

Fig.51 Variation in solar intensity and temp.with time for water at vol. flow rate of 60 l/h

2) Variation in temperature difference with time for water at different volume flow rate

Fig 52 shows the variation in temperature difference with time for water at volume flow rate of 20 l/h, 40 l/h and 60 l/h. As we know, temperature difference is directly related to solar intensity. At high solar intensity, temperature difference is also high and at low solar intensity, temperature difference is also low. Discontinuity in solar intensity also affects the temperature difference badly. Some other external factor like high wind speed and discontinuous power supply which is not only affects the temperature difference badly, also affects useful heat gain, instantaneous efficiency, thermal efficiency and overall thermal efficiency which are directly related to temperature difference. It also depends upon the temperature of working fluid.

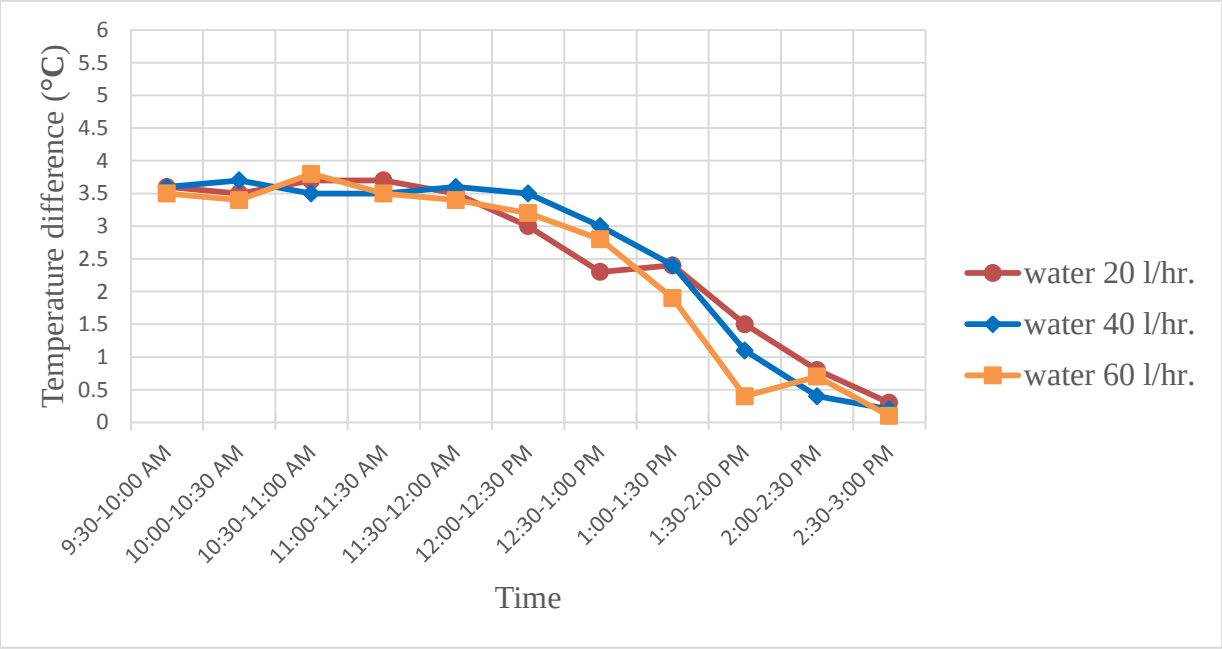

Fig.52 Variation in temperature difference with time for water at different volume flow rate

3) Variation in useful heat gain with time for water at different volume flow rate

Variation in useful heat gain with time for water at different volume flow rate is shown in fig.53. Useful heat gain is mainly depends upon volume flow rate, specific heat and temperature difference of working fluid. As the volume flow rate increases, useful heat gain also increases. Specific heat is same for water at different volume flow rate. Temperature difference varies according to the variation in solar intensity. As the temperature difference increases, useful heat gain also increases at particular volume flow rate.

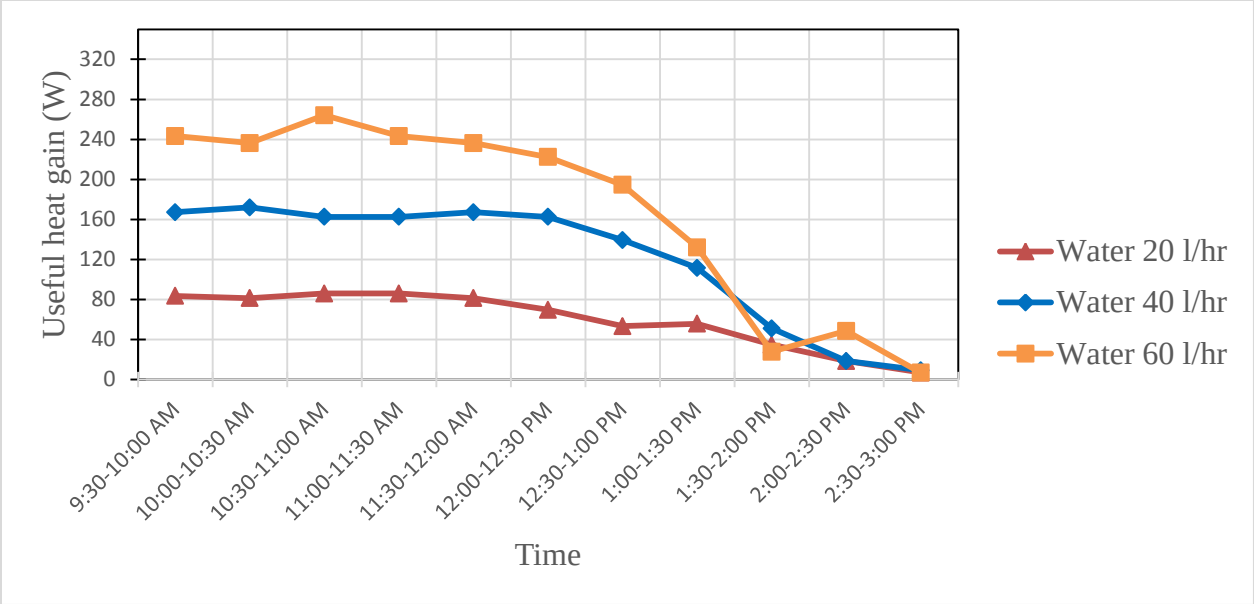

Fig.53 Variation in useful heat gain with time for water at different volume flow rate

4) Variation in instantaneous efficiency with time for water at different volume flow rate

Variation in instantaneous efficiency with time for water at different volume flow rate is shown in fig.54. Instantaneous efficiency depends upon the useful heat gain, solar intensity and aperture area. Aperture area is same for all cases which is inversely proportional to the instantaneous efficiency, thermal efficiency and overall thermal efficiency. Useful heat gain is directly proportional to instantaneous efficiency. More the useful heat gain, more will be instantaneous efficiency. Solar intensity is inversly proportional to instantaneous efficiency. Higher solar intensity decreases the instantaneous efficiency but increases temperature difference which increase the useful heat gain. So, instantaneous efficiency increases. The maximum instantaneous efficiency is 29.34% at volume flow rate of 60 l/h around 10:30-11:00 am as shown in fig.54.

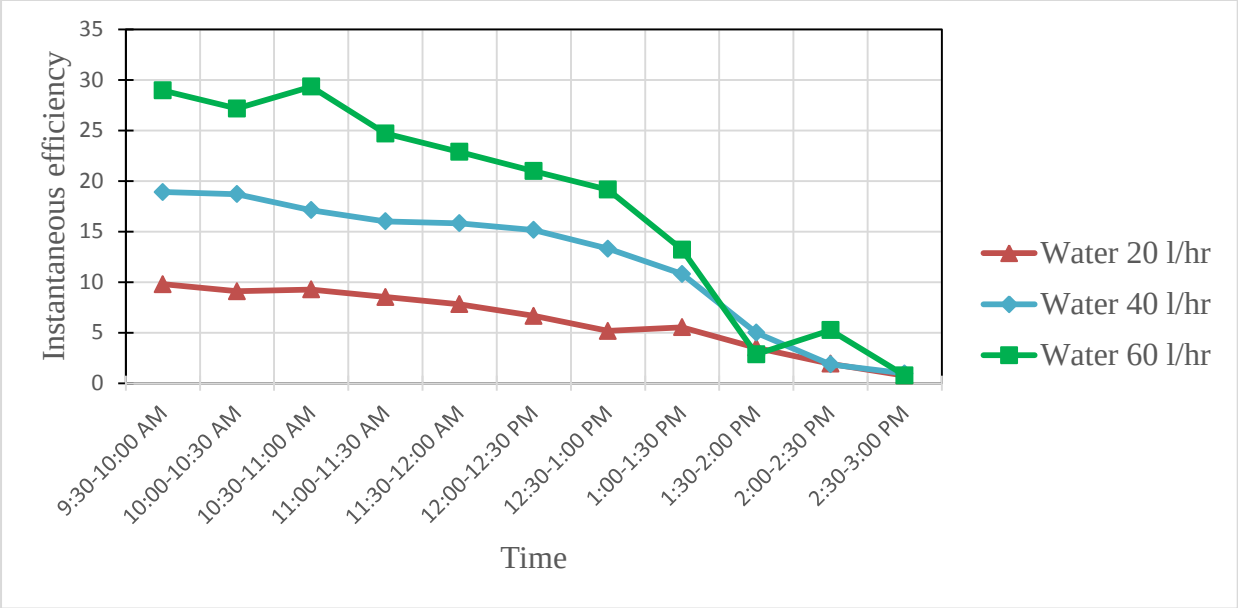

Fig.54 Variation in instantaneous efficiency with time for water at different volume flow rate

5) Variation in thermal efficiency with time for water at different volume flow rate

Variation in thermal efficiency with time for water at different volume flow rate is shown in fig.55. Thermal efficiency is directly related to specific heat, temperature difference and volume of working fluid in storage tank but inversely proportional to solar intensity. Volume of water in storage tank and specific heat is same for all cases. So, the variational parameters are temperature difference and solar intensity. More the temperature difference, more will be thermal efficiency and more the solar intensity, less will be thermal efficiency.

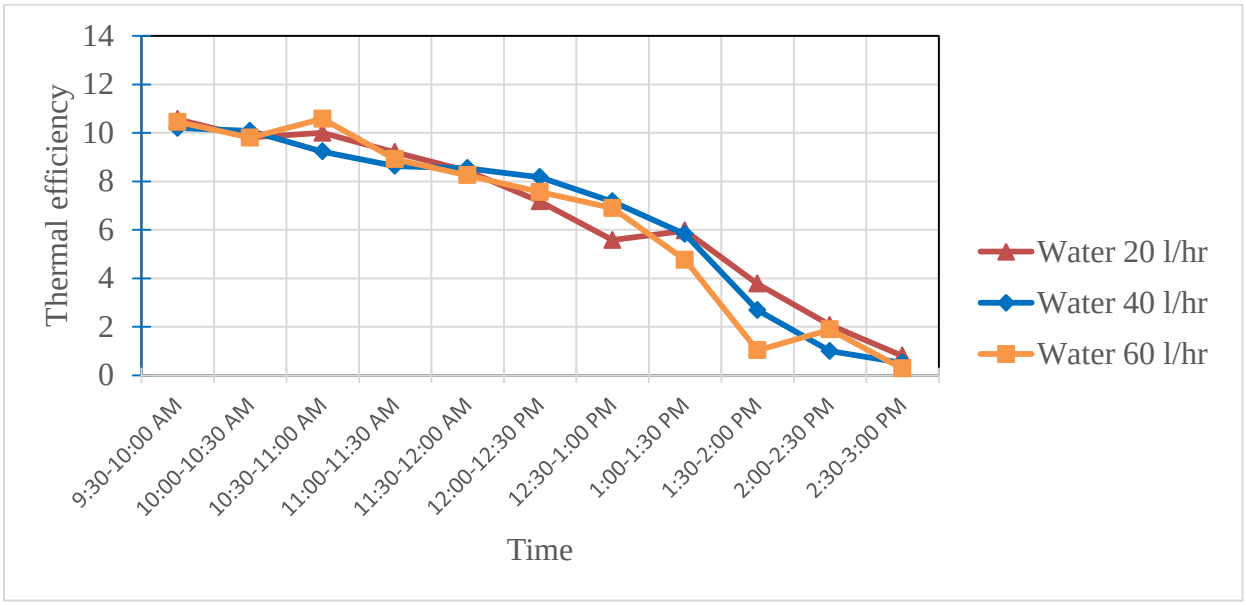

Fig.55 Variation in thermal efficiency with time for water at different volume flow rate

6.3 PERFORMANCE OF PARABOLIC SOLAR COLLECTOR USING NANOFLUIDS

1) Variation in solar intensity and temperature with time

a) For SiO_2-water based nanofluid (0.01% conc.) at volume flow rate of 20 l/h

In this case, the solar intensity is continuously increases upto 1:00 pm and the maximum solar intensity is 926 W/m^2 at 1:00 pm as shown in fig.56. After 1:00 pm, solar intensity is continuously decreases. In case of temperature, both inlet and outlet temperatures of nanofluid are continuously increases upto 3:00 pm. The maximum outlet temperature of SiO_2 nanofluid is 62.9^0 C and the initial temperature of nanofluid is 31.5^0 C. The reading of this has been taken on 8 May, 2014 from 9:30 am to 3:00 pm.

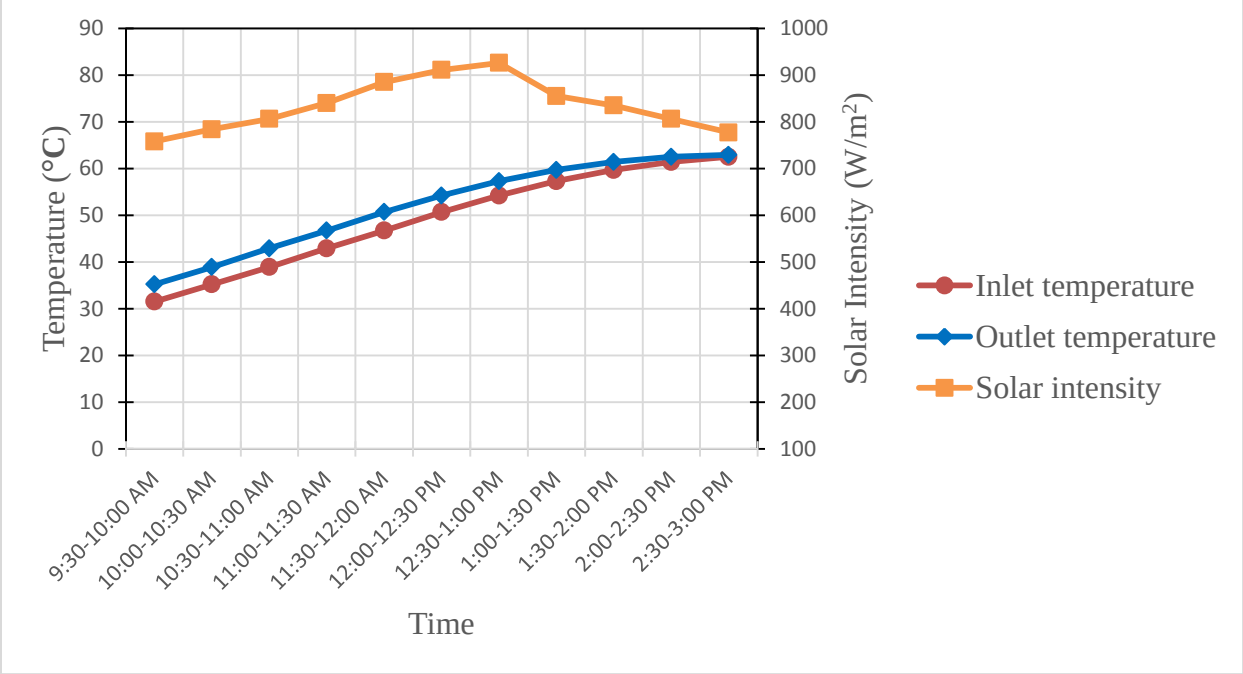

Fig.56 Variation in solar intensity and temperature with time for SiO_2-water based nanofluid (0.01% conc.) at volume flow rate of 20 l/h

b) For SiO_2-water based nanofluid (0.01% conc.) at volume flow rate of 40 l/h

The reading of SiO_2 nanofluid at volume flow rate of 40 l/h is taken on 9 May, 2014 from 9:30 am to 3:00 pm. In this case, the maximum solar intensity is at 1:00 pm which is 881 W/m^2 and the maximum outlet temperature is 61.6^0 C. The outlet temperature is increases continuously upto 2:30 pm. The initial temperature in this case is 31.2^0 C.

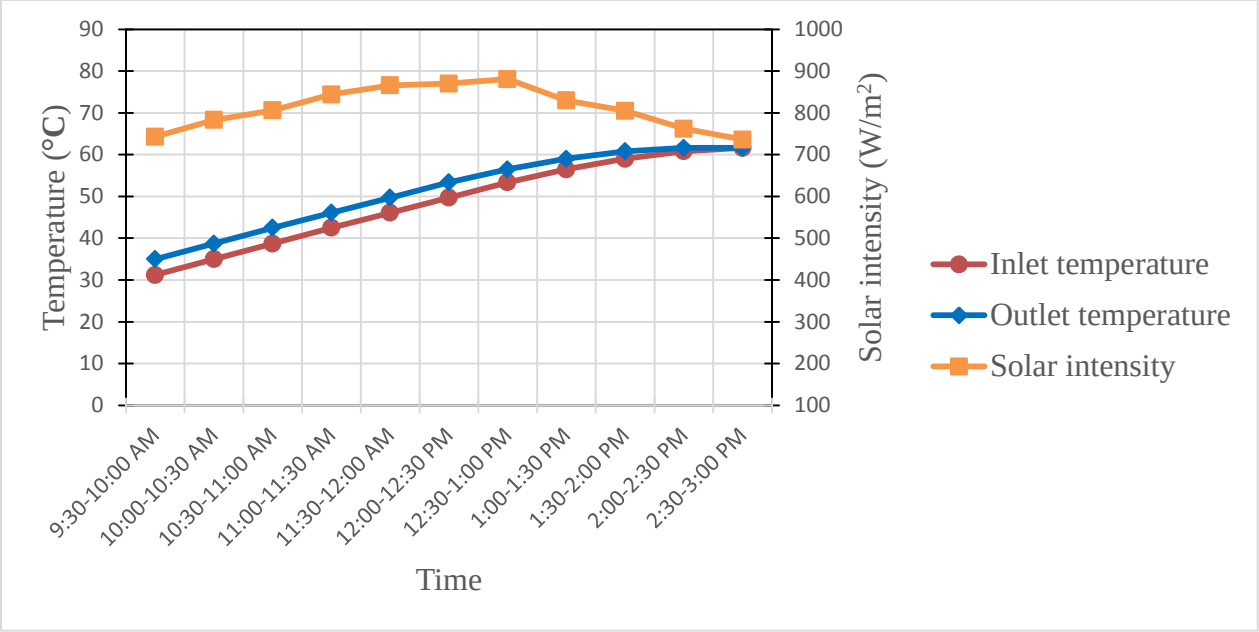

Fig.57 Variation in solar intensity and temp.with time for SiO_2 nanofluid (0.01% conc.) at volume flow rate of 40 l/h

c) For SiO_2-water based nanofluid (0.01% conc.) at volume flow rate of 60 l/h

The reading for this at volume flow rate of 60 l/h is taken on 10 May, 2014 from 9:30 am to 3:00 pm. The maximum solar intensity is 926 W/m^2 at 1:00 pm and the maximum outlet temperature is 60.8^0 C at 2:30 pm. The initial temperature of the nanofluid is 33.1^0 C. In this case, the solar intensity at 2:30 pm is more as compared to solar intensity at 2:00 pm. So, the trend of variation of solar intensity with time is something different from others.

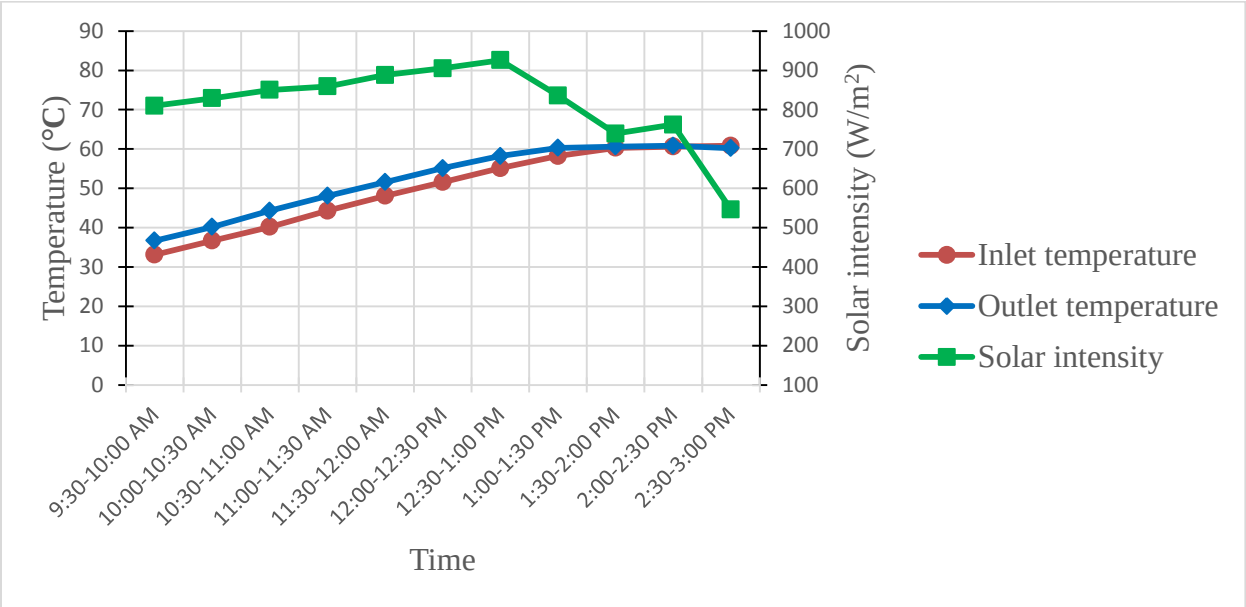

Fig.58 Variation in solar intensity and temperature with time for SiO_2 nanofluid (0.01% conc.) at volume flow rate of 60 l/h

2) Variation in temperature difference with time for SiO_2-water based nanofluid (0.01% conc.) at different volume flow rate

Fig.59 shows the variation in temperature difference with time for SiO_2-water based nanofluid (0.01% conc.) at different volume flow rate. The absorbing heat capacity of working fluid decreases due to discontinuity in solar intensity. If increasing solar intensity falls continuously on the reflector, then it reflects maximum solar radiations on receiver tube and due to this, absorbing heat capacity of working fluid also increases. Temperature of the working fluid can also affects the temperature difference.

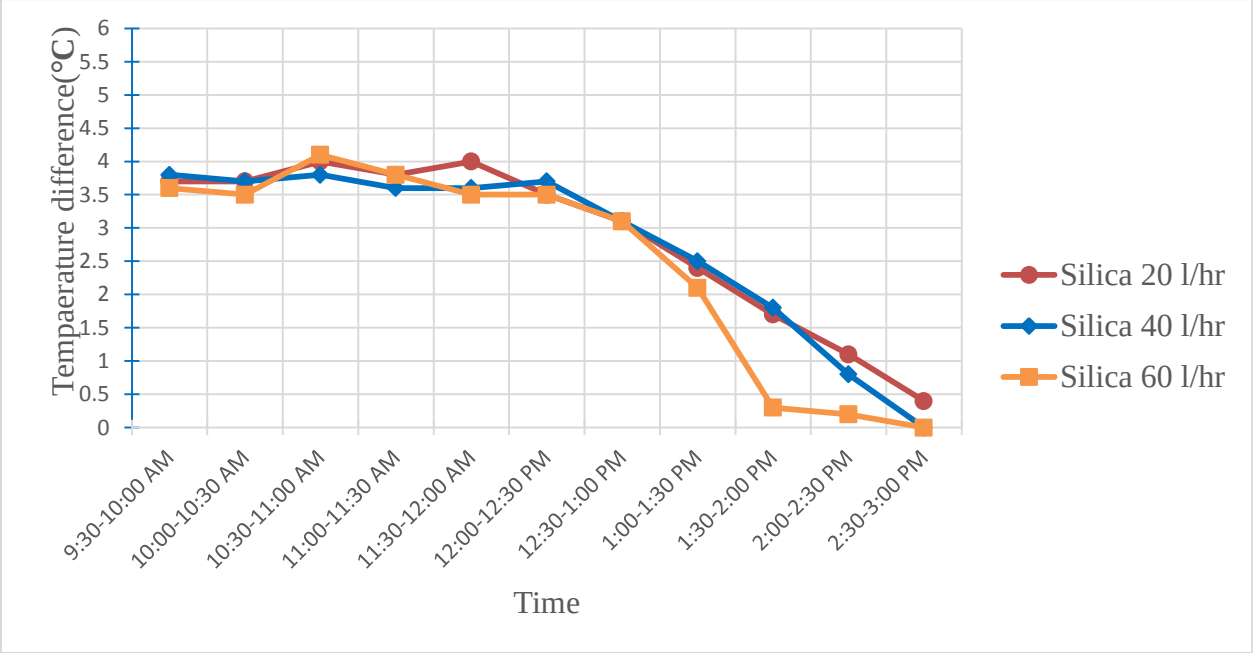

Fig.59 Variation in temperature difference with time for SiO_2-water based nanofluid (0.01% conc.) at different volume flow rate

3) Variation in useful heat gain with time for SiO_2-water based nanofluid (0.01% conc.) at different volume flow rate

Fig.60 shows variation in useful heat gain with time for SiO_2-water based nanofluid (0.01% conc.) at different volume flow rate. Volume flow rate is same for water and nanofluid but due to variation in density, volume flow rate is different for water and nanofluid. The specific heat of nanofluid is less as compared to water. In this case also, as the volume flow rate increases, useful

heat gain also increases. Useful heat gain in case of nanofluid is more as compared to water at particular volume flow rate. Temperature difference also more for nanofluid as compared to water.

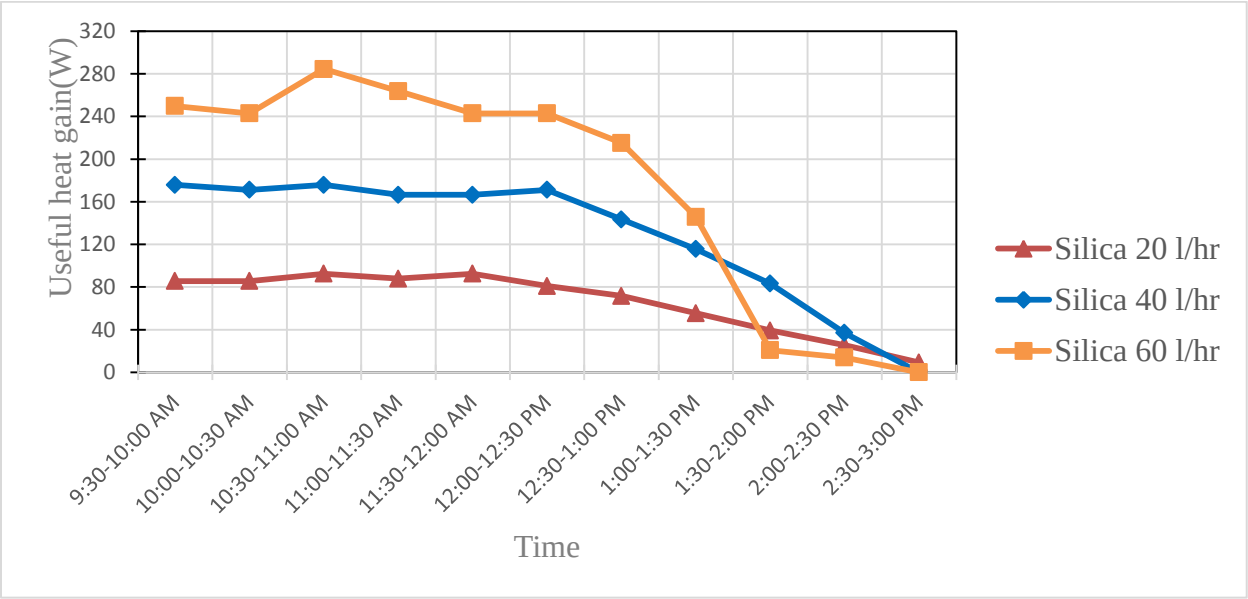

Fig.60 Variation in useful heat gain with time for SiO_2-water based nanofluid (0.01% conc.) at different volume flow

4) Variation in instantaneous efficiency with time for SiO_2-water based nanofluid (0.01% conc.) at different volume flow rate

The instantaneous efficiency is maximum at volume flow rate of 60 l/h for SiO_2-water based nanofluid (0.01% conc.) except the instantaneous efficiency around 1:30-3:00 pm as shown in fig.61. The reasons for this are high volume flow rate, high useful heat gain. The maximum instantaneous efficiency obtained for SiO_2-water based nanofluid (0.01% conc.) is 30.48% at volume flow rate of 60 l/h around 10:30-11:00 pm.

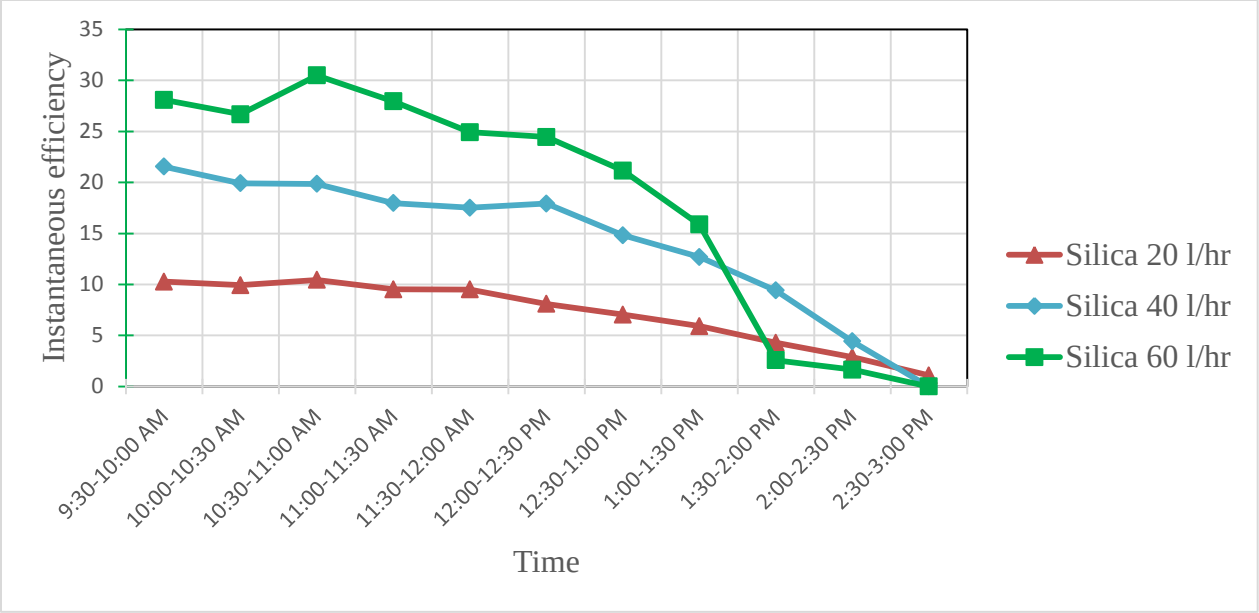

Fig.61 Variation in instantaneous efficiency with time for SiO_2-water based nanofluid (0.01% conc.) at different volume flow rate

5) Variation in thermal efficiency with time for SiO_2-water based nanofluid (0.01% conc.) at different volume flow rate

In this case, volume of nanofluid in storage tank and specific heat is different from water but same for different volume flow rate of nanofluid. Temperature difference in this case is good as compared to water. So, improvement in thermal efficiency has been observed as compared to thermal efficiency of water. Aperture area and time is same for all kinds of working fluid.

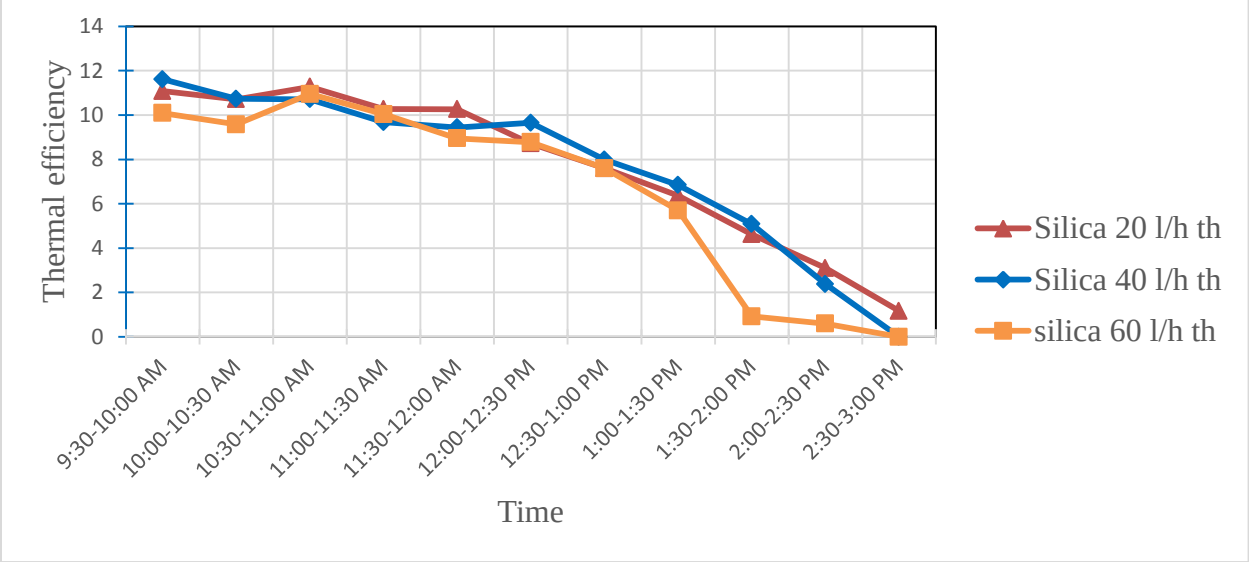

Fig.62 Variation in thermal efficiency with time for SiO_2-water based nanofluid (0.01% conc.) at different volume flow rate

1) Variation in solar intensity and temperature with time

a) For SiO_2-water based nanofluid (0.05% conc.) at volume flow rate of 20 l/h

The reading of this has been taken on 15 May, 2014 from 9:30 am to 3:00 pm. The maximum solar intensity in this case is 929 W/m^2 at 1:00 pm and after 1:00 pm, solar intensity continuously decreases as shown in fig.64. The maximum outlet temperature is 63.9^0 C at 3:00 pm and the initial temperature is 32^0 C. In this case, both inlet and outlet temperatures of nanofluid are increases continuously upto 3:00 pm as shown in fig.63.

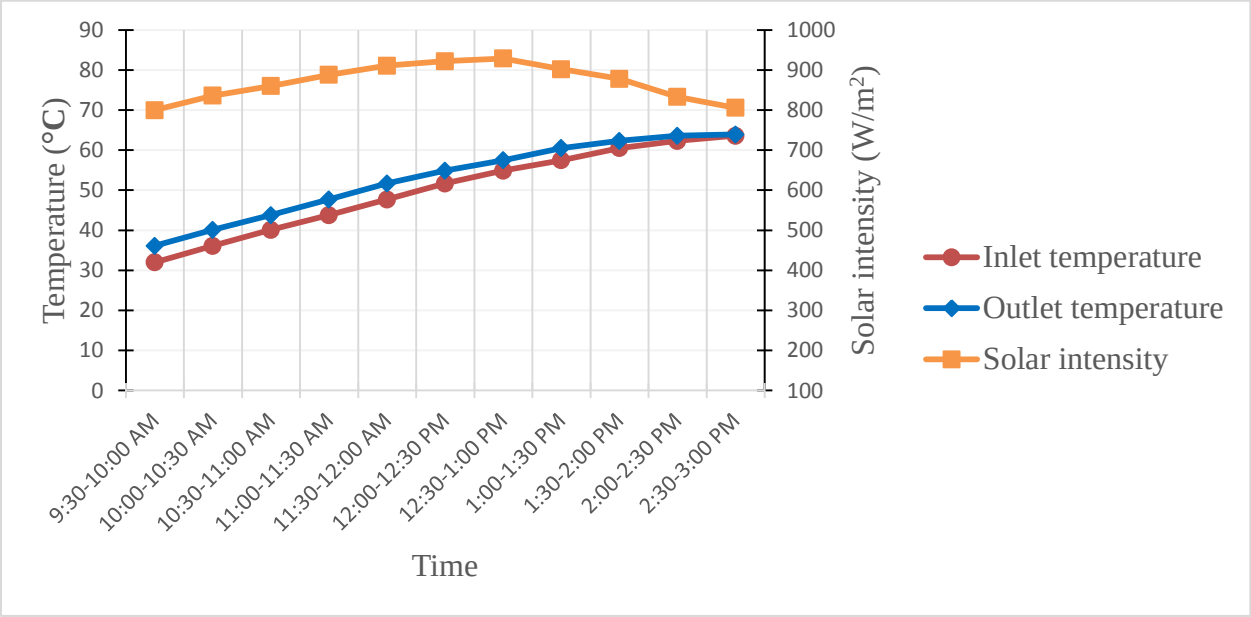

Fig.63 Variation in solar intensity and temperature with time for SiO_2 nanofluid (0.05% conc.) at volume flow rate of 20 l/h

b) For SiO_2-water based nanofluid (0.05% conc.) at volume flow rate of 40 l/h

The reading of this has been taken on 16 May, 2014 from 9:30 am to 3:00 pm. The maximum solar intensity in this case is 954 W/m^2 at 12:30 pm and after 12:30 pm, solar intensity continuously decreases as shown in fig.65. The maximum outlet temperature is 63.2^0 C at 2:30 pm and the initial temperature is 32.5^0 C. In this case, the outlet temperatures of nanofluid increases continuously upto 2:30 pm as shown in fig.64.

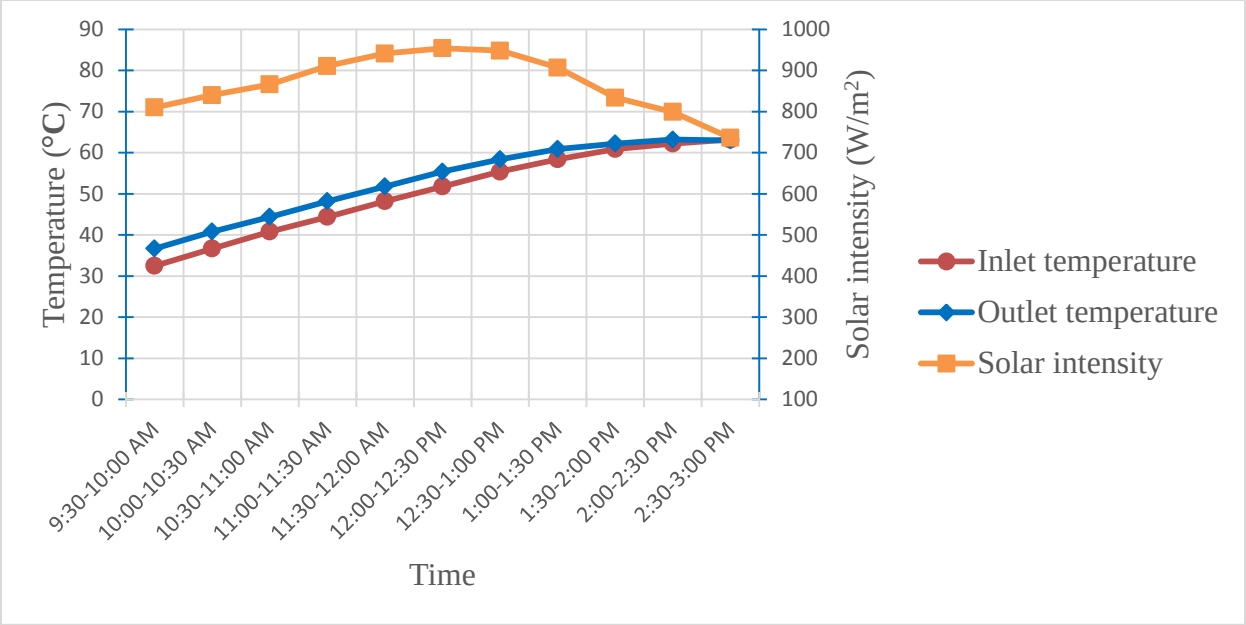

Fig.64 Variation in solar intensity and temperature with time for SiO_2 nanofluid (0.05% conc.) at volume flow rate of 40 l/h

c) For SiO_2-water based nanofluid (0.05% conc.) at volume flow rate of 60 l/h

The reading of SiO_2 nanofluid (0.05% conc.) at volume flow rate of 60 l/h is taken on 18May, 2014 from 9:30 am to 3:00 pm. In this case, the maximum solar intensity is at 1:00 pm which is 961 W/m^2 and the maximum outlet temperature is 65.4^0 C. Both the inlet and outlet temperatures are increases continuously upto 3:00 pm and the solar intensity increases continuously upto 1:00 pm as shown in fig.65. The initial temperature in this case is 31.1^0 C.

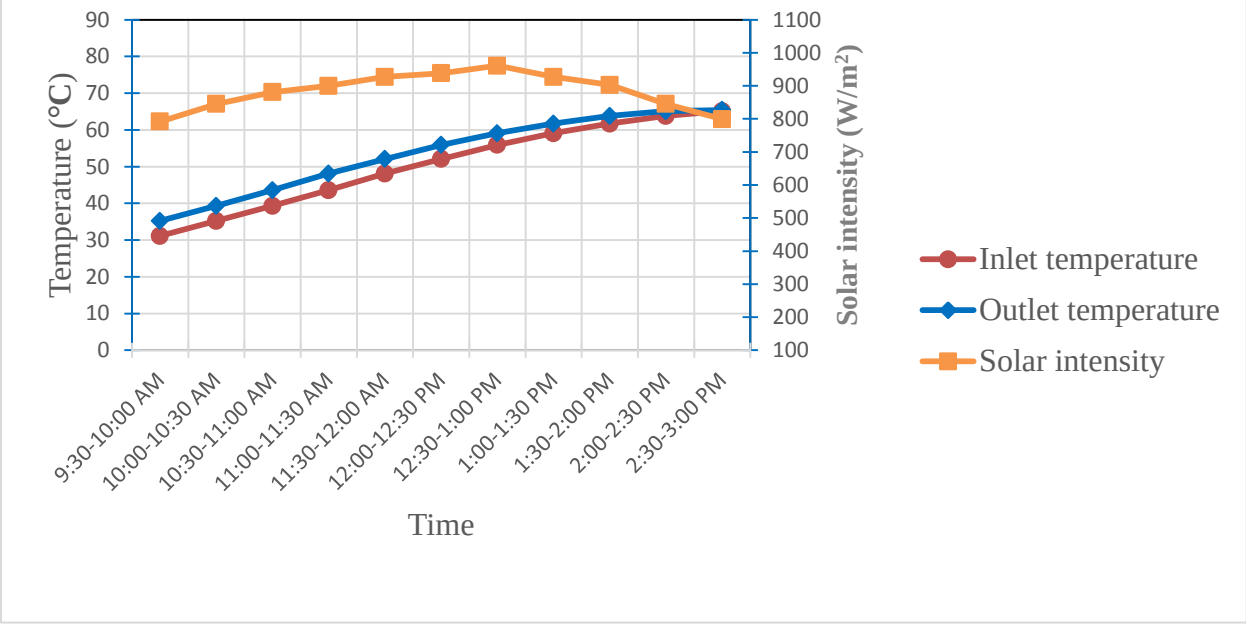

Fig.65 Variation in solar intensity and temperature with time for SiO_2 nanofluid (0.05% conc.) at volume flow rate of 60 l/h

2) Variation in temperature difference with time for SiO_2 nanofluid (0.05% conc.) at different volume flow rate

Fig.66 shows the variation in temperature difference with time for SiO_2-water based nanofluid (0.05% conc.) at different volume flow rate. The absorbing heat capacity of working fluid decreases due to discontinuity in solar intensity. If increasing solar intensity falls continuously on the reflector, then it reflects maximum solar radiations on receiver tube and due to this, absorbing heat capacity of working fluid also increases. Temperature of the working fluid can also affects the temperature difference.

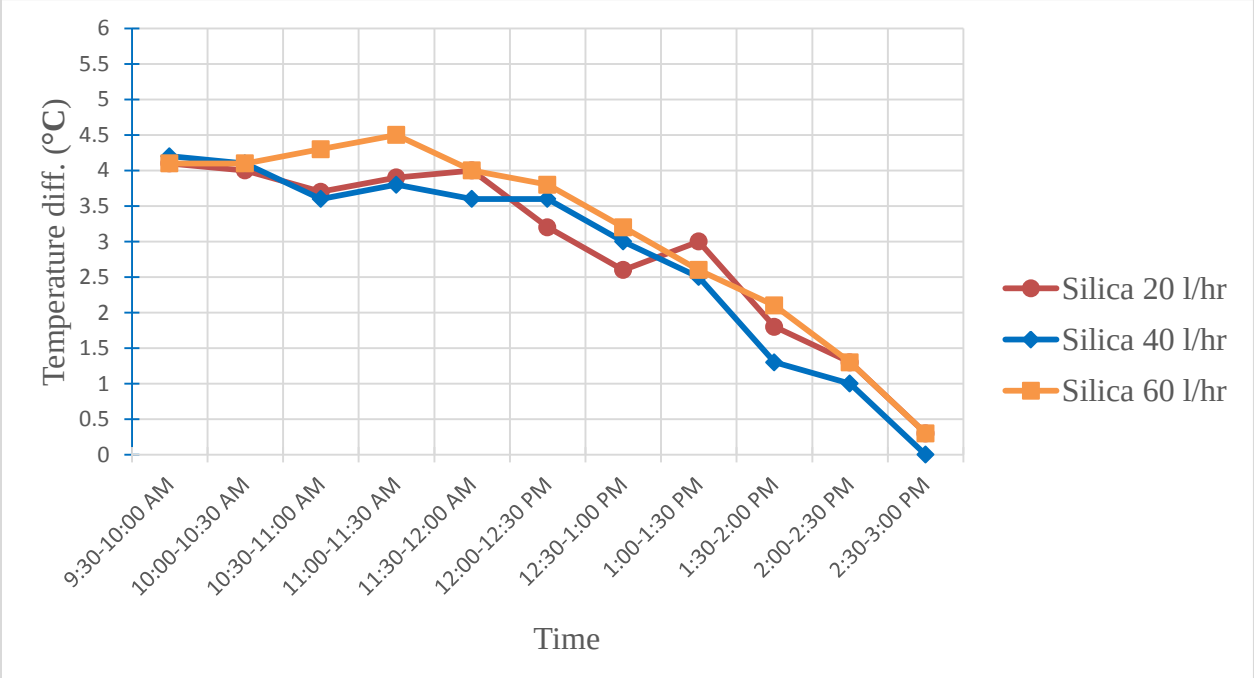

Fig.66 Variation in temperature difference with time for SiO_2-water based nanofluid (0.05% conc.) at different volume flow rate

3) Variation in useful heat gain with time for SiO_2 nanofluid (0.05% conc.) at different volume flow rate

For SiO_2-water based nanofluid (0.05% conc.) at different volume flow rate, variation in useful heat gain with time is shown in fig.67. The maximum useful heat gain is 305.03 W at volume flow rate of 60 l/h. Discontinuity in solar intensity affects the useful heat gain because due to

this, temperature difference decreases. As the volume flow rate increases, useful heat gain also increases as shown in fig.68. Specific heat is less in SiO_2-water based nanofluid (0.05% conc.) as compared to SiO_2-water based nanofluid (0.01% conc.) and water. Useful heat gain also varies according to the variation in temperature difference.

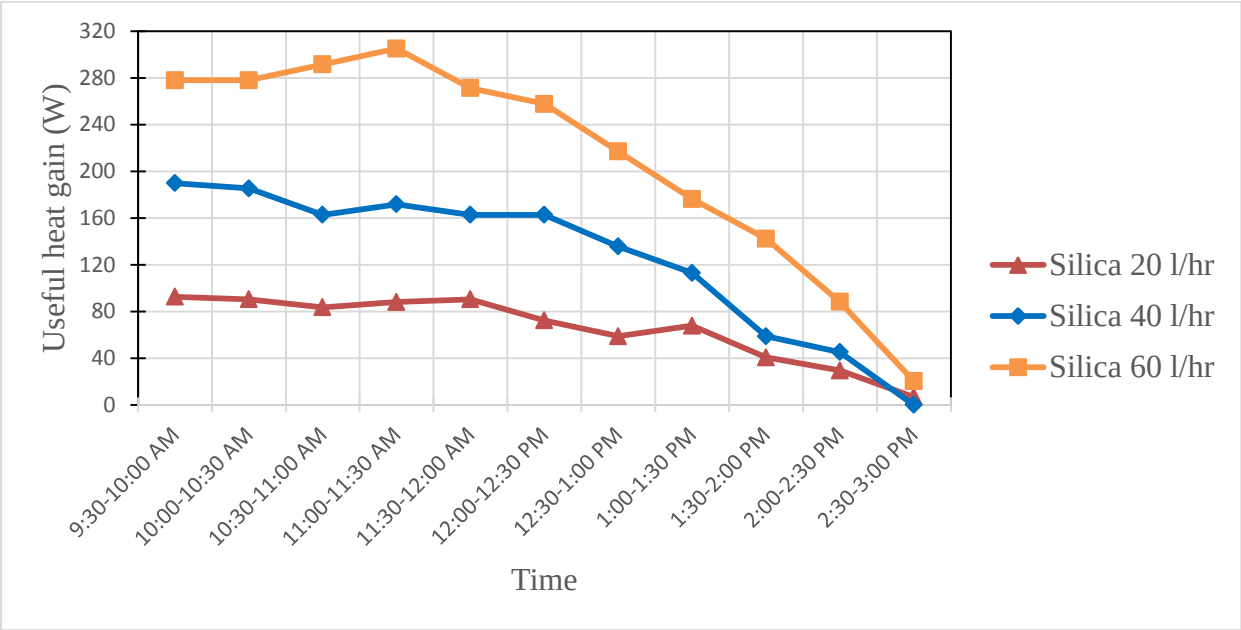

Fig.67 Variation in useful heat gain with time for SiO_2-water based nanofluid (0.05% conc.) at different volume flow rate

4) Variation in instantaneous efficiency with time for SiO_2-water based nanofluid (0.05% conc.) at different volume flow rate

Variation in instantaneous efficiency with time for SiO_2-water based nanofluid (0.05% conc.) at different volume flow rate is shown in fig.68. The instantaneous efficiency is more at volume flow rate of 60 l/h for SiO_2-water based nanofluid (0.05% conc.) as compared to volume flow rate of 20 l/h and 40 l/h. The reasons for this are high volume flow rate, high useful heat gain, continuous solar intensity, high temperature difference. The specific heat taken is same for all volume flow rate of SiO_2-water based nanofluid (0.05% conc.) to avoid increasing no. of calculations.

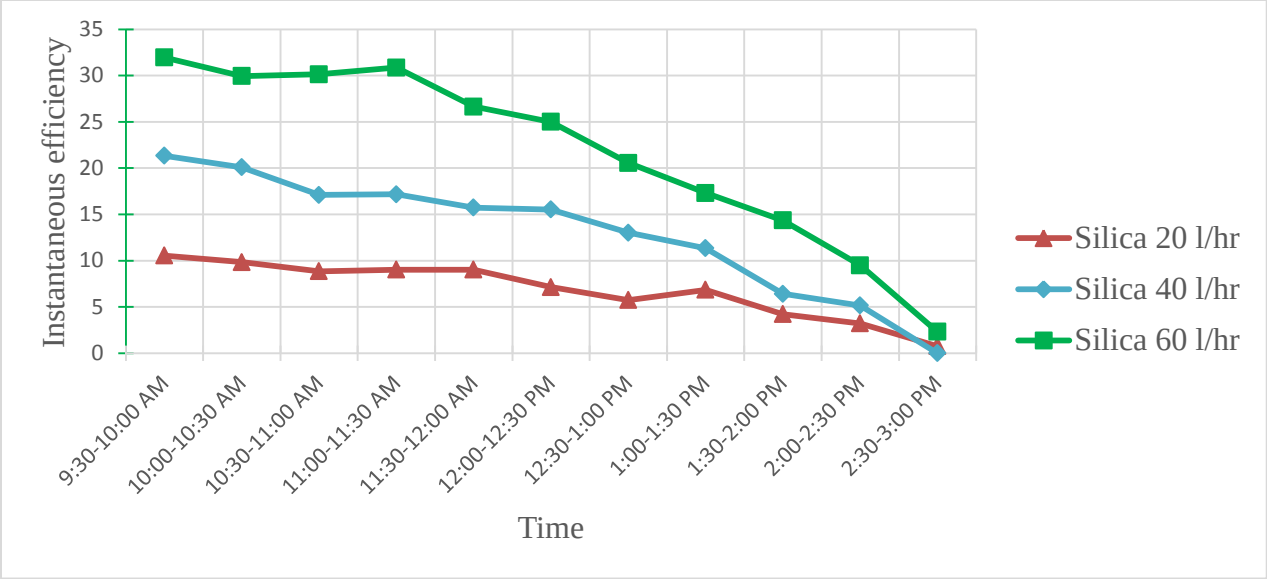

Fig.68 Variation in instantaneous efficiency with time for SiO_2-water based nanofluid (0.05% conc.) at different volume flow rate

5) Variation in thermal efficiency with time for SiO_2-water based nanofluid (0.05% conc.) at different volume flow rate

The density of nanofluid at 0.05% conc. is more as compared to water and nanofluid at 0.01% conc. Due to this, volume of nanofluid at this conc. is also increases but remains same for different volume flow rate of nanofluid. Temperature difference is also better at this conc. But the specific heat of nanofluid at 0.05% conc. is less as compared to water and nanofluid at 0.01% conc. Due to this reason, reduction in efficiency at this concentration is observed. Other reasons for reduction in thermal efficiency are high agglomeration of nanoparticle and instability of nanofluid at higher concentration. The thermal efficiency of SiO_2-water based nanofluid (0.05% conc.) is high at volume flow rate of 60l/h as shown in fig.69.

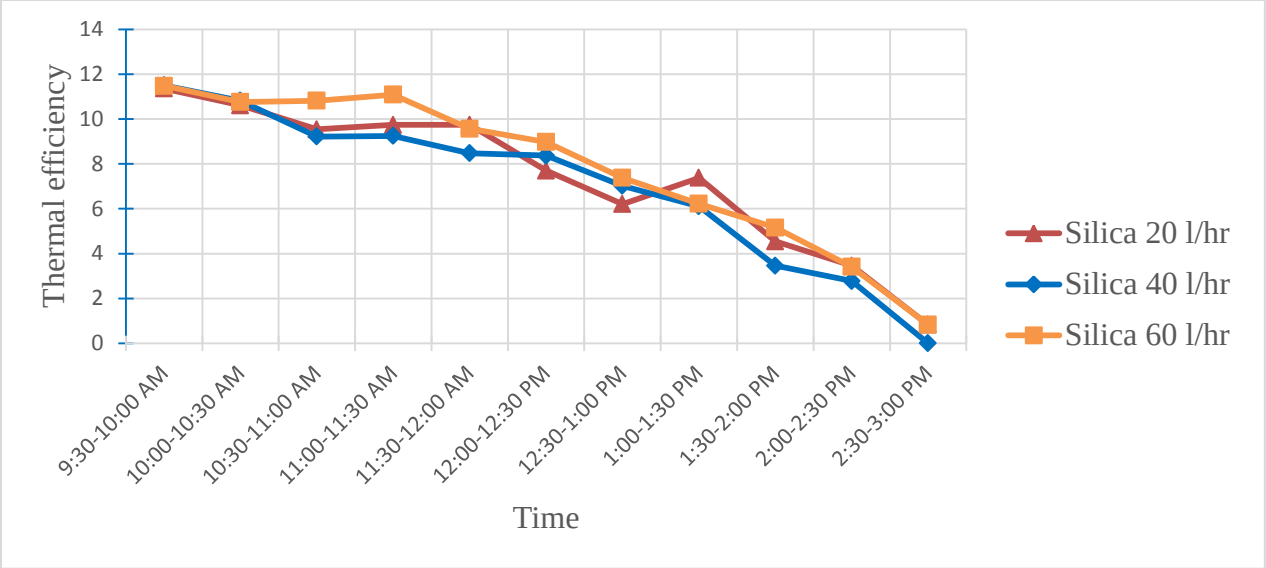

Fig.69 Variation in thermal efficiency with time for SiO_2-water based nanofluid (0.05% conc.) at different volume flow rate

1) Variation in solar intensity and temperature with time

a) For CuO-water based nanofluid (0.01% conc.) at volume flow rate of 20 l/h

The reading of CuO nanofluid has been taken on 26 May, 2014 from 9:30 am to 3:00 pm. In this case, the solar intensity increases continuously upto 1:30 pm and after that starts decreases as shown in fig. 70. The maximum solar intensity is 900 W/m^2 at 1:30 pm and the maximum outlet temperature is 64.8^0 C at 3:00 pm. Both the temperatures are continuously increases upto 3:00 pm. The initial temperature of the nanofluid is 30^0 C.

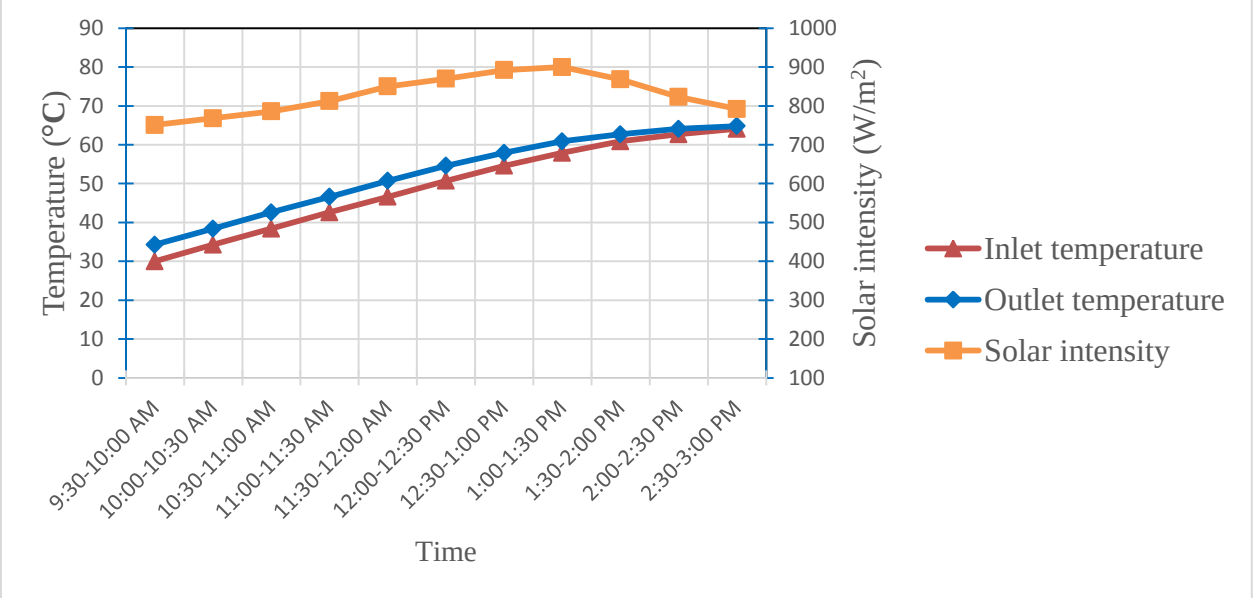

Fig.70 Variation in solar intensity and temperature with time for CuO nanofluid (0.01% conc.) at volume flow rate of 20 l/h

b) For CuO-water based nanofluid (0.01% conc.) at volume flow rate of 40 l/h

The reading of CuO nanofluid has been taken on 28 May, 2014 from 9:30 am to 3:00 pm. In this case, the solar intensity increases continuously upto 1:00 pm and after that starts decreases as shown in fig.71. The maximum solar intensity is 907 W/m^2 at 1:00 pm and the maximum outlet temperature is 68.4^0 C at 3:00 pm. Both the temperatures are continuously increases upto 3:00 pm. The initial temperature of the nanofluid is 33.5^0 C.

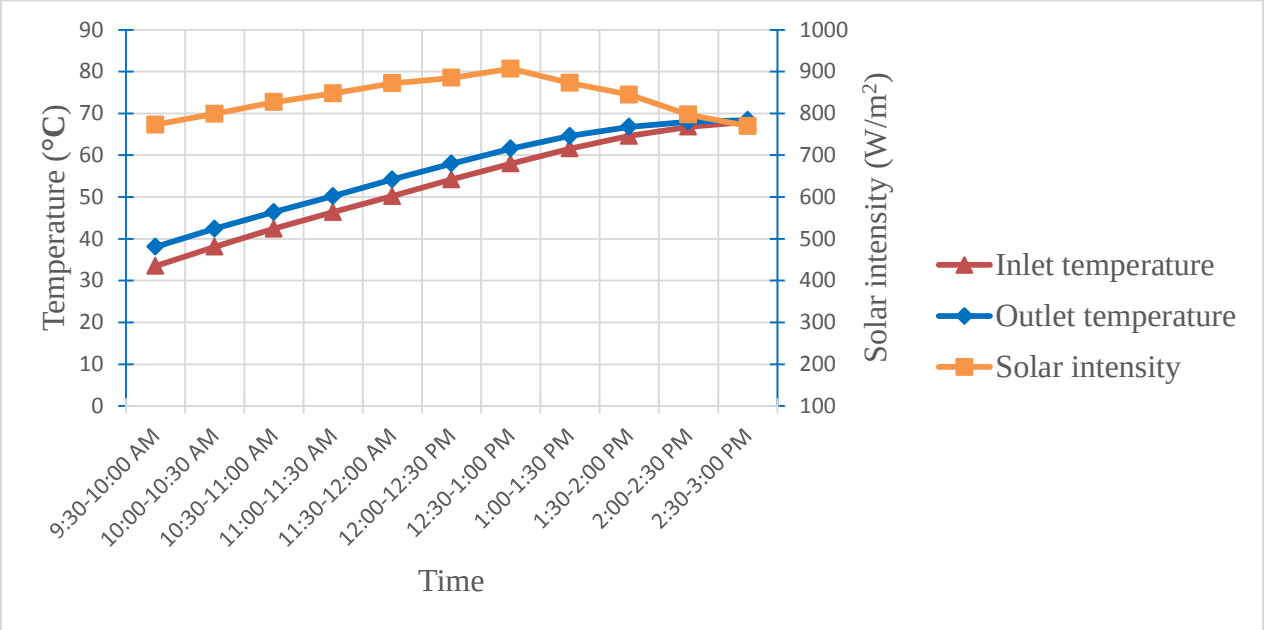

Fig.71 Variation in solar intensity and temperature with time for CuO nanofluid (0.01% conc.) at volume flow rate of 40 l/h

c) For CuO-water based nanofluid (0.01% conc.) at volume flow rate of 60 l/h

The reading of CuO nanofluid (0.01% conc.) at volume flow rate of 60 l/h is taken on 29May, 2014 from 9:30 am to 3:00 pm. In this case, the maximum solar intensity is at 1:00 pm which is 885 W/m^2 and the maximum outlet temperature is 70.2^0 C. Both the inlet and outlet temperatures are increases continuously upto 3:00 pm and the solar intensity increases continuously upto 1:00 pm as shown in fig.72. The initial temperature in this case is 34.5^0 C.

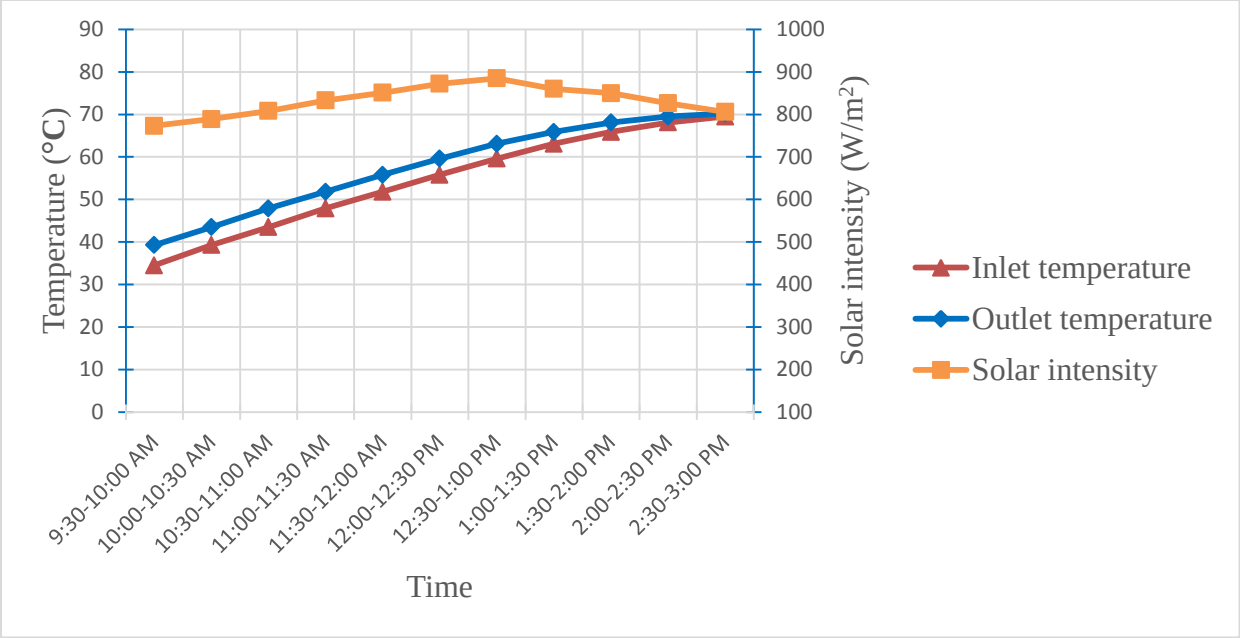

Fig.72 Variation in solar intensity and temperature with time for CuO nanofluid (0.01% conc.) at volume flow rate of 60 l/h

2) Variation in temperature difference with time for CuO-water based nanofluid (0.01% conc.) at different volume flow rate

Variation in temperature difference with time for CuO-water based nanofluid (0.01% conc.) at different volume flow rate is shown in fig.73. Temperature difference varies according to the variation in solar intensity. The overall temperature difference is better in case of CuO-water based nanofluid at volume flow rate of 60 l/h. The temperature difference in other volume flow rates are also good.

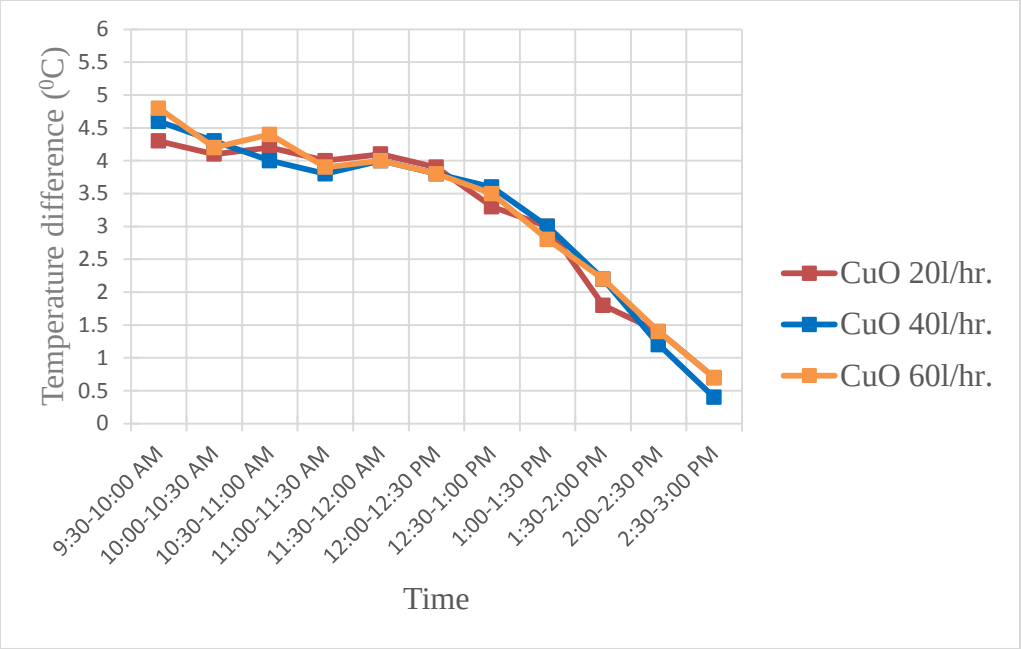

Fig.73 Variation in temperature difference with time for CuO-water based nanofluid (0.01% conc.) at different volume flow rate

3) Variation in useful heat gain with time for CuO-water based nanofluid (0.01% conc.) at different volume flow rate

Variation in useful heat gain with time for CuO-water based nanofluid (0.01% conc.) at different volume flow rate is shown in fig. 74. Due to its better thermophysical properties, useful heat gain also more as compared to water and SiO_2-water based nanofluid at particular volume flow rate. The maximum useful heat gain is 334.33 W at volume flow rate of 60 l/h. As the volume flow rate increases, useful heat gain also increases. The specific heat of CuO-water based nanofluid (0.01% conc.) is less as compared to water and SiO_2-water based nanofluid But temperature difference is more.

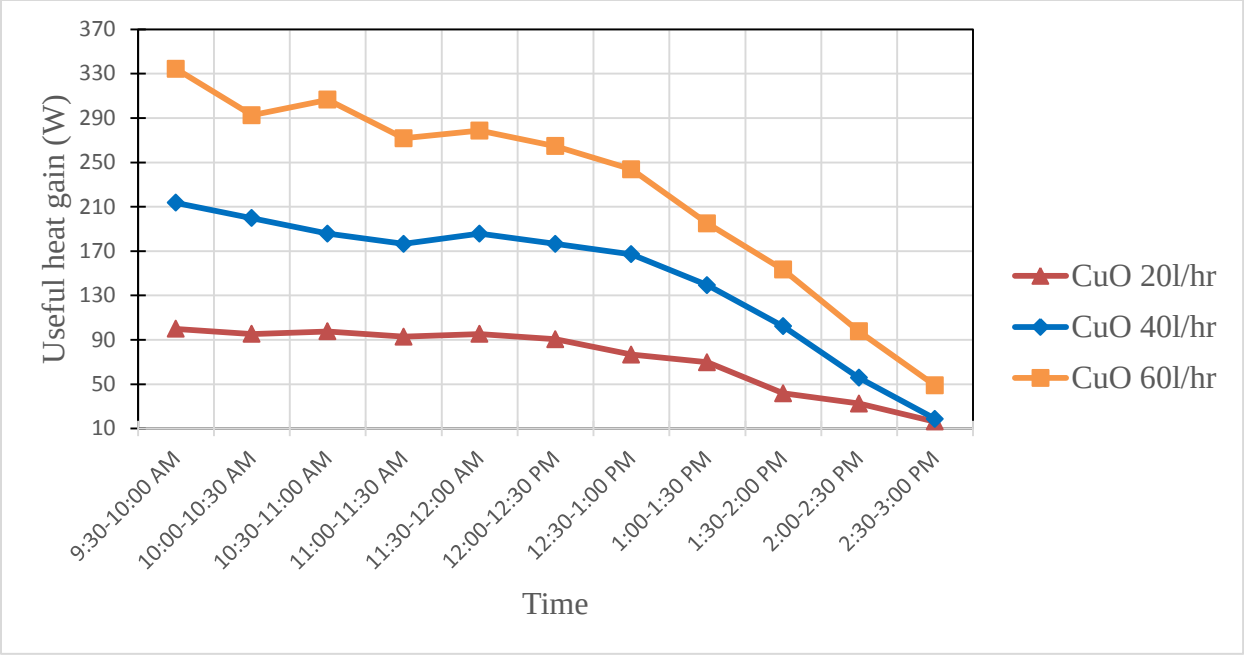

Fig.74 Variation in useful heat gain with time for CuO-water based nanofluid (0.01% conc.) at different volume flow rate

4) Variation in instantaneous efficiency with time for CuO-water based nanofluid (0.01% conc.) at different volume flow rate

Variation in instantaneous efficiency with time for CuO-water based nanofluid (0.01% conc.) at different volume flow rate is shown in fig.75. The maximum instantaneous efficiency is 39.39% at volume flow rate of 60 l/h around 9:30-10:00 pm. The other thing is instantaneous efficiency is more at various times for CuO-water based nanofluid (0.01% conc.) at volume flow rate of 60 l/h as compared to CuO-water based nanofluid (0.01% conc.) at volume flow rate of 20 l/h and 40 l/h as shown in fig.75. The reasons for this are high volume flow rate, high useful heat gain, continuous solar intensity, high temperature difference. The specific heat taken is same for all volume flow rates of CuO-water based nanofluid (0.01% conc.) to avoid increasing no. of calculations.

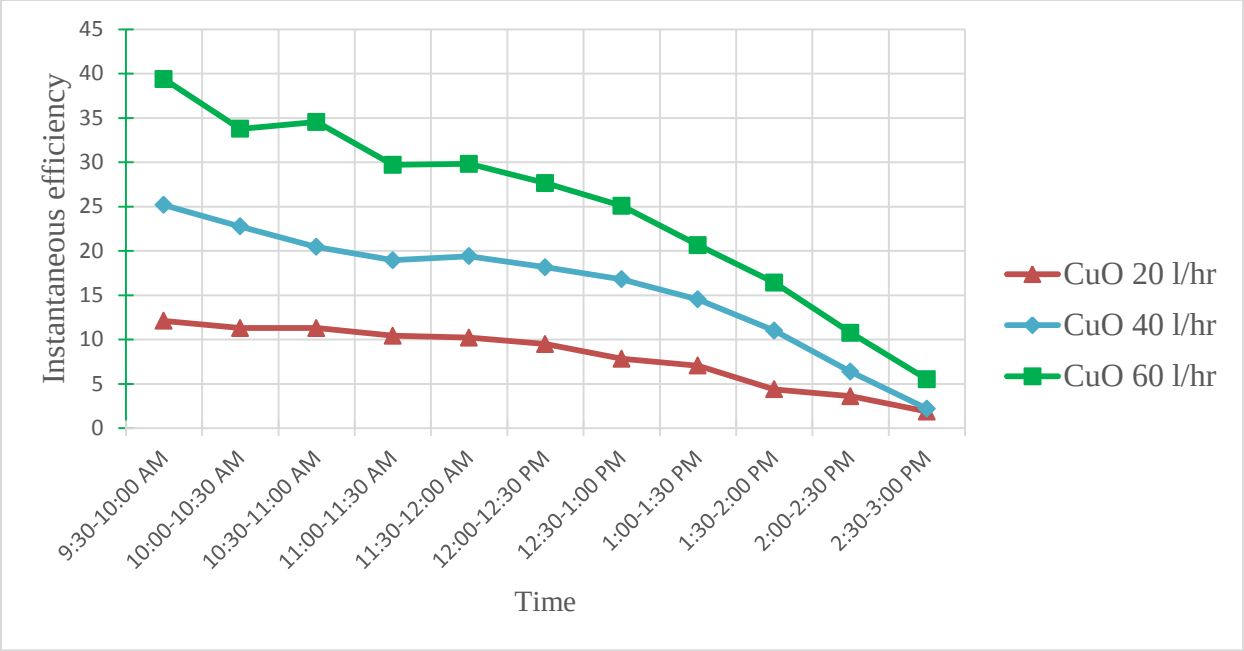

Fig.75 Variation in instantaneous efficiency with time for CuO-water based nanofluid (0.01% conc.) at different volume flow rate

5) Variation in thermal efficiency with time for CuO-water based nanofluid (0.01% conc.) at different volume flow rate

CuO-water based nanofluid has excellent thermophysical properties as compared to SiO_2-water based nanofluid and water. So, the thermal efficiency at this conc. is high for CuO-water based nanofluid as compared to SiO_2-water based nanofluid and water. Also, the temperature difference is more in this case. The maximum thermal efficiency is obtained at volume flow rate of 60 l/h for CuO-water based nanofluid (0.01% conc.) as shown in fig.76.

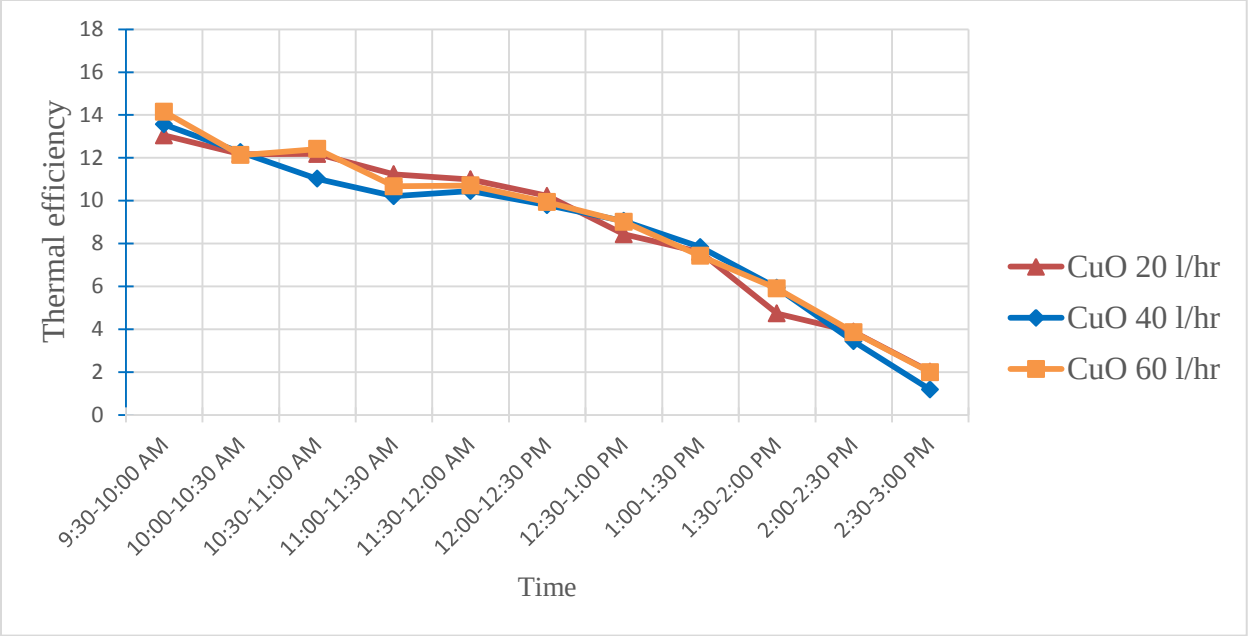

Fig.76 Variation in thermal efficiency with time for CuO-water based nanofluid (0.01% conc.) at different volume flow rate

1) Variation in solar intensity and temperature with time

a) For CuO-water based nanofluid (0.05% conc.) at volume flow rate of 20 l/h

The reading is taken on 2 June, 2014 from 9:30 to 3:00 pm at 0.05% concentration of CuO nanofluid and volume flow rate of 20 l/h. The solar intensity continuously increases upto 1:30 pm and after that starts decreases continuously. Both the temperatures are continuously increases upto 3:00 pm as shown in fig.77. The maximum solar intensity and outlet temperature are 948 W/m^2 at 1:30 pm and 68.9^0 C at 3:00 pm respectively. The initial temperature is 32^0 C at 9:30 am.

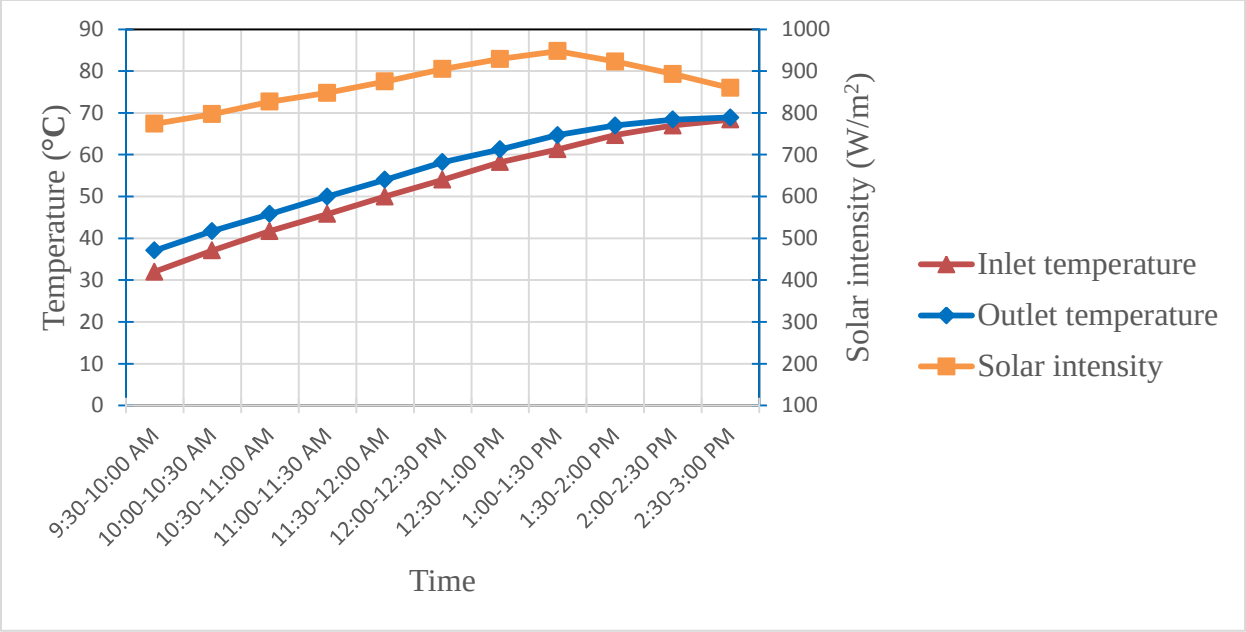

Fig.77 Variation in solar intensity and temperature with time for CuO nanofluid (0.05% conc.) at volume flow rate of 20 l/h

b) For CuO-water based nanofluid (0.05% conc.) at volume flow rate of 40 l/h

The reading is taken on 3 June, 2014 from 9:30 to 3:00 pm at 0.05% concentration of CuO nanofluid and volume flow rate of 40 l/h. The solar intensity continuously increases upto 1:00 pm and after that starts decreases continuously. Both the temperatures are continuously increases upto 3:00 pm as shown in fig.78. The maximum solar intensity and outlet temperature are 944 W/m^2 at 1:00 pm and 70.6^0 C at 3:00 pm respectively. The initial temperature is 36.2^0 C at 9:30 am.

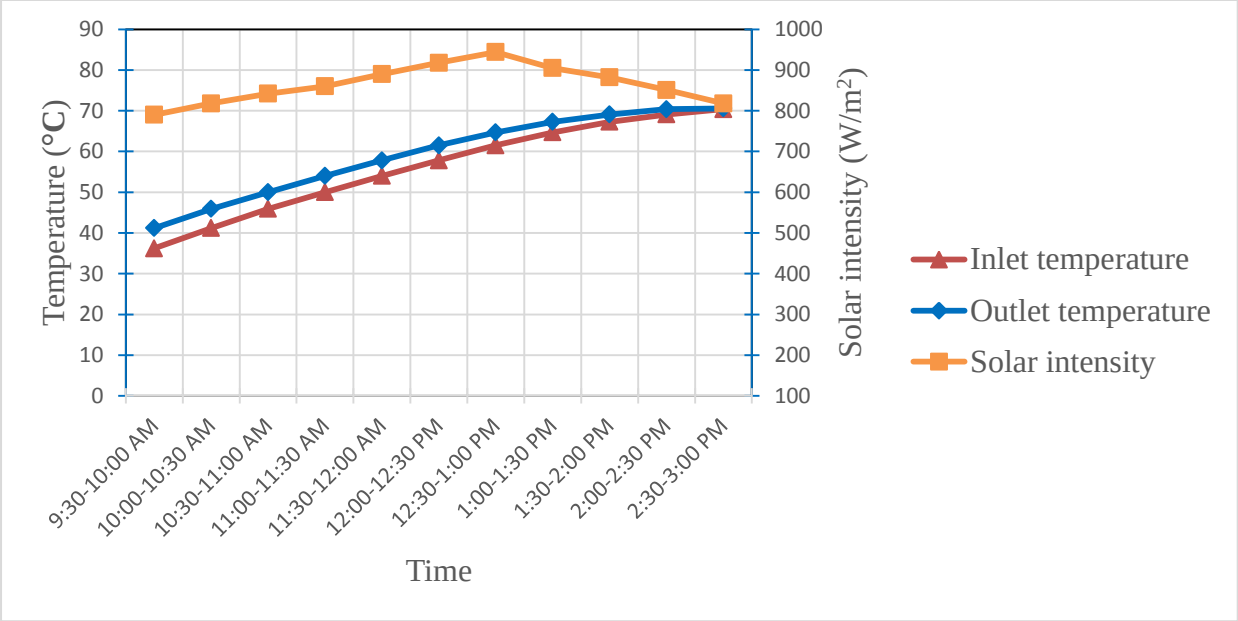

Fig.78 Variation in solar intensity and temperature with time for CuO nanofluid (0.05% conc.) at volume flow rate of 40 l/h

c) For CuO-water based nanofluid (0.05% conc.) at volume flow rate of 60 l/h

In this case, the solar intensity is continuously increases upto 1:00 pm and the maximum solar intensity is 946 W/m^2 at 1:00 pm as shown in fig.79. After 1:00 pm, solar intensity is continuously decreases. In case of temperature, both inlet and outlet temperatures of nanofluid are continuously increases upto 3:00 pm. The maximum outlet temperature of CuO nanofluid is 77^0 C and the initial temperature of nanofluid is 36.5^0 C. The reading of this has been taken on 4 June, 2014 from 9:30 am to 3:00 pm.

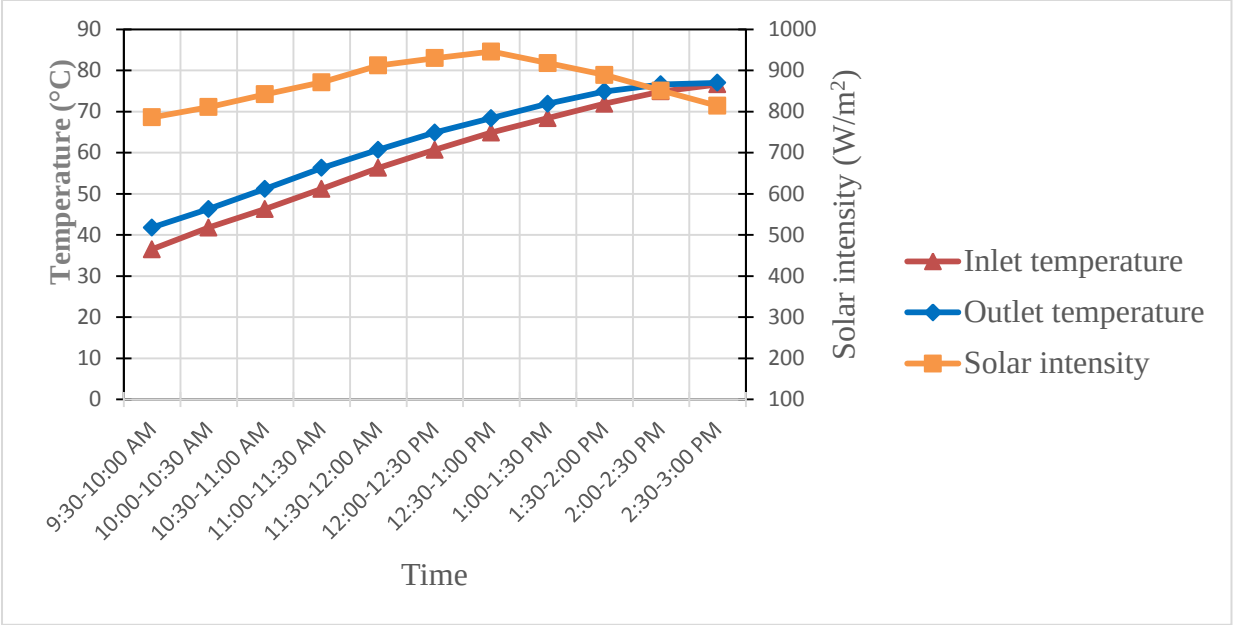

Fig.79 Variation in solar intensity and temperature with time for CuO nanofluid (0.05% conc.) at volume flow rate of 60 l/h

2) Variation in temperature difference with time for CuO-water based nanofluid (0.05% conc.) at different volume flow rate

The maximum variation in temperature difference for CuO-water based nanofluid (0.05% conc.) is at volume flow rate of 60 l/ due to high solar intensity all over the day. Also, for other two volume flow rates, temp. difference is good but less than that of 60 l/h as shown in fig.80.

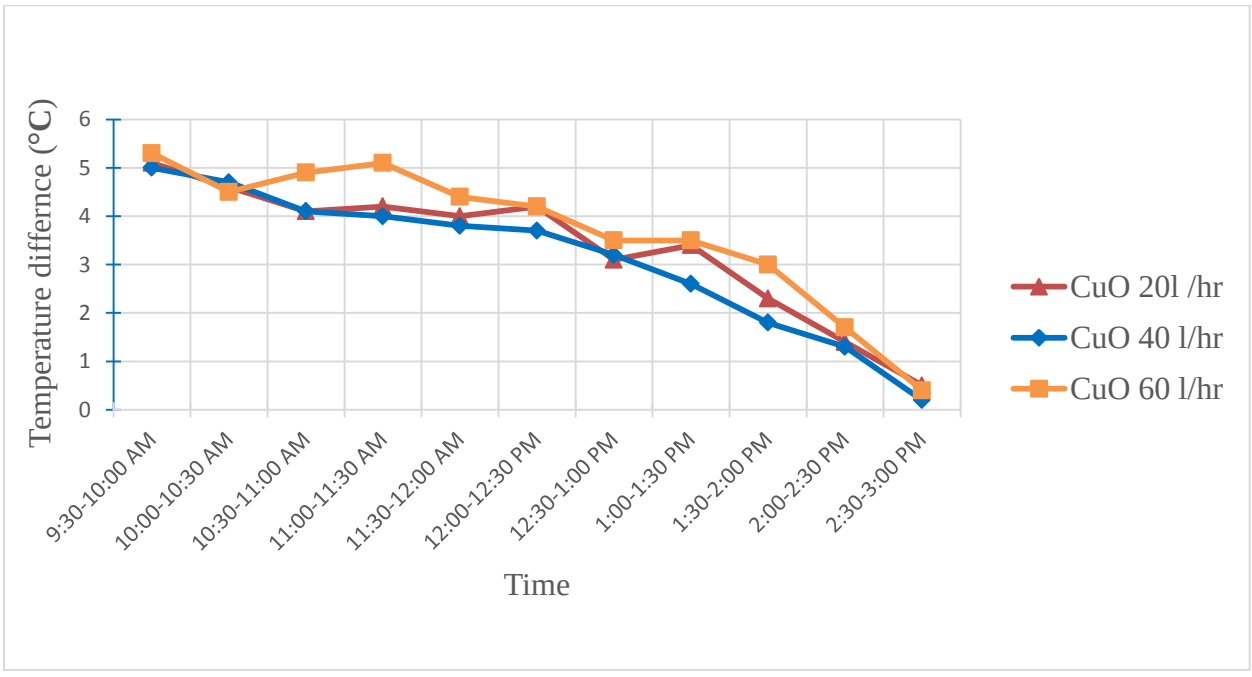

Fig.80 Variation in temperature difference with time for CuO-water based nanofluid (0.05% conc.) at different volume flow rate

3) Variation in useful heat gain with time for CuO-water based nanofluid (0.05% conc.) at different volume flow rate

The maximum useful heat gain obtained is 366.39 W at volume flow rate of 60 l/h which is highest all over the experiment as shown in fig.81. If the solar intensity is high, then the temperature difference also increases at particular volume flow rate which is the main cause of increase in useful heat gain. The specific heat is less as compared to CuO-water based nanofluid (0.01% conc.), SiO_2-water based nanofluid (0.01% conc.), SiO_2-water based nanofluid (0.05% conc.) and water. But the volume flow rate is high as compared to others due to its high density.

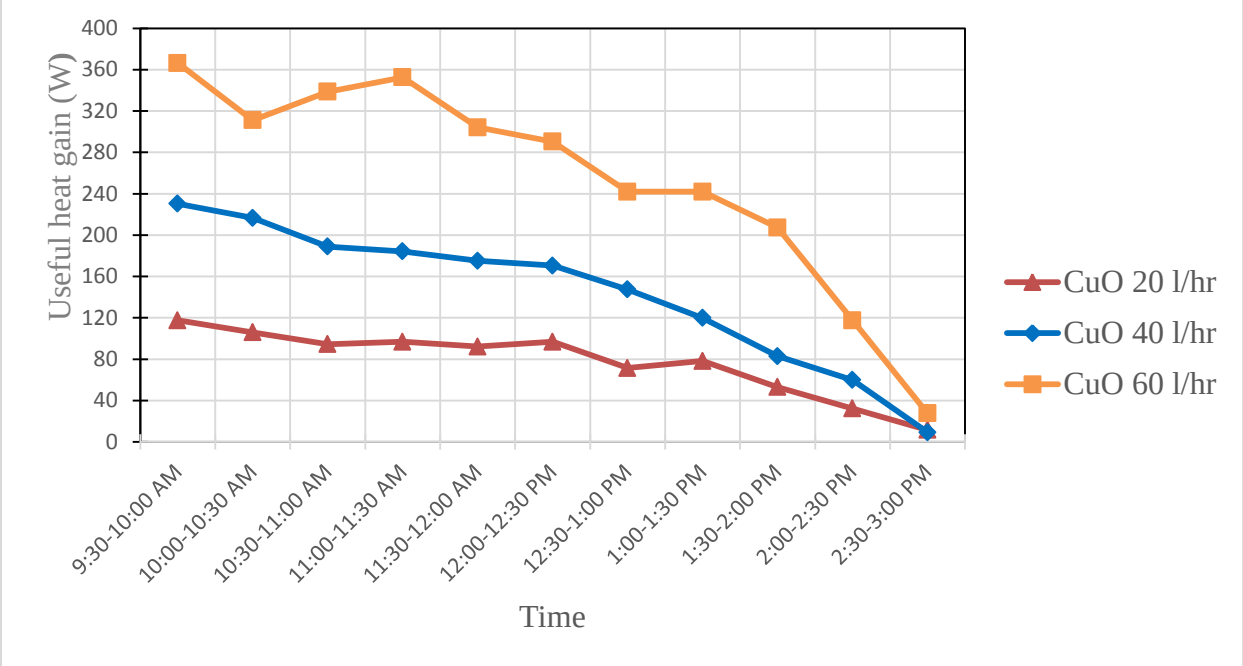

Fig.81 Variation in useful heat gain with time for CuO-water based nanofluid (0.05% conc.) at different volume flow rate

4) Variation in instantaneous efficiency with time for CuO-water based nanofluid (0.05% conc.) at different volume flow rate

Fig.82 shows the variation in instantaneous efficiency with time for CuO-water based nanofluid (0.05% conc.) at different volume flow rate. The maximum instantaneous efficiency is 42.45% at volume flow rate of 60 l/h around 9:30-10:00 pm which is maximum all over the experiment. Due to its excellent thermophysical properties like thermal conductivity, density, viscosity and

specific heat as compared to water and SiO_2-water based nanofluid, the instantaneous efficiency is high for CuO-water based nanofluid as compared to water and SiO_2-water based nanofluid.

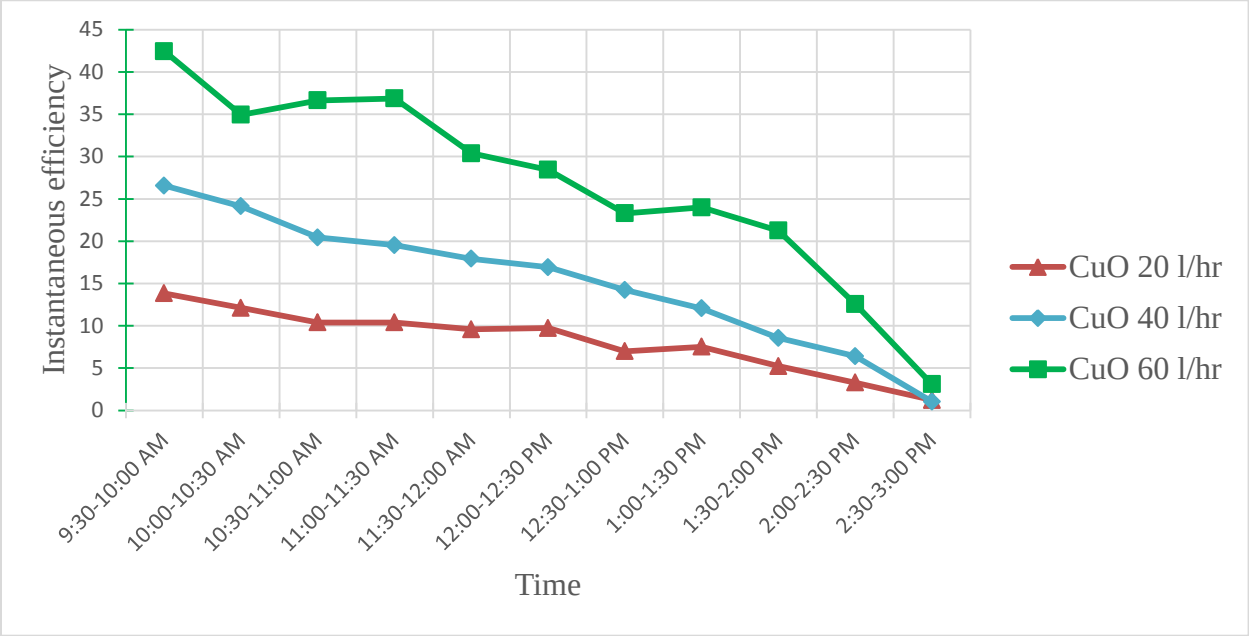

Fig.82 Variation in instantaneous efficiency with time for CuO-water based nanofluid (0.05% conc.) at different volume flow rate

5) Variation in thermal efficiency with time for CuO-water based nanofluid (0.05% conc.) at different volume flow rate

The variation in thermal efficiency with time at different volume flow rate for CuO-water based nanofluid (0.05% conc.) is shown in fig.83. The maximum thermal efficiency obtained is at volume flow rate of 60 l/h as compared to volume flow rate of 20 l/h and 40 l/h. The reason for this is higher temperature difference, excellent thermophysical properties and continuous solar intensity falling on the system.

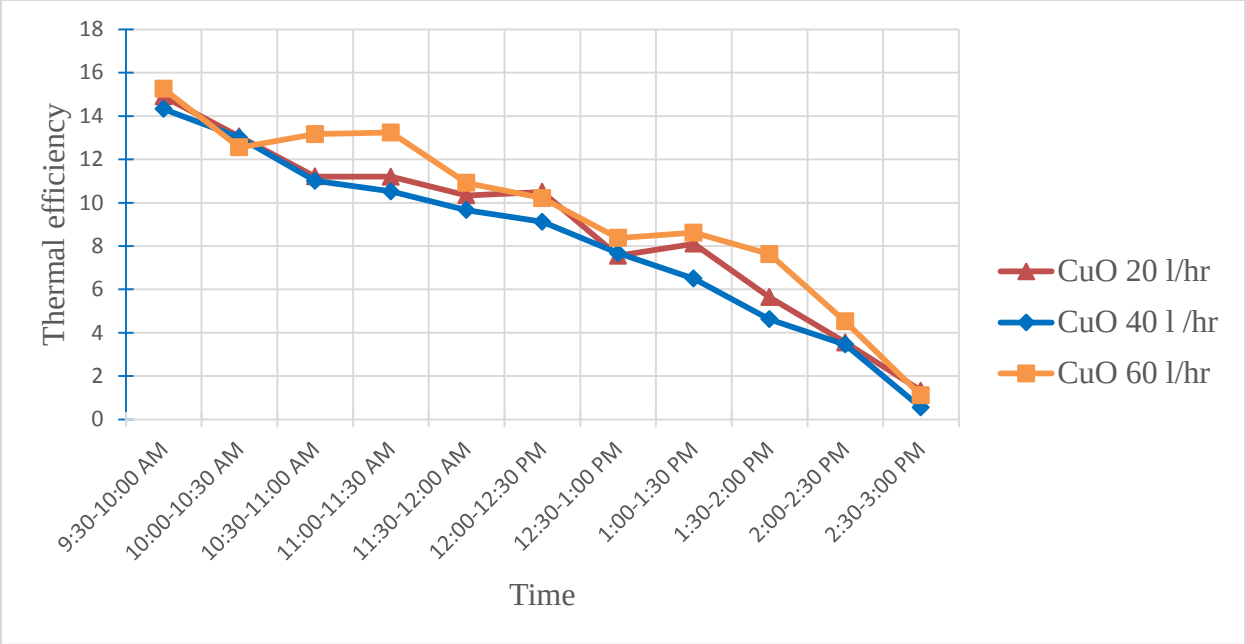

Fig.83 Variation in thermal efficiency with time for CuO-water based nanofluid (0.05% conc.) at different volume flow rate

6) Comparisons of instantaneous efficiency of water with nanofluids (0.01% conc.) at volume flow rate of 20 l/h

Fig.84 shows variation in instantaneous efficiency with time for water and nanofluids (0.01% conc.) at volume flow rate of 20 l/h. As we know, the thermophysical properties of water are not so good as compared to nanofluids. Nanoparticles are suspended in water to prepare the nanofluids which improves the thermophysical properties of water depend upon the type of nanoparticle used. The instantaneous efficiency of CuO-water based nanofluid (0.01% conc.) at volume flow rate of 20 l/h and at various time interval is more as compared to SiO_2-water based nanofluid (0.01% conc.) at volume flow rate of 20 l/h and water at volume flow rate of 20 l/h.

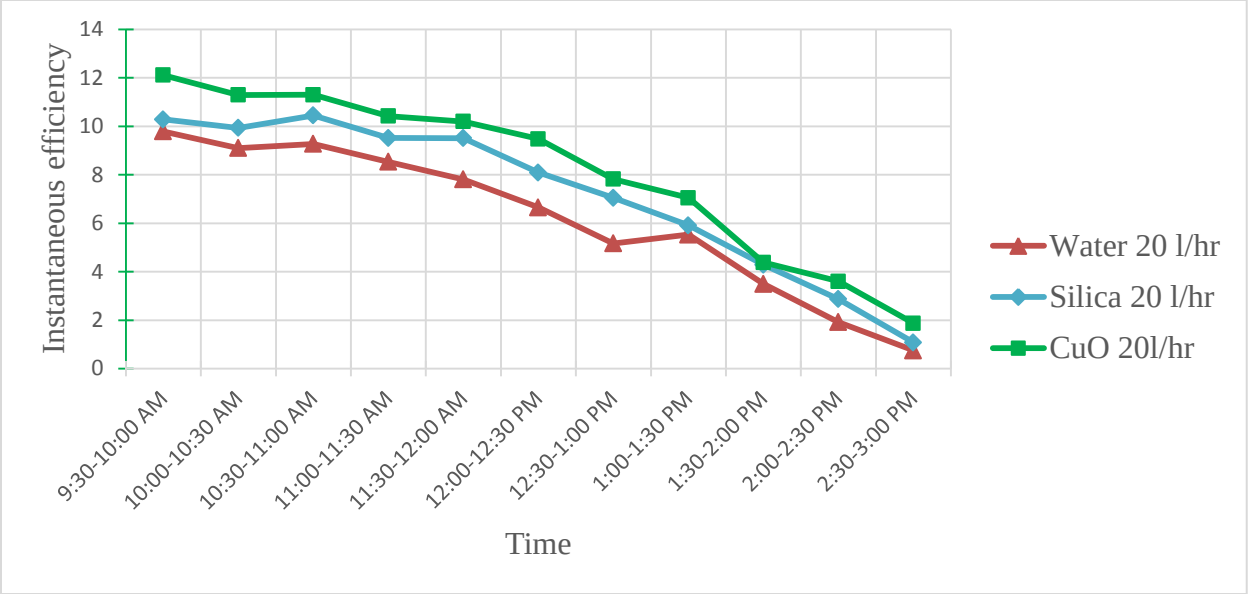

Fig.84 Variation in instantaneous efficiency with time for water and nanofluids (0.01% conc.) at volume flow rate of 20 l/h

7) Comparisons of instantaneous efficiency of water with nanofluids (0.01% conc.) at volume flow rate of 40 l/h

Variation in instantaneous efficiency with time for water and nanofluids (0.01% conc.) at volume flow rate of 40 l/h is shown in fig.85. The instantaneous efficiency increases as the volume flow rate increases for water and nanofluids but the maximum instantaneous efficiency is found to be in case of CuO-water based nanofluid at various time interval and at particular volume flow rate. So, CuO-water based nanofluid is most effective one as compared to water and SiO_2-water based nanofluid due to its excellent thermophysical properties like thermal conductivity, density etc.

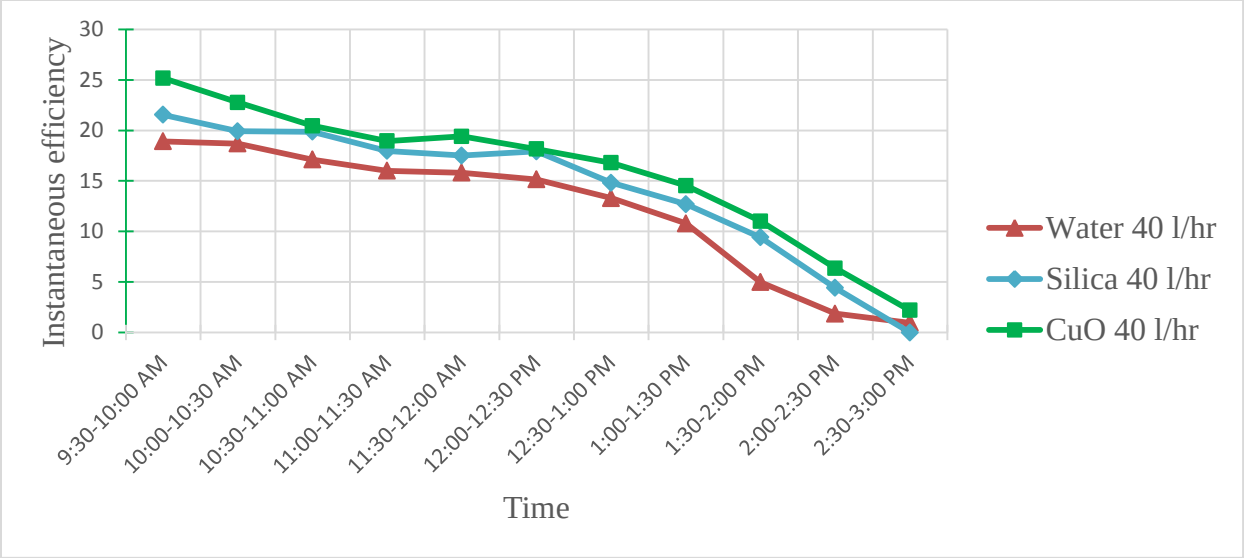

Fig.85 Variation in instantaneous efficiency with time for water and nanofluids (0.01% conc.) at volume flow rate of 40 l/h

8) Comparisons of instantaneous efficiency of water with nanofluids (0.01% conc.) at volume flow rate of 60 l/h

Fig.86 shows the variation in instantaneous efficiency with time for water and nanofluids (0.01% conc.) at volume flow rate of 60 l/h. The maximum instantaneous efficiencies for CuO-water based nanofluid, SiO_2-water based nanofluid and water at volume flow rate of 60 l/h having nanoparticles conc. 0.01% are found to be 39.39%, 30.48% and 29.34% respectively which means that CuO-water based nanofluid enhances more than 10% instantaneous efficiency of the system compared to water.

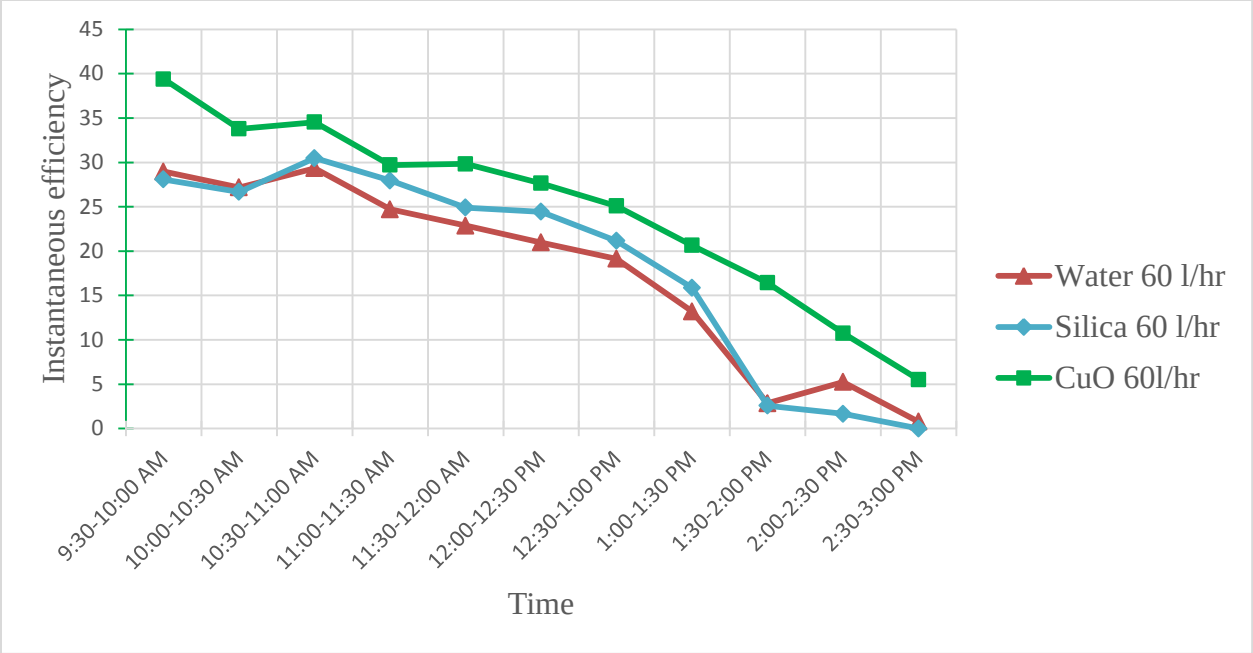

Fig.86 Variation in instantaneous efficiency with time for water and nanofluids (0.01% conc.) at volume flow rate of 60 l/h

9) Comparisons of instantaneous efficiency of water with nanofluids (0.05% conc.) at volume flow rate of 20 l/h

As the nanoparticles concentration increases in water, the thermophysical properties are also improved which means that system is more effective and perform better. In this case also, the maximum instantaneous efficiency of CuO-water based nanofluid (0.05% conc.) is 13.83% which is more as compared to maximum instantaneous efficiency of CuO-water based nanofluid (0.01% conc.) which has 12.11%. But some external factors like high wind speed, discontinuity in solar intensity and off power supply for sometime decreases the efficiency of high concentrated nanofluid also. The other factors are instability and agglomeration of nanoparticles in water at high concentration. Fig.87 shows variation in instantaneous efficiency with time for water and nanofluids (0.05% conc.) at volume flow rate of 20 l/h.

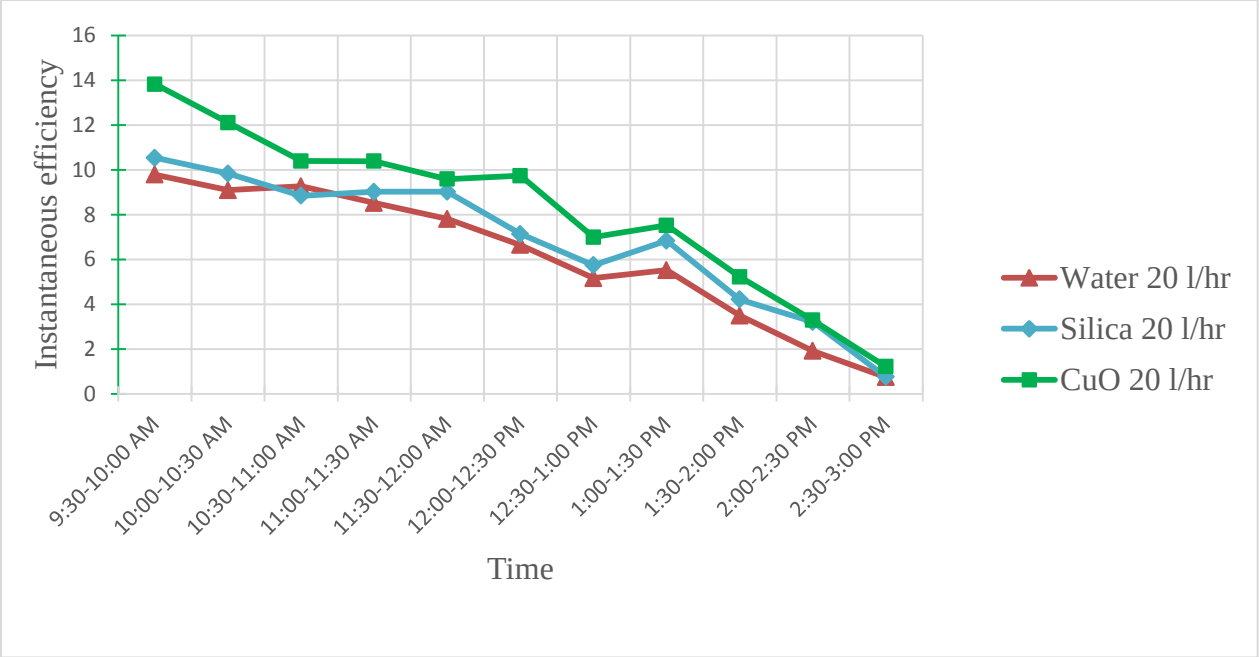

Fig.87 Variation in instantaneous efficiency with time for water and nanofluids (0.05% conc.) at volume flow rate of 20 l/h

10) Comparisons of instantaneous efficiency of water with nanofluids (0.05% conc.) at volume flow rate of 40 l/h

Variation in instantaneous efficiency with time for water and nanofluids (0.05% conc.) at volume flow rate of 40 l/h is shown in fig.88. The instantaneous efficiency at this flow rate is more as compared to instantaneous efficiency at volume flow rate of 20 l/h but less than the instantaneous efficiency at volume flow rate of 60 l/h. The maximum instantaneous efficiencies for CuO-water based nanofluid, SiO_2-water based nanofluid and water at volume flow rate of 40 l/h having nanoparticles conc. 0.05% are found to be 26.56%, 21.34% and 18.91% respectively. From this graph, it is also found that CuO-water based nanofluid is most effective one .

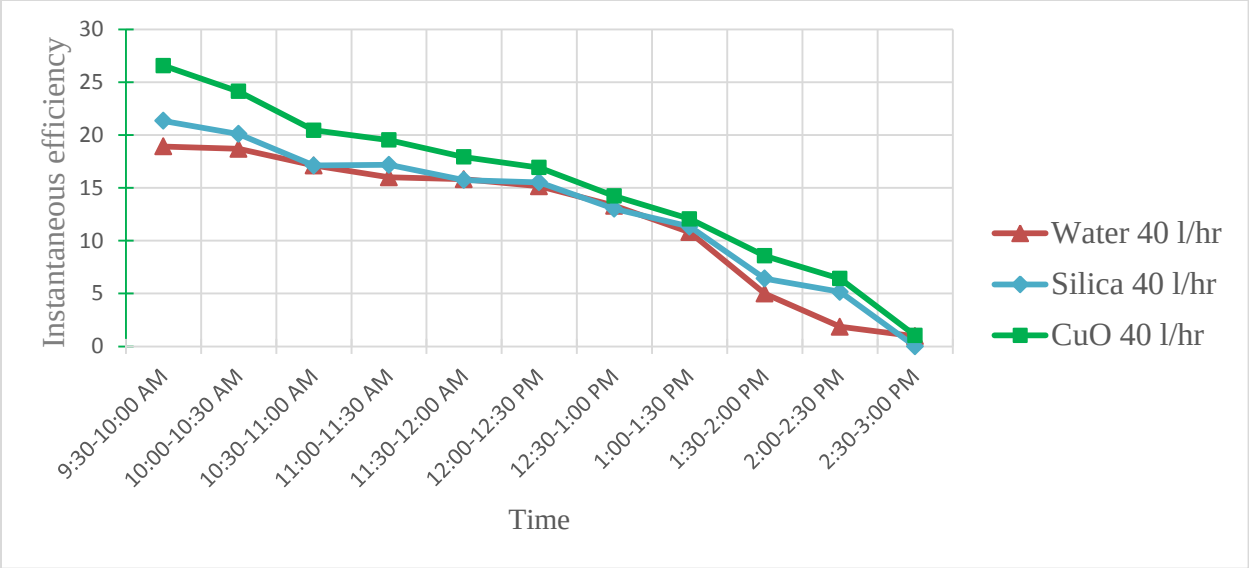

Fig.88 Variation in instantaneous efficiency with time for water and nanofluids (0.05% conc.) at volume flow rate of 40 l/h

11) Comparisons of instantaneous efficiency of water with nanofluids (0.05% conc.) at volume flow rate of 60 l/h

Fig.89 shows variation in instantaneous efficiency with time for water and nanofluids (0.05% conc.) at volume flow rate of 60 l/h. The maximum instantaneous efficiencies for CuO-water based nanofluid, SiO_2-water based nanofluid and water at volume flow rate of 60 l/h having nanoparticles conc. 0.05% are found to be 42.45%, 31.96% and 29.34% respectively. From the above results, it has been found that CuO-water based nanofluid gives better results at any concentration and at any volume flow rate as compared to SiO_2-water based nanofluid and water which means that CuO-water based nanofluid is more efficient one as compared to SiO_2-water based nanofluid and water.

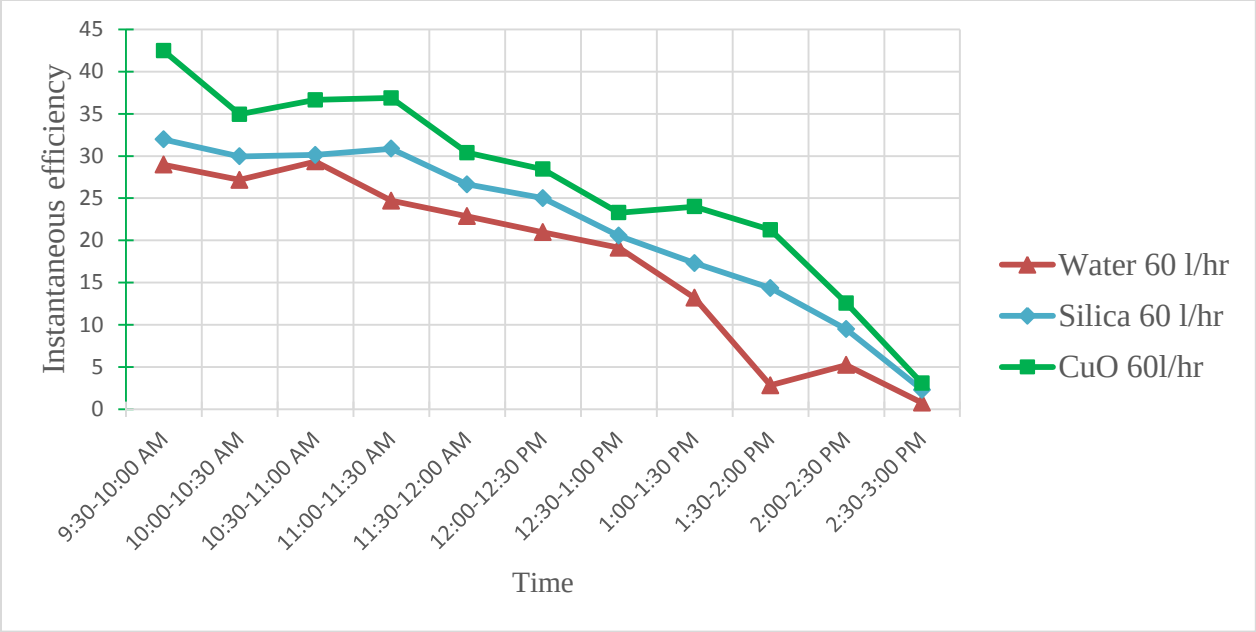

Fig.89 Variation in instantaneous efficiency with time for water and nanofluids (0.05% conc.) at volume flow rate of 60 l/h

12) Comparisons of thermal efficiency of water with nanofluids (0.01% conc.) at volume flow rate of 20 l/h

The thermal efficiency of CuO-water based nanofluid at 0.01% conc. is higher than SiO_2-water based nanofluid and water for the volume flow rate of 20 l/h as shown in fig.90. The main reasons for this is excellent thermophysical properties and higher temperature difference as compared to SiO_2-water based nanofluid and water.

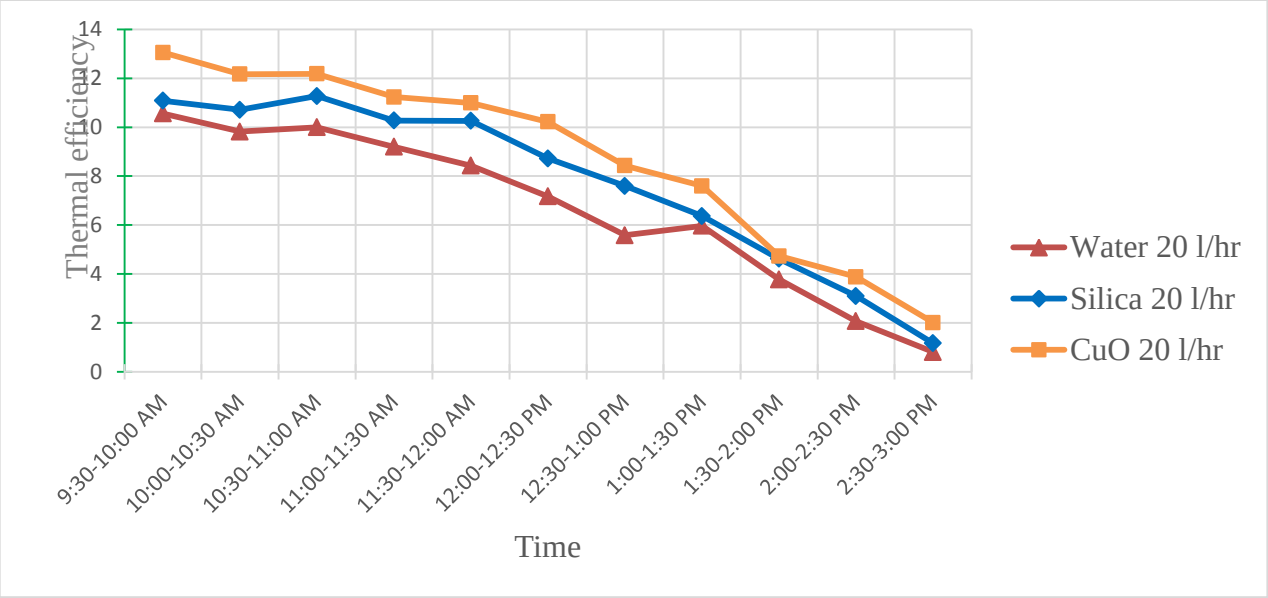

Fig.90 Variation in thermal efficiency with time for water and nanofluids (0.01% conc.) at volume flow rate of 20 l/h

13) Comparisons of thermal efficiency of water with nanofluids (0.01% conc.) at volume flow rate of 40 l/h

The thermal efficiency of CuO-water based nanofluid at 0.01% conc. is higher than SiO_2-water based nanofluid and water for the volume flow rate of 40 l/h as shown in fig.91. The main reasons for this is excellent thermophysical properties and higher temperature difference as compared to SiO_2-water based nanofluid and water.

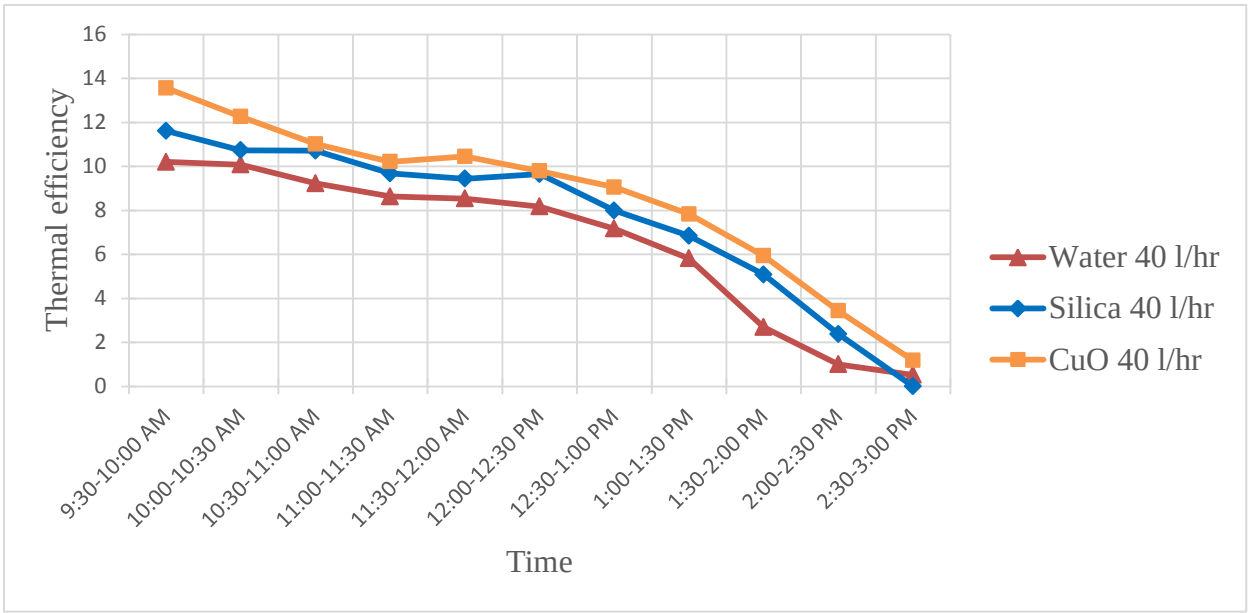

Fig.91 Variation in thermal efficiency with time for water and nanofluids (0.01% conc.) at volume flow rate of 40 l/h

14) Comparisons of thermal efficiency of water with nanofluids (0.01% conc.) at volume flow rate of 60 l/h

The thermal efficiency of CuO-water based nanofluid at 0.01% conc. is higher than SiO_2-water based nanofluid and water for the volume flow rate of 60 l/h as shown in fig.92. The main reasons for this is excellent thermophysical properties and higher temperature difference as compared to SiO_2-water based nanofluid and water.

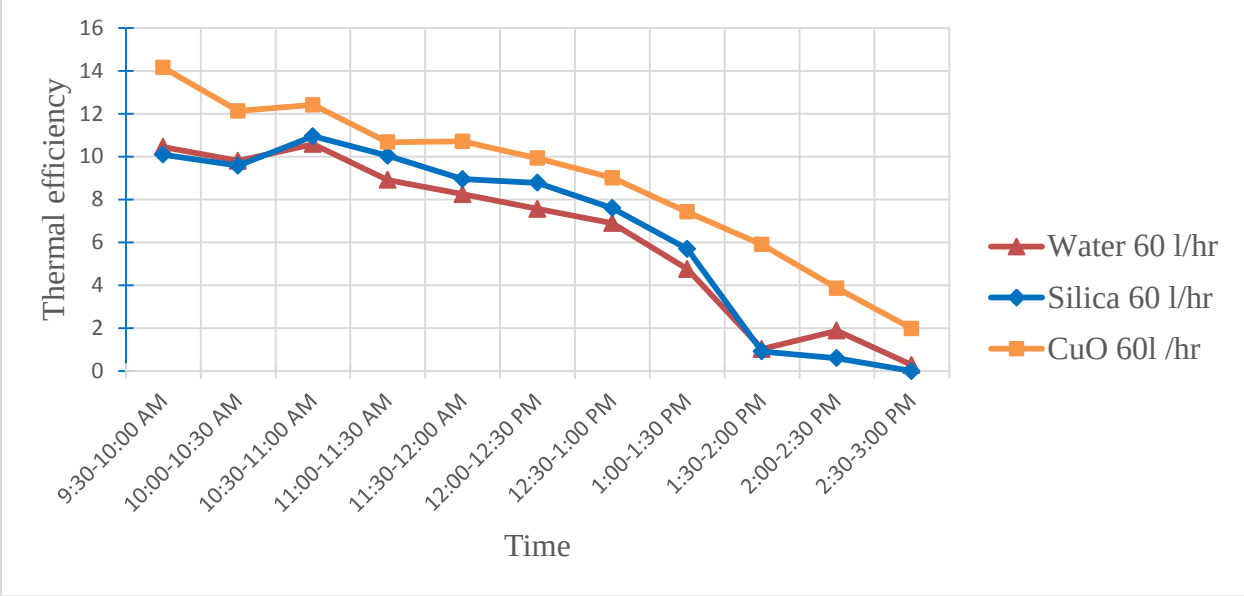

Fig.92 Variation in thermal efficiency with time for water and nanofluids (0.01% conc.) at volume flow rate of 60 l/h

15) Comparisons of thermal efficiency of water with nanofluids (0.05% conc.) at volume flow rate of 20 l/h

Fig.93 shows the variation in thermal efficiency with time for water and nanofluid (0.05% conc.) at volume flow rate of 20 l/h. The thermal efficiency of CuO-water based nanofluid at 0.05% conc. is higher than SiO_2-water based nanofluid and water for the volume flow rate of 20 l/h The main reasons for this is excellent thermophysical properties and higher temperature difference as compared to SiO_2-water based nanofluid and water.

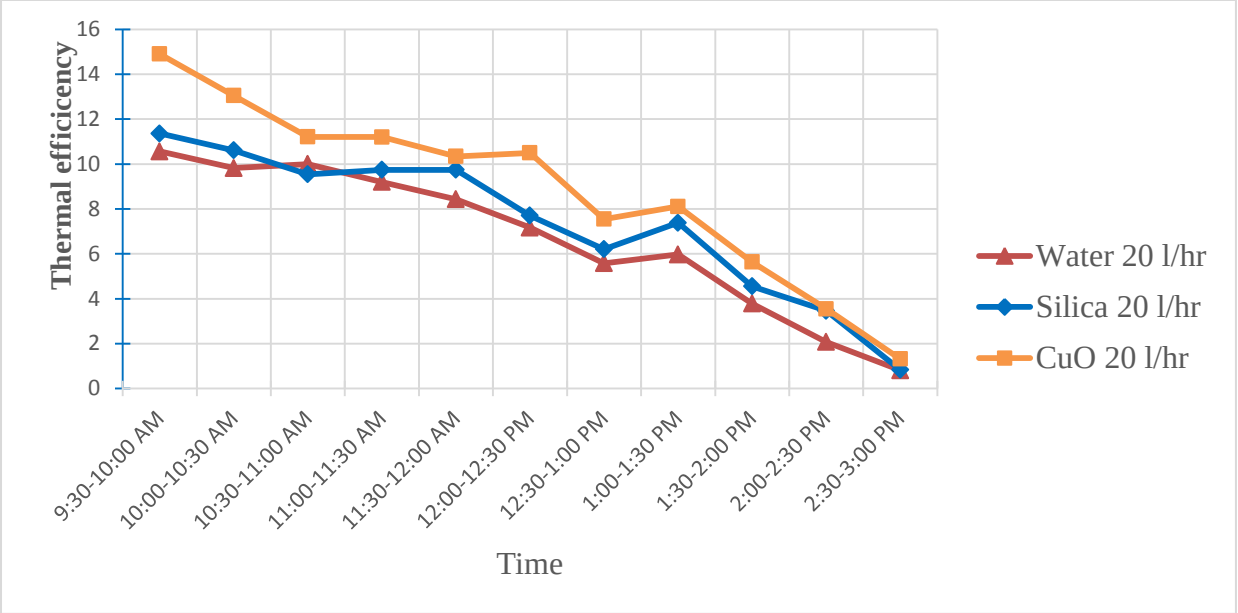

Fig.93 Variation in thermal efficiency with time for water and nanofluids (0.05% conc.) at volume flow rate of 20 l/h

16) Comparisons of thermal efficiency of water with nanofluids (0.05% conc.) at volume flow rate of 40 l/h

The thermal efficiency of CuO-water based nanofluid at 0.05% conc. is higher than SiO_2-water based nanofluid and water for the volume flow rate of 40 l/h as shown in fig.94. The main reasons for this is excellent thermophysical properties and higher temperature difference as compared to SiO_2-water based nanofluid and water.

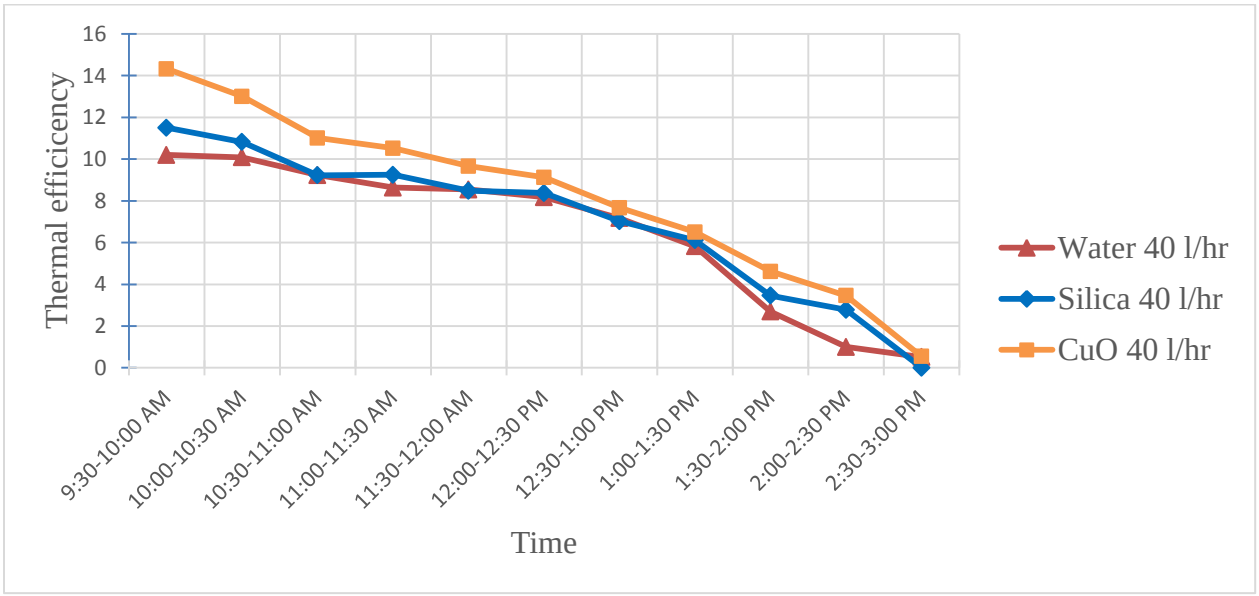

Fig.94 Variation in thermal efficiency with time for water and nanofluids (0.05% conc.) at volume flow rate of 40 l/h

17) Comparisons of thermal efficiency of water with nanofluids (0.05% conc.) at volume flow rate of 60 l/h

The thermal efficiency of CuO-water based nanofluid at 0.05% conc. is higher than SiO_2-water based nanofluid and water for the volume flow rate of 60 l/h as shown in fig.95. The main reasons for this is excellent thermophysical properties and higher temperature difference as compared to SiO_2-water based nanofluid and water.

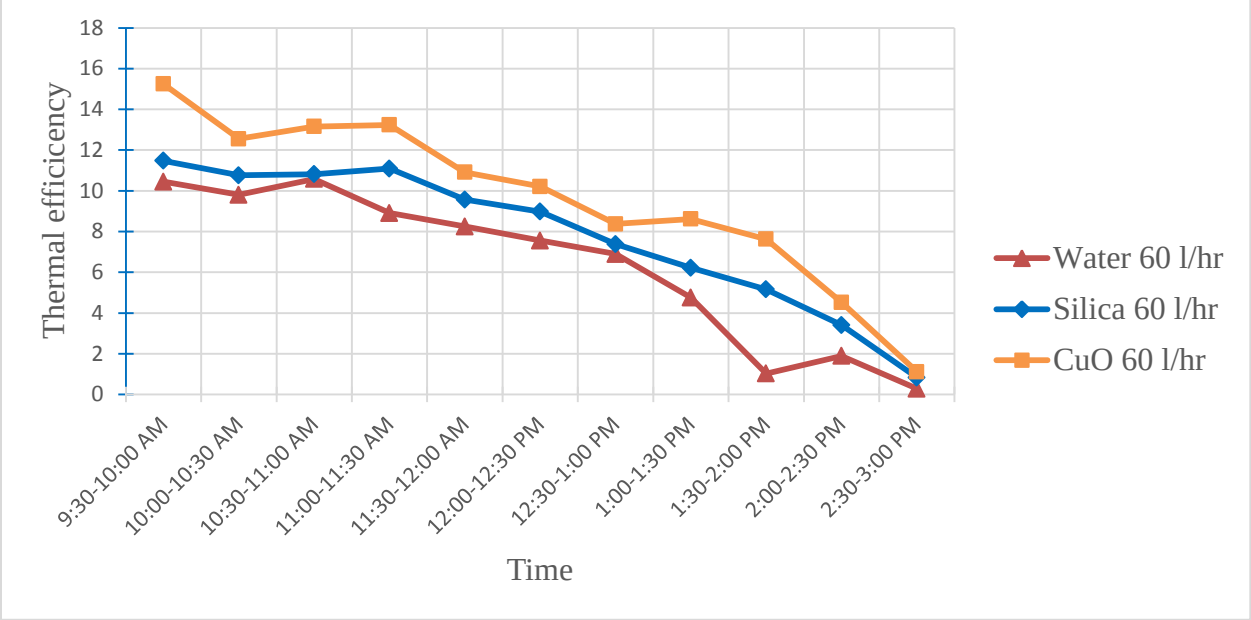

Fig.95 Variation in thermal efficiency with time for water and nanofluids (0.05% conc.) at volume flow rate of 60 l/h

CHAPTER 7
CONCLUSION

The present work examines experimentally the performance of parabolic solar collector using SiO_2-water based and CuO-water based nanofluids and then compares it with the conventional fluid i.e. water. The parameters taken are different volume flow rates, nanoparticles volume concentration and working fluids. For each working fluid, instantaneous efficiency, thermal efficiency and overall thermal efficiency is calculated. Manual tracking system is used to absorb maximum solar radiation. Convective heat transfer coefficient and collector heat removal factor are also calculated for water and nanofluids at different mass flow rate and at different nanoparticles volume concentration. From the results, the following points are concluded as shown below:

1) The optical efficiency of the system is 70.6% which is same for both water and nanofluids used as a working fluid because glass mirror strips are used as a reflector in both cases.
2) The maximum temperature obtains from water, SiO_2-water based and CuO-water based nanofluids is 61^0C, 65.4^0C and 77^0C respectively at 3:00 pm.
3) Instantaneous efficiency increases with increase in volume flow rates. The maximum instantaneous efficiency obtains from water, SiO_2-water based and CuO-water based nanofluids is 29.34%, 31.96% and 42.45% respectively.
4) The maximum thermal efficiency obtains from water, SiO_2-water based and CuO-water based nanofluids is 10.58%, 11.61% and 15.25% respectively.
5) The maximum overall thermal efficiency obtains from water, SiO_2-water based and CuO-water based nanofluids is 6.63%, 7.83% and 9.57% respectively.
6) At 20 l/h volume flow rate, the instantaneous efficiency is upto 2% in SiO_2-water based nanofluid (0.01% vol. conc.) and upto 2.4% in CuO-water based nanofluid (0.01% vol. conc.) more as compared to water. The instantaneous efficiency is upto 1.5% in SiO_2-water based nanofluid (0.05% vol. conc.) and upto 3.04% in CuO-water based nanofluid (0.05% vol. conc.) more as compared to water.
7) At 40 l/h volume flow rate, the instantaneous efficiency is upto 2.64% in SiO_2-water based nanofluid (0.01% vol. conc.) and upto 6.26% in CuO-water based nanofluid

(0.01% vol. conc.) more as compared to water. The instantaneous efficiency is upto 2.43% in SiO_2-water based nanofluid (0.05% vol. conc.) and upto 7.65% in CuO-water based nanofluid (0.05% vol. conc.) more as compared to water.

8) At 60 l/h volume flow rate, the instantaneous efficiency is upto 3.25% in SiO_2-water based nanofluid (0.01% vol. conc.) and upto 10.43% in CuO-water based nanofluid (0.01% vol. conc.) more as compared to water. The instantaneous efficiency is upto 6.17% in SiO_2-water based nanofluid (0.05% vol. conc.) and upto 12.49% in CuO-water based nanofluid (0.05% vol. conc.) more as compared to water.
9) At 20 l/h volume flow rate, the thermal efficiency is upto 2% in SiO_2-water based nanofluid (0.01% vol. conc.) and upto 3.05% in CuO-water based nanofluid (0.01% vol. conc.) more as compared to water. The thermal efficiency is upto 1.41% in SiO_2-water based nanofluid (0.05% vol. conc.) and upto 4.34% in CuO-water based nanofluid (0.05% vol. conc.) more as compared to water.
10) At 40 l/h volume flow rate, the thermal efficiency is upto 2.39% in SiO_2-water based nanofluid (0.01% vol. conc.) and upto 3.36% in CuO-water based nanofluid (0.01% vol. conc.) more as compared to water. The thermal efficiency is upto 1.78% in SiO_2-water based nanofluid (0.05% vol. conc.) and upto 4.12% in CuO-water based nanofluid (0.05% vol. conc.) more as compared to water.
11) At 60 l/h volume flow rate, the thermal efficiency is upto 1.13% in SiO_2-water based nanofluid (0.01% vol. conc.) and upto 4.87% in CuO-water based nanofluid (0.01% vol. conc.) more as compared to water. The thermal efficiency is upto 4.13% in SiO_2-water based nanofluid (0.05% vol. conc.) and upto 6.6% in CuO-water based nanofluid (0.05% vol. conc.) more as compared to water.
12) The maximum convective heat transfer coefficient and heat removal factor is 406.85W/m^2K and 0.9579 respectively in CuO-water based nanofluid (0.05% vol. conc.).

CHAPTER 8
FUTURE SCOPE

Very limited experimental work has been done on parabolic solar collector. So, it has wide scope in future. In the present experimental work, lot of things which are not taken into account can be employed in future to enhance the performance of parabolic solar collector. These are:

1) Concentration ratio of the system is 9.66 and it can be increased by varying the diameter and length of the receiver tube and can also vary the aperture area of the collector.
2) In order to reduce heat loss, glass cover tube is used on receiver tube. In future, the material and diameter of the cover tube can vary to prevent it from losses as much as possible.
3) The receiver tube used is of copper material. One can use pyrex glass receiver tube, receiver tube made of quartz, stainless steel etc.
4) Material of the storage tank is plastic in the present experiment, one can change it to reduce heat losses.
5) Manual tracking mechanism is used in the experiment. To enhance the performance of PSC, automatic tracking mechanism can be used.
6) Stopwatch system is used in the present experiment to measure volume flow rate. For exact measurement of volume flow rate, rotameter can be used.
7) The support structure is made up of cast iron in present experiment to withstand from stress and wind load etc. Other suitable material can be used to prevent the system from stress and wind load etc.
8) While preparing the nanofluid, surfactant is not used. Surfactant increases the stability of nanoparticles in base fluid. So, one can use surfactant which is helpful for improving the performance of parabolic solar system.
9) Nanoparticles concentration taken are 0.01% and 0.05% in present experiment. One can increase the concentration of nanoparticle in base fluid to enhance the performance of parabolic solar collector.
10) Volume flow rates taken in present experiment are 20 l/h, 40 l/h and 60 l/h. One can vary it to check the performance of PSC.

11) Average nanoparticles size used in the experiment is 20-30 nm and one can check the performance of PSC using different sizes of nanoparticles.
12) No. of glass mirror strips are used in the present experiment as reflector. One can use proper reflector for reflecting maximum solar radiation onto the receiver tube.
13) The value of specific heat is taken as constant at different mass flow rate to avoid increasing no. of calculations. One can take exact value of specific heat.

REFERENCES

Akoh, H., Tsukasaki, Y., Yatsuya S., and Tasaki A., 1978, Magnetic properties of ferromagnetic ultrafine particles prepared by vacuum evaporation on running oil substrate, "*Journal of Crystal Growth*", vol.45, pp. 495–500.

Chaji H., Ajabshirchi Y., Esmaeilzadeh E., HerisSaeid Z., Hedayatizadeh M. , Kahani M.,(2013), Experimental study on thermal efficiency of flat plate solar collector using TiO_2/Water nanofluid, "*Modern Applied Science*", published by Canadian Centre of Science and Education, vol. 7, issue 10, pp.60-69.

Chang M. H., Liu H. S., Tai C. Y, 2011, Preparation of copper oxide nanoparticles and its application in nanofluid, "*Powder Technology*", vol. 207, pp. 378 – 386.

Choi, S.U.S., 1995, Enhancing thermal conductivity of fluids with nanoparticles, in Developments and Applications of Non-Newtonian Flows, D. A. Singer and H. P.Wang, Eds., "*American Society of Mechanical Engineers*", New York, FED–231/MD-66, pp.99–105.

Chow T.T., 2009, A review on photovoltaic/thermal hybrid solar technology, "*Applied Energy*", vol.87, issue 2, pp. 365–379.

Chougule S. S., Dr. Pise A.T., Madane P. A., 2012, Performance of nanofluid-charged solar water heater by solar tracking system, "*IEEE-International Conference On Advances In Engineering, Science And Management (ICAESM -2012)*", March 30, 31,2012, ISBN: 978-81-909042-2-3 ©2012 IEEE.

Das S. K., Choi S.U.S., Yu W., Pradeep T., 2008, Nanofluids science and technology, Wiley Publication.

David B., Ruxandra V., Pieter S., 2011, Innovation in concentrated solar power, Review, "*Solar Energy Materials & Solar Cells*", vol.95, issue 10, pp. 2703–2725.

Dr. Kumar D. S., 2009-2010, Heat and mass transfer, "*S. K. Kataria& Sons Publications*", 7th revised edition, pp. 819.

Granqvist C.G and Buhrman R.A, 1976, Ultra-fine metal particles, "*J.Appl. Physics*", vol. 47, issue 5, pp. 2200.

Gunge V.C., Kapatkar V.N. 2012, Performance analysis of parabolic trough collector with step tube receiver, "*International Journal of Engineering & Science Research*", IJESR, June 2012, vol. 2, Issue 6, Article No-5,436-448, ISSN 2277-2685.

Gorji B., Ghasri M., Fazaeli R., Niksirat N., 2012, Synthesis and characterizations of silica nanoparticles by a new sol-jel method, "*Journal of Applied Chemical Research*" vol. 6, issue 3, pp. 22-26.

He Y., Wang S., Ma J., Tian F., Ren Y., 2011, Experimental study on the light-heat conversion characteristics of nanofluids, "*Nanosci. Nanotechnol. Lett.*", vol. 3, issue 4 , pp. 494–496.

http://www6.cityu.edu.hk/tto/Admin/Data/ATPhoto%5CHybridPhotovoltaicThermalCollector%5CHybrid%20Photovoltaic.JPG; [accessed 28.11.13].

Javadi F.S., Sadeghipour S., Saidur R., BoroumandJazi G., Rahmati B., Elias M.M., Sohel M.R., 2013, The effects of nanofluid on thermophysical properties and heat transfer characteristics of a plate heat exchanger, "*International Communications in Heat and Mass Transfer*", vol. 44, pp. 58–63.

Kalogirou S.A., 2004, Solar thermal collectors and applications, "*Progress in Energy and Combustion Science*", vol. 30, pp.231–295.

Khullar Vikrant, Tyagi Himanshu, 2010, Application of nanofluids as the working fluid in concentrating parabolic solar collectors, Proceedings of the 37th National & 4th "*International Conference on Fluid Mechanics and Fluid Power",* December 16-18, 2010, IIT Madras, Chennai, India.

Khullar V., Tyagi H., Phelan P.E., Otanicar T.P., Singh H., Taylor R.A., 2012, Solar energy harvesting using nanofluids-based concentrating solar collector, "*Journal of Nanotechnology in Engineering and Medicine*", vol.3, pp. 031003-1-9.

Khullar V., Tyagi H., 2012, A study on environmental impact of nanofluid based concentrating solar water heating system, "*International Journal of Environmental Studies*", vol. 69, issue 2, pp. 220–232.

Lee S., Choi S. U.-S., Li S., Eastman J. A., 1999, Measuring thermal conductivity of fluids containing oxide nanoparticles, "*Journal of Heat Transfer*" vol. 121, pp. 280-289.

Maddah H., Rezazadeh M., Maghsoudi M., NasiriKokhdanS., (2013), the effect of silver and aluminium oxide nanoparticles on thermophysical properties of nanofluids, "*Journal of Nanostructure in Chemistry*", vol. 3, pp.1-6.

Mahian Omid, Kianifar Ali , Kalogirou Soteris A., Pop Ioan , Wongwises Somchai, 2013, A review of the applications of nanofluids in solar energy, "*International Journal of Heat and Mass Transfer*", vol.57, issue 2, pp. 582–594.

Natrajan E, Sathish R, 2008, Role of nanofluids in solar water heater, "*Int J Adv Manuf Technol*",special issue, doi 10.1007/s00170-008-1876-8.

Otanicar T.P., Phelan P.E., Prasher R.S., Rosengarten G., Taylor R.A., 2010, Nanofluid based direct absorption solar collector, "*J. Renew. Sustain. Energy*", vol.2, issue 3, pp.033102-1 to 13.

Rai.G.D., 2011, Non-conventional energy sources, "*Khanna Publishers*", fifth edition, New Delhi, pp. 1-224.

Reddy K.S., Kumar K. Ravi, 2012, Solar collector field design and viability analysis of standalone parabolic trough power plants for Indian conditions, "*Energy for Sustainable Development*", vol.16, issue 4, pp. 456–470.

Reddy S.P.M., Dr. Venkataramaiah P., Sairam Mr.P., 2012, Optimization of process parameters of a solar parabolic trough in winter using Grey-Taguchi approach, "*International Journal of Engineering Research and Applications*", Vol. 2, Issue 1, pp.816-821.

Risi A. de, Milanese M., Laforgia D., 2013, Modelling and optimization of transparent parabolic trough collector based on gas-phase nanofluids, "*Renewable Energy*"**,** vol.58, pp. 134-139.

Roman A., 2011, Simulation analysis of thermal storage for concentrating solar power, "*Applied Thermal Engineering"*, vol. 31, pp. 3588-3594.

Romano J.M, Parker J.C, and Ford Q.B, 1997: Application opportunities for nanoparticles made from condensation of physical vapors, "*Adv. Powder Methal. Partic. Mater*", vol. 2, pp.12-13.

Saidur R., Meng T.C., Said Z., Hasanuzzaman M., Kamyar A., 2012, Evaluation of the effect of nanofluid-based absorbers on direct solar collector, "*Int. J. Heat Mass Transfer*", vol.55,issue 21-22, pp. 5899–5907.

Sani E., Barison S., Pagura C., Mercatelli L., Sansoni P., Fontani D., Jafrancesco D. and Francini F., 2010, Carbon nanohorns-based nanofluids as direct sunlight absorbers, "*Journal Optics Express*", vol. 18, issue 5, pp. 1-9.

Shah M.A. and Ahmed T., 2010, Principles of nanoscience and nanotechnology, "*Narosa Publications*".

Sharma A., 2011, A comprehensive study of solar power in India and World, "*Renew. Sustain. Energy Rev.*", vol.15, pp. 1767–1776.

Sukhatme S. P., 1984, Solar energy-Principles of thermal collection and storage, "*Tata McGraw –Hill Publications*", pp. 158-180.

Taylor R.A., Phelan P.E., Otanicar T.P., Adrian R., Prasher R.P., 2011, Nanofluid optical property characterization: towards efficient direct absorption solar collectors, "*Nanoscale Res. Lett.*", vol.6, issue 1, pp. 1-11.

Taylor R.A., Phelan P.E., Otanicar T.P., Walker C.A., Nguyen M., Trimble S., Prasher R., 2011, Applicability of nanofluids in high flux solar collectors, "*J. Renew. Sustain. Energy*", vol.3, issue 2, pp.023104-1 to 15.

Tiwari Arun Kumar, Ghosh Pradyumna, Sarkar Jahar, 2013, Solar water heating using nanofluids - a comprehensive overview and environmental impact analysis, "*International Journal of Emerging Technology and Advanced Engineering*", vol. 3, issue 3: ICERTSD 2013, pp. 221-224.

Tyagi H., Phelan P., Prasher R., 2009, Predicted efficiency of a low-temperature nanofluid – based direct absorption solar collector, "*J. Solar Energy Eng.*", vol.131 , pp.041004-1 to 7.

Variability of wind power and other renewable, Management options and strategies, IEA, 2005, http://www.uwig.org/IEA_Report_on variability.pdf.

Wong K.V. and Leon O.D., 2009, Applications of nanofluids: current and future, "*Advances in Mechanical Engineering*", Hindawi Publishing Corporationvol. 2010, Article ID 519659, doi:10.1155/2010/519659, pp.1-12.

Yousefi T., Veysi F., Shojaeizadeh E., Zinadini S., 2012, An experimental investigation on the effect of Al_2O_3–H_2O nanofluid on the efficiency of flat-plate solar collectors, "*Renewable Energy*", vol.39, pp. 293–298.

Yousefi T., Veysi F., Shojaeizadeh E., Zinadini S., 2012, An experimental investigation on the effect of MWCNT–H_2O nanofluid on the efficiency of flat-plate solar collector, "*Exp. Therm. Fluid Sci.*", vol. 39, pp. 207–212.

Yousefi T., Veysi F., Shojaeizadeh E., Zinadini S., 2012, An experimental investigation on the effect of pH variation of MWCNT–H_2O nanofluid on the efficiency of flat-plate solar collector, "*Solar Energy*", vol. 86, pp. 771–779.

Yu W., Xie H., 2011, A review on nanofluids: preparation, stability mechanisms and applications, "*Journal of Nanomaterials*", vol. 2012, Article ID 435873, pp.17, doi:10.1155/2012/435873.

Zhu, H., Lin, Y., and Yin, Y., 2004, A novel one-step chemical method for preparation of copper nanofluids, "*Journal of Colloid and Interface Science*", vol. 227, pp.100–103.

ANNEXURE

Annexure A

XRD Details of Purchased SiO_2 Nanoparticles From SAI Lab

Measurement Conditions: (Bookmark 1)

Dataset Name	SiO_2
File name	C:\Documents and Settings\Administrator\Desktop\SAI Labs\TU\Kundan Lal\Sunil Kumar\SiO_2.xrdml
Comment	Configuration=Spinner Reflection-Transmission, Owner=User-1, Creation date=6/25/2009 11:03:49 AM
	Goniometer=PW3050/60 (Theta/Theta); Minimum step size 2Theta:0.001; Minimum step size Omega:0.001
	Sample stage=Reflection-Transmission Spinner PW3064/60; Minimum step size Phi:0.1
	Diffractometer system=XPERT-PRO
	Measurement program=Thapar_Spinner Stage, Owner=User-1, Creation date=2/5/2010 5:38:09 PM
Measurement Date / Time	6/12/2014 10:53:41 AM
Operator	Administrator
Raw Data Origin	XRD measurement (*.XRDML)
Scan Axis	Gonio
Start Position [°2Th.]	20.0116
End Position [°2Th.]	109.9846
Step Size [°2Th.]	0.0130
Scan Step Time [s]	29.0700
Scan Type	Continuous
PSD Mode	Scanning
PSD Length [°2Th.]	3.35
Offset [°2Th.]	0.0000
Divergence Slit Type	Automatic
Irradiated Length [mm]	10.00
Specimen Length [mm]	10.00

Measurement Temperature [°C] 25.00

Anode Material Cu

K-Alpha1 [Å] 1.54060

Generator Settings 40 mA, 45 kV

Diffractometer Type 0000000011059259

Diffractometer Number 0

Goniometer Radius [mm] 240.00

Dist. Focus-Diverg. Slit [mm] 100.00

Incident Beam Monochromator No

Spinning Yes

Main Graphics, Analyze View: (Bookmark 2)

Peak List: (Bookmark 3)

Pos. [°2Th.]	Height [cts]	d-spacing [Å]	Rel. Int. [%]	Area [cps*°2Th.]	Area [cts*°2Th.]	FWHM [°2Th.]
22.5602	274.27	3.93802	100.00	2.83	82.28	0.3000
31.7958	20.17	2.81209	7.35	1.04	30.20	0.7488

Pattern List: (Bookmark 4)

Visible	Ref. Code	Score	Compound Name	Displacement [°2Th.]	Scale Factor	Chemical Formula	SemiQuant [%]
*	01-082-0512	35	Cristobalite, syn	0.807	0.812	SiO_2	100

XRD Details of Purchased CuO Nanoparticles From SAI Lab

Measurement Conditions: (Bookmark 1)

Dataset Name CuO

File name C:\Documents and Settings\Administrator\Desktop\SAI Labs\TU\Kundan Lal\Sunil Kumar\CuO.xrdml

Comment	Configuration=Spinner Reflection-Transmission, Owner=User-1, Creation date=6/25/2009 11:03:49 AM
	Goniometer=PW3050/60 (Theta/Theta); Minimum step size 2Theta:0.001; Minimum step size Omega:0.001
	Sample stage=Reflection-Transmission Spinner PW3064/60; Minimum step size Phi:0.1
	Diffractometer system=XPERT-PRO
	Measurement program=Thapar_Spinner Stage, Owner=User-1, Creation date=2/5/2010 5:38:09 PM
Measurement Date / Time	6/12/2014 10:20:29 AM
Operator	Administrator
Raw Data Origin	XRD measurement (*.XRDML)
Scan Axis	Gonio
Start Position [°2Th.]	20.0116
End Position [°2Th.]	109.9846
Step Size [°2Th.]	0.0130
Scan Step Time [s]	29.0700
Scan Type	Continuous
PSD Mode	Scanning
PSD Length [°2Th.]	3.35
Offset [°2Th.]	0.0000
Divergence Slit Type	Automatic
Irradiated Length [mm]	10.00
Specimen Length [mm]	10.00
Measurement Temperature [°C]	25.00
Anode Material	Cu
K-Alpha1 [Å]	1.54060
Generator Settings	40 mA, 45 kV
Diffractometer Type	0000000011059259
Diffractometer Number	0
Goniometer Radius [mm]	240.00

Dist. Focus-Diverg. Slit [mm] 100.00

Incident Beam Monochromator No

Spinning Yes

Main Graphics, Analyze View: (Bookmark 2)

Peak List: (Bookmark 3)

Pos. [°2Th.]	Height [cts]	d-spacing [Å]	Rel. Int. [%]	Area [cps*°2Th.]	Area [cts*°2Th.]	FWHM [°2Th.]
23.2173	0.38	3.82803	0.01	5.71	166.07	4.0000
32.5625	384.24	2.74761	11.77	5.53	160.89	0.3410
35.5462	1583.53	2.52352	48.51	59.76	1737.17	0.8702
38.8098	3264.31	2.31849	100.00	84.67	2461.31	0.5961
45.3935	5.18	1.99635	0.16	0.73	21.32	0.0010
48.8624	256.98	1.86242	7.87	16.91	491.66	1.5133
51.3164	12.84	1.77898	0.39	0.00	0.00	0.4048
53.5594	103.20	1.70964	3.16	5.38	156.51	1.2359
58.2462	297.75	1.58274	9.12	8.30	241.14	0.6495
61.6300	371.27	1.50370	11.37	14.97	435.10	0.9345
66.1754	333.21	1.41100	10.21	19.71	572.88	1.3849
68.0606	622.39	1.37644	19.07	14.29	415.38	0.5449
72.3674	93.19	1.30476	2.85	5.12	148.70	1.3267
74.9903	102.42	1.26549	3.14	6.36	184.96	1.4696
75.2067	1279.05	1.26239	39.18	1.90	55.33	0.0335
80.5177	3.63	1.19197	0.11	0.00	0.00	0.0010
82.6209	95.14	1.16687	2.91	3.02	87.91	0.9362
83.3976	118.81	1.15797	3.64	3.94	114.60	0.8912
86.7146	4.65	1.12199	0.14	0.45	13.04	3.5115
89.9424	88.90	1.08992	2.72	1.97	57.39	0.5199
91.7358	23.54	1.07323	0.72	1.08	31.49	1.1171
99.2081	34.81	1.01144	1.07	2.45	71.10	1.6645
103.5198	77.05	0.98074	2.36	4.69	136.31	1.4082
107.0812	81.67	0.95775	2.50	0.41	11.84	0.1150

Pattern List: (Bookmark 4)

Visible	Ref. Code	Score	Compound Name	Displacement [°2Th.]	Scale Factor	Chemical Formula	SemiQuant [%]
*	01-089-5897	86	Copper Oxide	0.026	1.111	Cu O	53
*	01-073-6023	81	Tenorite	0.009	1.007	Cu O	47

Annexure B

Table 3 Values of Re, Pr, Nu, h_f, F' and F_R for water at different vol. flow rates

	20 l/hr	40 l/hr	60 l/hr
Re	631.08	1262.17	1886.75
Pr	2.605	2.605	2.605
Nu	5.863	10.208	14.08
h_f (W/m^2K)	144.84	252.175	347.84
F'	0.9132	0.9482	0.9619
F_R	0.8885	0.9348	0.9592

Table 4 Values of Re, Pr, Nu, h_f, F' and F_R for SiO_2 nanofluid (0.01% conc.) at different vol. flow rates

	20 l/hr	40 l/hr	60 l/hr
Re	637.36	1275.77	1913.26
Pr	2.545	2.545	2.545
Nu	5.855	10.20	14.107
h_f (W/m^2K)	145.79	253.98	351.26
F'	0.914	0.949	0.9623
F_R	0.8891	0.9355	0.953

Table 5 Values of Re, Pr, Nu, h_f, $F^{'}$ and F_R for SiO_2 nanofluid (0.05% conc.) at different vol. flow rates

	20 l/hr	40 l/hr	60 l/hr
Re	606.875	1213.75	1820
Pr	2.532	2.532	2.532
Nu	5.618	9.782	13.526
h_f (W/m^2K)	144.4	251.43	347.67
F'	0.913	0.9481	0.9619
F_R	0.8876	0.9343	0.9524

Table 6 Values of Re, Pr, Nu, h_f, $F^{'}$ and F_R for CuO nanofluid (0.01% conc.) at different vol. flow rates

	20 l/hr	40 l/hr	60 l/hr
Re	662.045	1323.82	1985.73
Pr	2.4089	2.4089	2.4089
Nu	5.904	10.278	14.2165
h_f (W/m^2K)	150.23	261.522	361.74
F'	0.91603	0.94997	0.9633
F_R	0.8912	0.9365	0.95403

Table 7 Values of Re, Pr, Nu, h_f, $F^{'}$ and F_R for CuO nanofluid (0.05% conc.) at different vol. flow rates

	20 l/hr	40 l/hr	60 l/hr
Re	720.247	1440.495	2160.3
Pr	1.9015	1.9015	1.9015
Nu	5.746	10.004	13.835
h_f (W/m^2K)	168.97	294.192	406.85
F'	0.92464	0.9553	0.9673
F_R	0.8991	0.9416	0.9579

Annexure C

$k / k_0 = 1.03$ at 0.01% conc. for CuO-water based nanofluid (Lee et al. 1999)

$k / k_0 = 1.19$ at 0.05% conc. for CuO-water based nanofluid (Lee et al. 1999)

Where,

k = thermal conductivity of CuO-water based nanofluid

k_0 = thermal conductivity of base fluid i.e. water

Table 8 Thermophysical properties of the nanoparticles (Javadi et al. 2013)

Properties	SiO_2	TiO_2	Al_2O_3
ρ (Kg/m^3)	2220	4157	3970
c_p (J/kg K)	745	710	765
k (W/m.K)	1.38	8.4	36

Table 9 Physical properties of Water (Dr. D. S. Kumar, 2009-2010)

t ^0C	ρ Kg/m^3	c_p kJ/kg K	$k \times 10^{-2}$ W/mK	$\alpha \times 10^{-4}$ m^2/hr	$\mu \times 10^{-2}$ kg/hr-m	$\upsilon \times 10^{-6}$ m^2/s	Pr
0	999.9	4.212	55.093	4.71	644.093	1.789	13.67
10	999.7	4.191	57.418	4.94	469.818	1.306	9.54
20	998.2	4.183	59.859	5.16	361.892	1.006	7.02
30	995.7	4.174	61.718	5.35	288.668	0.805	5.42
40	992.2	4.174	63.345	5.51	235.602	0.659	4.31
50	988.1	4.178	64.740	5.65	197.771	0.556	3.54
60	983.2	4.178	65.902	5.78	169.305	0.478	2.98
70	977.8	4.187	66.716	5.87	146.370	0.415	2.55
80	971.8	4.195	67.413	5.96	127.924	0.365	2.21

Table 10 Thermophysical properties of working fluids

Thermophysical properties	Water	SiO_2-water based nanofluid (0.01% conc.)	SiO_2-water based nanofluid (0.05% conc.)	CuO-water based nanofluid (0.01% conc.)	CuO-water based nanofluid (0.05% conc.)
Density (kg/m^3)	1000	1014	1070	1054	1270
Specific heat (J/kg K)	4187	4106	3801	3965.05	3266
Thermal conductivity (W/m K)	0.667	0.6723	0.694	0.68701	0.794
Viscosity (m^2/s)	0.415×10^{-6}	0.411×10^{-6}	0.432×10^{-6}	0.396×10^{-6}	0.364×10^{-6}

Annexure D

Table 11 Values of temp., solar intensity and wind speed with time

Date26/04/2014 _ for water at vol. flow rate of 20 l/hr.					
Time	Inlet temperature (°C)	Outlet temperature (°C)	Temperature difference (°C)	Solar intensity (W/m^2)	Wind speed (m/sec)
9:30-10:00 AM	32	35.6	3.6	778	3.88
10:00-10:30 AM	35.6	39.1	3.5	814	3.88
10:30-11:00 AM	39.1	42.8	3.7	845	5
11:00-11:30 AM	42.8	46.5	3.7	918	5
11:30-12:00 AM	46.5	50	3.5	948	4.72
12:00-12:30 PM	50	53	3	955	4.72
12:30-1:00 PM	53	55.3	2.3	941	4.44
1:00-1:30 PM	55.3	57.7	2.4	918	4.44
1:30-2:00 PM	57.7	59.2	1.5	907	4.166
2:00-2:30 PM	59.2	60	0.8	881	4.166
2:30-3:00 PM	60	60.3	0.3	841	4.166

Table 12 Values of temp., solar intensity and wind speed with time

Date28/04/2014 _for water at vol. flow rate of 40 l/hr					
Time	Inlet temperature (°C)	Outlet temperature (°C)	Temperature difference (°C)	Solar intensity (W/m^2)	Wind speed (m/sec)
9:30-10:00 AM	32.5	36.1	3.6	806	3.333
10:00-10:30 AM	36.1	39.8	3.7	838	3.333
10:30-11:00 AM	39.8	43.3	3.5	866	4.166
11:00-11:30 AM	43.3	46.8	3.5	926	4.166
11:30-12:00 AM	46.8	50.4	3.6	963	4.166
12:00-12:30 PM	50.4	53.9	3.5	978	4.166
12:30-1:00 PM	53.9	56.9	3	955	4.444
1:00-1:30 PM	56.9	59.3	2.4	941	4.444
1:30-2:00 PM	59.3	60.4	1.1	933	4.722
2:00-2:30 PM	60.4	60.8	0.4	908	4.722
2:30-3:00 PM	60.8	61	0.2	884	4.722

Table 13 Values of temp., solar intensity and wind speed with time

Date 29/04/2014 _for water at vol. flow rate of 60 l/hr					
Time	Inlet temperature (°C)	Outlet temperature (°C)	Temperature difference (°C)	Solar intensity (W/m^2)	Wind speed (m/sec)
9:30-10:00 AM	33	36.5	3.5	765	2.222
10:00-10:30 AM	36.5	39.9	3.4	792	2.222
10:30-11:00 AM	39.9	43.7	3.8	820	2.777
11:00-11:30 AM	43.7	47.2	3.5	897	2.777
11:30-12:00	47.2	50.6	3.4	941	3.055

AM					
12:00-12:30 PM	50.6	53.8	3.2	966	3.055
12:30-1:00 PM	53.8	56.6	2.8	926	3.333
1:00-1:30 PM	56.6	58.5	1.9	911	3.333
1:30-2:00 PM	58.5	58.9	0.4	888	3.611
2:00-2:30 PM	58.9	59.6	0.7	844	3.611
2:30-3:00 PM	59.6	59.7	0.1	820	3.888

Table 14 Values of temp., solar intensity and wind speed with time

Date08/05/2014_for SiO_2-water based nanofluid(0.01% conc.) at vol. flow rate of 20 l/hr.					
Time	Inlet temperature (°C)	Outlet temperature (°C)	Temperature difference (°C)	Solar intensity (W/m^2)	Wind speed (m/sec)
9:30-10:00 AM	31.5	35.2	3.7	758	3.888
10:00-10:30 AM	35.2	38.9	3.7	784	3.888
10:30-11:00 AM	38.9	42.9	4	806	4.722
11:00-11:30 AM	42.9	46.7	3.8	840	4.722
11:30-12:00 AM	46.7	50.7	4	885	5
12:00-12:30 PM	50.7	54.2	3.5	911	5
12:30-1:00 PM	54.2	57.3	3.1	926	5
1:00-1:30 PM	57.3	59.7	2.4	855	5
1:30-2:00 PM	59.7	61.4	1.7	835	5.277
2:00-2:30 PM	61.4	62.5	1.1	806	5.277
2:30-3:00 PM	62.5	62.9	0.4	777	5

Table 15 Values of temp., solar intensity and wind speed with time

Date09/05/2014_for SiO_2-water based nanofluid(0.01% conc.) at vol. flow rate of 40 l/hr.					
Time	Inlet temperature (°C)	Outlet temperature (°C)	Temperature difference (°C)	Solar intensity (W/m^2)	Wind speed (m/sec)
9:30-10:00 AM	31.2	35	3.8	743	3.05
10:00-10:30 AM	35	38.7	3.7	783	3.05
10:30-11:00 AM	38.7	42.5	3.8	806	3.333
11:00-11:30 AM	42.5	46.1	3.6	844	3.333
11:30-12:00 AM	46.1	49.7	3.6	866	3.333
12:00-12:30 PM	49.7	53.4	3.7	870	3.333
12:30-1:00 PM	53.4	56.5	3.1	881	3.333
1:00-1:30 PM	56.5	59	2.5	830	3.333
1:30-2:00 PM	59	60.8	1.8	805	3.611
2:00-2:30 PM	60.8	61.6	0.8	762	3.611
2:30-3:00 PM	61.6	61.6	0	736	3.611

Table 16 Values of temp., solar intensity and wind speed with time

Date10/05/2014_for SiO_2-water based nanofluid(0.01% conc.) at vol. flow rate of 60 l/hr.					
Time	Inlet temperature (°C)	Outlet temperature (°C)	Temperature difference (°C)	Solar intensity (W/m^2)	Wind speed (m/sec)
9:30-10:00 AM	33.1	36.7	3.6	810	1.667
10:00-10:30 AM	36.7	40.2	3.5	829	1.667
10:30-11:00 AM	40.2	44.3	4.1	850	1.667
11:00-11:30 AM	44.3	48.1	3.8	859	1.667
11:30-12:00	48.1	51.6	3.5	888	1.667

AM					
12:00-12:30 PM	51.6	55.1	3.5	905	1.667
12:30-1:00 PM	55.1	58.2	3.1	926	1.667
1:00-1:30 PM	58.2	60.3	2.1	836	1.667
1:30-2:00 PM	60.3	60.6	0.3	739	1.667
2:00-2:30 PM	60.6	60.8	0.2	762	1.667
2:30-3:00 PM	60.8	60.2	-0.6	546	1.667

Table 17 Values of temp., solar intensity and wind speed with time

Date15/05/2014_for SiO_2-water based nanofluid(0.05% conc.) at vol. flow rate of 20 l/hr.					
Time	Inlet temperature (°C)	Outlet temperature (°C)	temperature difference (°C)	Solar intensity (W/m^2)	Wind speed (m/sec)
9:30-10:00 AM	32	36.1	4.1	800	4.722
10:00-10:30 AM	36.1	40.1	4	836	4.722
10:30-11:00 AM	40.1	43.8	3.7	860	4.444
11:00-11:30 AM	43.8	47.7	3.9	888	4.444
11:30-12:00 AM	47.7	51.7	4	911	4.166
12:00-12:30 PM	51.7	54.9	3.2	922	4.166
12:30-1:00 PM	54.9	57.5	2.6	929	4.166
1:00-1:30 PM	57.5	60.5	3	902	4.166
1:30-2:00 PM	60.5	62.3	1.8	878	3.888
2:00-2:30 PM	62.3	63.6	1.3	833	3.888
2:30-3:00 PM	63.6	63.9	0.3	806	3.888

Table 18 Values of temp., solar intensity and wind speed with time

Date16/05/2014_for SiO_2-water based nanofluid(0.05% conc.) at vol. flow rate of 40 l/hr.					
Time	Inlet temperature (°C)	Outlet temperature (°C)	Temperature difference (°C)	Solar intensity (W/m^2)	Wind speed (m/sec)
9:30-10:00 AM	32.5	36.7	4.2	810	3.333
10:00-10:30 AM	36.7	40.8	4.1	840	3.333
10:30-11:00 AM	40.8	44.4	3.6	866	3.611
11:00-11:30 AM	44.4	48.2	3.8	911	3.611
11:30-12:00 AM	48.2	51.8	3.6	941	3.611
12:00-12:30 PM	51.8	55.4	3.6	954	3.611
12:30-1:00 PM	55.4	58.4	3	948	3.333
1:00-1:30 PM	58.4	60.9	2.5	907	3.333
1:30-2:00 PM	60.9	62.2	1.3	834	3.333
2:00-2:30 PM	62.2	63.2	1	799	3.333
2:30-3:00 PM	63.2	63	-0.2	736	3.333

Table 19 Values of temp., solar intensity and wind speed with time

Date18/05/2014_for SiO_2-water based nanofluid(0.05% conc.) at vol. flow rate of 60 l/hr.					
Time	Inlet temperature (°C)	Outlet temperature (°C)	Temperature difference (°C)	Solar intensity (W/m^2)	Wind speed (m/sec)
9:30-10:00 AM	31.1	35.2	4.1	792	2.777
10:00-10:30 AM	35.2	39.3	4.1	845	2.777
10:30-11:00 AM	39.3	43.6	4.3	881	3.055
11:00-11:30 AM	43.6	48.1	4.5	900	3.055
11:30-12:00	48.1	52.1	4	927	3.333

AM					
12:00-12:30 PM	52.1	55.9	3.8	938	3.333
12:30-1:00 PM	55.9	59.1	3.2	961	3.333
1:00-1:30 PM	59.1	61.7	2.6	927	3.333
1:30-2:00 PM	61.7	63.8	2.1	903	3.611
2:00-2:30 PM	63.8	65.1	1.3	845	3.611
2:30-3:00 PM	65.1	65.4	0.3	799	3.611

Table 20 Values of temp., solar intensity and wind speed with time

Date26/05/2014_for CuO-water based nanofluid(0.01% conc.) at vol. flow rate of 20 l/hr .					
Time	Inlet temperature (°C)	Outlet temperature (°C)	Temperature Difference (°C)	Solar intensity (W/m^2)	Wind speed (m/sec)
9:30-10:00 AM	30	34.3	4.3	751	1.667
10:00-10:30 AM	34.3	38.4	4.1	768	1.667
10:30-11:00 AM	38.4	42.6	4.2	786	1.388
11:00-11:30 AM	42.6	46.6	4	812	1.388
11:30-12:00 AM	46.6	50.7	4.1	850	1.667
12:00-12:30 PM	50.7	54.6	3.9	870	1.667
12:30-1:00 PM	54.6	57.9	3.3	892	1.667
1:00-1:30 PM	57.9	60.9	3	900	1.667
1:30-2:00 PM	60.9	62.7	1.8	868	1.944
2:00-2:30 PM	62.7	64.1	1.4	823	1.944
2:30-3:00 PM	64.1	64.8	0.7	792	2.222

Table 21 Values of temp., solar intensity and wind speed with time

Date28/05/2014_for CuO-water based nanofluid(0.01% conc.) at vol. flow rate of 40 l/hr.					
Time	Inlet temperature (°C)	Outlet temperature (°C)	Temperature Difference (°C)	Solar intensity (W/m^2)	Wind speed (m/sec)
9:30-10:00 AM	33.5	38.1	4.6	773	1.666
10:00-10:30 AM	38.1	42.4	4.3	799	1.666
10:30-11:00 AM	42.4	46.4	4	827	2.222
11:00-11:30 AM	46.4	50.2	3.8	848	2.222
11:30-12:00 AM	50.2	54.2	4	872	2.777
12:00-12:30 PM	54.2	58	3.8	885	2.777
12:30-1:00 PM	58	61.6	3.6	907	3.888
1:00-1:30 PM	61.6	64.6	3	873	3.888
1:30-2:00 PM	64.6	66.8	2.2	845	4.722
2:00-2:30 PM	66.8	68	1.2	797	4.722
2:30-3:00 PM	68	68.4	0.4	770	5

Table 22 Values of temp., solar intensity and wind speed with time

Date29/05/2014_for CuO-water based nanofluid(0.01% conc.) at vol. flow rate of 60 l/hr.					
Time	Inlet temperature (°C)	Outlet temperature (°C)	Temperature Difference (°C)	Solar intensity (W/m^2)	Wind speed (m/sec)
9:30-10:00 AM	34.5	39.3	4.8	773	0.8333
10:00-10:30 AM	39.3	43.5	4.2	789	0.8333
10:30-11:00 AM	43.5	47.9	4.4	808	0.8333
11:00-11:30 AM	47.9	51.8	3.9	833	0.8333
11:30-12:00	51.8	55.8	4	851	1.388

AM					
12:00-12:30 PM	55.8	59.6	3.8	872	1.388
12:30-1:00 PM	59.6	63.1	3.5	885	1.944
1:00-1:30 PM	63.1	65.9	2.8	860	1.944
1:30-2:00 PM	65.9	68.1	2.2	850	2.5
2:00-2:30 PM	68.1	69.5	1.4	826	2.5
2:30-3:00 PM	69.5	70.2	0.7	806	2.777

Table 23 Values of temp., solar intensity and wind speed with time

Date02/06/2014_for CuO-water based nanofluid(0.05% conc.) at vol. flow rate of 20 l/hr.					
Time	Inlet temperature (°C)	Outlet temperature (°C)	Temperature Difference (°C)	Solar intensity (W/m^2)	Wind speed (m/sec)
9:30-10:00 AM	32	37.1	5.1	774	1.111
10:00-10:30 AM	37.1	41.7	4.6	797	1.111
10:30-11:00 AM	41.7	45.8	4.1	827	0.8333
11:00-11:30 AM	45.8	50	4.2	848	0.8333
11:30-12:00 AM	50	54	4	875	1.666
12:00-12:30 PM	54	58.2	4.2	905	1.666
12:30-1:00 PM	58.2	61.3	3.1	929	2.5
1:00-1:30 PM	61.3	64.7	3.4	948	2.5
1:30-2:00 PM	64.7	67	2.3	923	3.333
2:00-2:30 PM	67	68.4	1.4	893	3.333
2:30-3:00 PM	68.4	68.9	0.5	860	3.888

Table 24 Values of temp., solar intensity and wind speed with time

Date03/06/2014_for CuO-water based nanofluid(0.05% conc.) at vol. flow rate of 40 l/hr.					
Time	Inlet temperature (°C)	Outlet temperature (°C)	Temperature Difference (°C)	Solar intensity (W/m^2)	Wind speed (m/sec)
9:30-10:00 AM	36.2	41.2	5	790	3.888
10:00-10:30 AM	41.2	45.9	4.7	818	3.888
10:30-11:00 AM	45.9	50	4.1	842	4.722
11:00-11:30 AM	50	54	4	860	4.722
11:30-12:00 AM	54	57.8	3.8	890	5
12:00-12:30 PM	57.8	61.5	3.7	918	5
12:30-1:00 PM	61.5	64.7	3.2	944	5
1:00-1:30 PM	64.7	67.3	2.6	905	5
1:30-2:00 PM	67.3	69.1	1.8	882	5.277
2:00-2:30 PM	69.1	70.4	1.3	851	5.277
2:30-3:00 PM	70.4	70.6	0.2	818	5.277

Table 25 Values of temp., solar intensity and wind speed with time

Date04/06/2014_for CuO-water based nanofluid(0.05% conc.) at vol. flow rate of 60 l/hr.					
Time	Inlet temperature (°C)	Outlet temperature (°C)	Temperature Difference (°C)	Solar intensity (W/m^2)	Wind speed (m/sec)
9:30-10:00 AM	36.5	41.8	5.3	786	1.666
10:00-10:30 AM	41.8	46.3	4.5	811	1.666
10:30-11:00 AM	46.3	51.2	4.9	842	1.944
11:00-11:30 AM	51.2	56.3	5.1	871	1.944
11:30-12:00	56.3	60.7	4.4	912	2.5

AM					
12:00-12:30 PM	60.7	64.9	4.2	930	2.5
12:30-1:00 PM	64.9	68.4	3.5	946	3.333
1:00-1:30 PM	68.4	71.9	3.5	918	3.333
1:30-2:00 PM	71.9	74.9	3	889	3.888
2:00-2:30 PM	74.9	76.6	1.7	851	3.888
2:30-3:00 PM	76.6	77	0.4	814	3.888

Table 26 Values of absorbed heat flux, useful heat gain and efficiencies with time

Water at vol. flow rate of 20 l/hr.					
Time	Absorbed heat flux (W/m^2)	Useful heat gain (W)	Instantaneous efficiency (%)	Thermal efficiency (%)	Overall efficiency (%)
9:30-10:00 AM	544.39	83.66	9.79	10.56	6.63
10:00-10:30 AM	569.58	81.33	9.1	9.82	
10:30-11:00 AM	591.27	85.98	9.27	10	
11:00-11:30 AM	642.35	85.98	8.53	9.2	
11:30-12:00 AM	663.34	81.33	7.81	8.43	
12:00-12:30 PM	668.24	69.71	6.65	7.17	
12:30-1:00 PM	658.44	53.45	5.17	5.58	
1:00-1:30 PM	642.35	55.77	5.53	5.97	
1:30-2:00 PM	634.65	34.86	3.5	3.78	
2:00-2:30 PM	616.46	18.59	1.92	2.07	
2:30-3:00 PM	588.474	6.97	0.75	0.81	

Table 27 Values of absorbed heat flux, useful heat gain and efficiencies with time

Water at vol. flow rate of 40 l/hr.					
Time	Absorbed heat flux (W/m^2)	Useful heat gain (W)	Instantaneous efficiency (%)	Thermal efficiency (%)	Overall efficiency (%)
9:30-10:00 AM	563.98	167.31	18.91	10.2	6.51
10:00-10:30 AM	586.37	171.96	18.69	10.08	
10:30-11:00 AM	605.96	162.66	17.11	9.23	
11:00-11:30 AM	647.95	162.66	16	8.63	
11:30-12:00 AM	673.84	167.31	15.82	8.54	
12:00-12:30 PM	684.33	162.66	15.15	8.17	
12:30-1:00 PM	668.24	139.43	13.3	7.17	
1:00-1:30 PM	658.44	111.54	10.8	5.82	
1:30-2:00 PM	652.84	51.12	4.99	2.69	
2:00-2:30 PM	635.35	18.59	1.86	1	
2:30-3:00 PM	618.56	9.3	0.96	0.52	

Table 28 Values of absorbed heat flux, useful heat gain and efficiencies with time

Water at vol. flow rate of 60 l/hr.					
Time	Absorbed heat flux (W/m^2)	Useful heat gain (W)	Instantaneous efficiency (%)	Thermal efficiency (%)	Overall efficiency (%)
9:30-10:00 AM	535.29	243.26	28.96	10.45	
10:00-10:30 AM	554.18	236.31	27.17	9.8	
10:30-11:00 AM	573.78	264.16	29.34	10.58	
11:00-11:30 AM	627.65	243.26	24.7	8.91	
11:30-12:00	658.44	236.31	22.87	8.25	

AM					6.37
12:00-12:30 PM	675.94	222.41	20.97	7.56	
12:30-1:00 PM	647.95	194.61	19.14	6.9	
1:00-1:30 PM	637.45	132.06	13.2	4.76	
1:30-2:00 PM	621.36	27.8	2.85	1.03	
2:00-2:30 PM	590.57	48.65	5.25	1.89	
2:30-3:00 PM	573.78	6.95	0.77	0.28	

Table 29 Values of absorbed heat flux, useful heat gain and efficiencies with time

SiO_2-water based nanofluid having (0.01% particle concentration) at vol. flow rate of 20 l/hr.					
Time	Absorbed heat flux (W/m^2)	Useful heat gain (W)	Instantaneous efficiency (%)	Thermal efficiency (%)	Overall efficiency (%)
9:30-10:00 AM	530.39	85.52	10.28	11.08	7.76
10:00-10:30 AM	548.59	85.52	9.93	10.71	
10:30-11:00 AM	563.98	92.46	10.45	11.27	
11:00-11:30 AM	587.77	87.83	9.52	10.27	
11:30-12:00 AM	619.26	92.46	9.51	10.26	
12:00-12:30 PM	637.45	80.9	8.09	8.72	
12:30-1:00 PM	647.95	71.65	7.05	7.6	
1:00-1:30 PM	598.27	55.47	5.91	6.37	
1:30-2:00 PM	584.27	39.29	4.29	4.62	
2:00-2:30 PM	563.98	25.43	2.87	3.1	
2:30-3:00 PM	543.69	9.25	1.08	1.17	

Table 30 Values of absorbed heat flux, useful heat gain and efficiencies with time

SiO_2-water based nanofluid having (0.01% particle concentration) at vol. flow rate of 40 l/hr.					
Time	Absorbed heat flux (W/m^2)	Useful heat gain (W)	Instantaneous efficiency (%)	Thermal efficiency (%)	Overall efficiency (%)
9:30-10:00 AM	519.9	175.77	21.55	11.61	7.73
10:00-10:30 AM	547.89	171.15	19.91	10.73	
10:30-11:00 AM	563.98	175.77	19.86	10.71	
11:00-11:30 AM	590.57	166.52	17.97	9.68	
11:30-12:00 AM	605.97	166.52	17.51	9.44	
12:00-12:30 PM	608.77	171.15	17.92	9.65	
12:30-1:00 PM	616.46	143.39	14.82	7.99	
1:00-1:30 PM	580.78	115.64	12.69	6.84	
1:30-2:00 PM	563.28	83.26	9.42	5.08	
2:00-2:30 PM	533.19	37	4.42	2.38	
2:30-3:00 PM	515	0	0	0	

Table 31 Values of absorbed heat flux, useful heat gain and efficiencies with time

SiO_2-water based nanofluid having (0.01% particle concentration) at vol. flow rate of 60 l/hr.					
Time	Absorbed heat flux (W/m^2)	Useful heat gain (W)	Instantaneous efficiency (%)	Thermal efficiency (%)	Overall efficiency (%)
9:30-10:00 AM	566.78	249.78	28.08	10.09	
10:00-10:30 AM	580.08	242.84	26.68	9.58	
10:30-11:00 AM	594.77	284.47	30.48	10.95	
11:00-11:30 AM	601.07	263.66	27.95	10.04	
11:30-12:00 AM	621.36	242.84	24.91	8.95	

12:00-12:30 PM	633.26	242.84	24.44	8.78	7.48
12:30-1:00 PM	647.95	215.09	21.15	7.6	
1:00-1:30 PM	584.98	145.71	15.87	5.7	
1:30-2:00 PM	517.1	20.82	2.57	0.92	
2:00-2:30 PM	533.19	13.88	1.66	0.6	
2:30-3:00 PM	382.05	-	0	0	

Table 32 Values of absorbed heat flux, useful heat gain and efficiencies with time

SiO_2-water based nanofluid having (0.05% particle concentration) at vol. flow rate of 20 l/hr.					
Time	Absorbed heat flux (W/m^2)	Useful heat gain (W)	Instantaneous efficiency (%)	Thermal efficiency (%)	Overall Efficiency (%)
9:30-10:00 AM	559.78	92.57	10.54	11.36	7.4
10:00-10:30 AM	584.97	90.31	9.84	10.61	
10:30-11:00 AM	601.77	83.54	8.85	9.54	
11:00-11:30 AM	621.36	88.05	9.03	9.74	
11:30-12:00 AM	637.45	90.31	9.03	9.74	
12:00-12:30 PM	645.15	72.25	7.14	7.7	
12:30-1:00 PM	650.05	58.7	5.75	6.21	
1:00-1:30 PM	631.16	67.73	6.84	7.38	
1:30-2:00 PM	614.36	40.64	4.22	4.55	
2:00-2:30 PM	582.88	29.35	3.21	3.46	
2:30-3:00 PM	563.98	6.77	0.76	0.83	

Table 33 Values of absorbed heat flux, useful heat gain and efficiencies with time

SiO_2-water based nanofluid having (0.05% particle concentration) at vol. flow rate of 40 l/hr.					
Time	Absorbed heat flux (W/m^2)	Useful heat gain (W)	Instantaneous efficiency (%)	Thermal efficiency (%)	Overall Efficiency (%)
9:30-10:00 AM	566.78	189.8	21.34	11.5	7.73
10:00-10:30 AM	587.77	185.28	20.09	10.82	
10:30-11:00 AM	605.97	162.68	17.11	9.22	
11:00-11:30 AM	637.46	171.72	17.17	9.25	
11:30-12:00 AM	658.45	162.68	15.74	8.48	
12:00-12:30 PM	667.54	162.68	15.53	8.37	
12:30-1:00 PM	663.33	135.57	13.02	7.02	
1:00-1:30 PM	634.66	112.97	11.34	6.11	
1:30-2:00 PM	583.58	58.75	6.42	3.46	
2:00-2:30 PM	559.08	45.19	5.15	2.78	
2:30-3:00 PM	515	-	0	0	

Table 34 Values of absorbed heat flux, useful heat gain and efficiencies with time

SiO_2-water based nanofluid having (0.05% particle concentration) at vol. flow rate of 60 l/hr.					
Time	Absorbed heat flux (W/m^2)	Useful heat gain (W)	Instantaneous efficiency (%)	Thermal efficiency (%)	Overall Efficiency (%)
9:30-10:00 AM	554.19	277.91	31.96	11.48	7.83
10:00-10:30 AM	591.27	277.91	29.95	10.76	
10:30-11:00 AM	616.46	291.47	30.13	10.82	
11:00-11:30 AM	629.76	305.03	30.87	11.09	

11:30-12:00 AM	648.65	271.14	26.64	9.57	
12:00-12:30 PM	656.35	257.58	25.01	8.98	
12:30-1:00 PM	672.44	216.91	20.56	7.38	
1:00-1:30 PM	648.65	176.24	17.31	6.22	
1:30-2:00 PM	631.86	142.35	14.36	5.16	
2:00-2:30 PM	591.27	88.12	9.5	3.41	
2:30-3:00 PM	559.08	20.34	2.32	0.83	

Table 35 Values of absorbed heat flux, useful heat gain and efficiencies with time

CuO-water based nanofluid having (0.01% particle concentration) at vol. flow rate of 20 l/hr.					
Time	Absorbed heat flux (W/m^2)	Useful heat gain (W)	Instantaneous efficiency (%)	Thermal efficiency (%)	Overall efficiency (%)
9:30-10:00 AM	525.5	99.84	12.11	13.05	8.7
10:00-10:30 AM	537.39	95.19	11.29	12.17	
10:30-11:00 AM	550	97.51	11.3	12.18	
11:00-11:30 AM	568.18	92.87	10.42	11.23	
11:30-12:00 AM	594.77	95.19	10.2	10.99	
12:00-12:30 PM	608.77	90.55	9.48	10.22	
12:30-1:00 PM	624.16	76.62	7.82	8.43	
1:00-1:30 PM	629.76	69.65	7.05	7.6	
1:30-2:00 PM	607.37	41.79	4.38	4.73	
2:00-2:30 PM	575.88	32.5	3.6	3.88	
2:30-3:00 PM	554.2	16.25	1.87	2.01	

Table 36 Values of absorbed heat flux, useful heat gain and efficiencies with time

CuO-water based nanofluid having (0.01% particle concentration) at vol. flow rate of 40 l/hr.					
Time	Absorbed heat flux (W/m^2)	Useful heat gain (W)	Instantaneous efficiency (%)	Thermal efficiency (%)	Overall efficiency (%)
9:30-10:00 AM	540.89	213.6	25.17	13.56	8.65
10:00-10:30 AM	559.09	199.67	22.76	12.26	
10:30-11:00 AM	578.68	185.74	20.45	11.02	
11:00-11:30 AM	593.37	176.45	18.95	10.21	
11:30-12:00 AM	610.17	185.74	19.4	10.45	
12:00-12:30 PM	619.26	176.45	18.16	9.79	
12:30-1:00 PM	634.66	167.17	16.79	9.05	
1:00-1:30 PM	610.87	139.31	14.53	7.83	
1:30-2:00 PM	591.27	102.16	11.01	5.93	
2:00-2:30 PM	557.69	55.72	6.37	3.43	
2:30-3:00 PM	538.79	18.57	2.2	1.18	

Table 37 Values of absorbed heat flux, useful heat gain and efficiencies with time

CuO-water based nanofluid having (0.01% particle concentration) at vol. flow rate of 60 l/hr.					
Time	Absorbed heat flux (W/m^2)	Useful heat gain (W)	Instantaneous efficiency (%)	Thermal efficiency (%)	Overall efficiency (%)
9:30-10:00 AM	540.89	334.33	39.39	14.15	8.9
10:00-10:30 AM	552.09	292.54	33.77	12.13	
10:30-11:00 AM	565.38	306.47	34.54	12.41	
11:00-11:30 AM	582.88	271.65	29.7	10.67	
11:30-12:00 AM	595.47	278.61	29.82	10.71	

12:00-12:30 PM	610.17	264.68	27.64	9.93	
12:30-1:00 PM	619.26	243.78	25.09	9.01	
1:00-1:30 PM	601.77	195.03	20.65	7.42	
1:30-2:00 PM	594.77	153.24	16.42	5.9	
2:00-2:30 PM	577.98	97.51	10.75	3.86	
2:30-3:00 PM	563.98	48.76	5.51	1.98	

Table 38 Values of absorbed heat flux, useful heat gain and efficiencies with time

CuO-water based nanofluid having (0.05% particle concentration) at vol. flow rate of 20 l/hr.					
Time	Absorbed heat flux (W/m^2)	Useful heat gain (W)	Instantaneous efficiency (%)	Thermal efficiency (%)	Overall efficiency (%)
9:30-10:00 AM	541.59	117.52	13.83	14.9	8.71
10:00-10:30 AM	557.69	106	12.11	13.05	
10:30-11:00 AM	578.68	94.48	10.4	11.21	
11:00-11:30 AM	593.37	96.78	10.39	11.2	
11:30-12:00 AM	612.27	92.17	9.59	10.34	
12:00-12:30 PM	633.26	96.78	9.74	10.5	
12:30-1:00 PM	650.05	71.43	7	7.55	
1:00-1:30 PM	663.35	78.35	7.53	8.11	
1:30-2:00 PM	645.85	53	5.23	5.64	
2:00-2:30 PM	624.86	32.26	3.29	3.55	
2:30-3:00 PM	601.77	11.52	1.22	1.32	

Table 39 Values of absorbed heat flux, useful heat gain and efficiencies with time

CuO-water based nanofluid having (0.05% particle concentration) at vol. flow rate of 40 l/hr.					
Time	Absorbed heat flux (W/m^2)	Useful heat gain (W)	Instantaneous efficiency (%)	Thermal efficiency (%)	Overall efficiency (%)
9:30-10:00 AM	552.79	230.43	26.56	14.32	8.17
10:00-10:30 AM	572.38	216.61	24.12	13	
10:30-11:00 AM	589.17	188.96	20.44	11.01	
11:00-11:30 AM	601.77	184.35	19.52	10.52	
11:30-12:00 AM	622.76	175.13	17.92	9.66	
12:00-12:30 PM	642.35	170.52	16.92	9.12	
12:30-1:00 PM	660.55	147.48	14.23	7.67	
1:00-1:30 PM	633.26	119.83	12.06	6.5	
1:30-2:00 PM	617.16	82.96	8.57	4.62	
2:00-2:30 PM	595.47	59.91	6.41	3.46	
2:30-3:00 PM	572.38	9.22	1.03	0.55	

Table 40 Values of absorbed heat flux, useful heat gain and efficiencies with time

CuO-water based nanofluid having (0.05% particle concentration) at vol. flow rate of 60 l/hr.					
Time	Absorbed heat flux (W/m^2)	Useful heat gain (W)	Instantaneous efficiency (%)	Thermal efficiency (%)	Overall efficiency (%)
9:30-10:00 AM	549.99	366.39	42.45	15.25	
10:00-10:30 AM	567.48	311.09	34.94	12.55	
10:30-11:00 AM	589.17	338.74	36.64	13.16	
11:00-11:30 AM	609.47	352.56	36.86	13.24	
11:30-12:00 AM	638.16	304.17	30.38	10.91	

12:00-12:30 PM	650.75	290.35	28.43	10.21	9.57
12:30-1:00 PM	661.95	241.96	23.29	8.37	
1:00-1:30 PM	642.35	241.96	24	8.62	
1:30-2:00 PM	622.06	207.39	21.25	7.63	
2:00-2:30 PM	595.47	117.52	12.58	4.52	
2:30-3:00 PM	569.58	27.65	3.09	1.11	